Food structure modification in the gastrointestinal environment and its impact on the delivery of lipophilic bioactive compounds

A thesis presented in partial fulfilment of the requirements for the degree of

Doctor of Philosophy

in

Food Technology

Riddet Institute, Massey University, Palmerston North,

New Zealand

Haroon Jamshaid Qazi

2023

To my parents and family,

thank you for continuously reminding me

“The fear of the Allah is the beginning of knowledge”.

Here I present my PhD thesis for you

MASSEY UNIVERSITY
TE KUNENGA KI PŪREHUROA
UNIVERSITY OF NEW ZEALAND

GRADUATE RESEARCH SCHOOL

Note for Examiners of Doctoral Theses
Explanation of COVID-19 Impacts

The Doctoral Research Committee recognises the impacts of Covid-19 on research, particularly for doctoral candidates, and we appreciate the efforts made by supervisors and candidates to ensure timely completion of the doctoral thesis. We know that in some cases this has meant the project has needed to be changed in some way, including its final presentation. For students whose work has been impacted, we invite supervisors to provide a note for examiners explaining the circumstances.

Instructions for Supervisors:

The note is designed to enable you to communicate to examiners your desire for them to take account of certain factors in their assessment of a thesis to address delays and disruptions experienced by a thesis student as a result of the Covid-19 pandemic.

The attached form should be used to provide **an explanation** to the examiners on what to consider in their evaluation. It should detail how the project was altered or how the final product of the thesis has been affected as a result of the disruption. Statements should be clear and succinct for the benefit of the examiners and in fairness to the student and others in the student cohort.

The form should be signed by the student, the supervisor and the Head of Academic Unit, or nominee, and included in the information that is sent out with the thesis.

For doctoral candidates, the completed form should be inserted into the front of the thesis before the abstract by the candidate when submitting their digital thesis for examination in the Student Portal. At the completion of the examination, the amended form which excludes any confidential comments to the examiners, should be included in the appendices.

Please be sure to indicate whether a student has received a suspension of studies due to Covid-19 and/or an extension, as it is important to note if students have already had some special consideration.

September 2021

MASSEY UNIVERSITY
TE KUNENGA KI PŪREHUROA
UNIVERSITY OF NEW ZEALAND

GRADUATE RESEARCH SCHOOL

Note for Examiners
Explanation of COVID-19 Impacts

Thank you for taking the time to examine this thesis, which has been undertaken during the Covid-19 pandemic. The New Zealand Government's response to Covid-19 includes a system of Alert Levels which have impacted upon researchers. Our University's pandemic plan applied the Government's expectations to our research environment to ensure the health and safety of our researchers, however, research was impacted by restrictions and disruptions, as outlined below.

For a six-week period from March 26 to April 27 2020, New Zealand was placed under very strict lockdown conditions (Level 4 – Lockdown), with students and staff unable to physically access University facilities, unless they were involved in essential research related to Covid-19. All field work ceased and data collection with humans was restricted to online methods, if appropriate. The restrictions were partially lifted on April 27, but students and staff were not generally allowed back into University facilities until May 13.

Ongoing disruptions have also been encountered for some students due to uncertainties over the potential for future Covid-19-related restrictions on activities, and a Covid-19 cluster outbreak based in Auckland in New Zealand on 12 August 2020 led to the imposition of rolling Level 2 (Reduce) and Level 3 (Restrict) conditions until 23 September 2020. Auckland campus based students remained on Level 2 until 7 October 2020.

This Alert Level system continues to be utilised throughout 2021, and in particular from 17 August 2021 when the whole of New Zealand again moved to Level 4 lockdown for an extended period. The Auckland region remained in alert level 3 or 4 for a number of months. Please see the NZ Government website for more information on lockdown dates.

These changing Alert Levels have meant that some research students had experimental, clinical, laboratory, field work, and/or data collection or analysis interrupted, and consequently may have had to adjust their research plans. For some students, the impacts of Covid-19 have been substantial as they may have had to significantly revise their research plans.

Overseas travel is not permitted by the University and restrictions have been placed on the New Zealand borders which are closed to non-New Zealand citizens and permanent residents. This meant that international students who were based offshore at the time of lockdown, were unable to return to New Zealand. A small number of offshore students were provided permission to return to New Zealand in early 2021. Many students have also suffered from anxiety and stress-related issues, and have had financial impacts, meaning their research progress has been significantly delayed.

This form, as completed by the supervisor and student, outlines the extent that the research has been affected by Covid-19 conditions.

Approved by DRC 10/Feb/2021
DRC 21/02/03
Updated September 2021

Please consider the factors listed below in your assessment of the work.

This statement has been prepared by the candidate's supervisor in consultation with the student and has been endorsed by the relevant Head of Academic Unit.

Student Name:	Haroon Jamshaid Qazi	ID Number:	[redacted]
Supervisor Name:	Prof. Aiqian Ye	Date:	27-Jun-23
Thesis title:	Food structure modification in the gastro-intestinal environment and its impact on the delivery of lipophilic bioactive compounds.		

Considerations to be taken into account. Note: This statement will remain in the final copy of the thesis which will be available from the Massey University Library following the examination process.
[*Enter key considerations here for the examiners. This can include but is not limited to change of scope, scale, topic, focus; limitations in relation to data collection, access to necessary literature or archival materials, laboratories, field sites; disruptions as a result of lockdown and various alert levels, medical or health considerations etc*]

In February 2020, I traveled to Pakistan to see my parents and siblings. But I was unable to return because of COVID-19 international border restrictions. I was unable to conduct the research work abroad during this time. As a result, I requested a suspension of my degree before starting my studies again in May 2021. The second lock-down in 2021 likewise impacted my research's progress. All of these factors compel us to change our initial research plans and therefore we have to drop our last research goal of examining gastrointestinal digestion of a real food system enriched with curcumin nanoemulsion.

Approved by DRC 10/Feb/2021
DRC 21/02/03
Updated September 2021

Confidential for Examiners Only: [*Please enter any other considerations which are confidential for examiners only and should not be placed in the final thesis version submitted to Library following the examination process]*

Signed, confirming this is a fair reflection of the impact of Covid-19 on this research.

Student	Haroon Jamshaid Qazi	Digitally signed by Haroon Jamshaid Qazi DN: cn=Haroon Jamshaid Qazi, c=NZ, ou=Riddet Institute, email=h.j.qazi@massey.ac.nz Date: 2023.06.28 08:35:58 +12'00'
Supervisor	Aiqian Ye	Digitally signed by Aiqian Ye DN: cn=Aiqian Ye, c=NZ, o=Massey University, ou=SF&AT, email=a.m.ye@massey.ac.nz Date: 2023.06.28 09:23:34 +12'00'
Head of Academic Unit (or nominee)	Steve Flint	Digitally signed by Steve Flint DN: cn=Steve Flint, c=NZ, email=s.h.flint@massey.ac.nz Date: 2023.06.28 09:50:05 +12'00'

Approved by DRC 10/Feb/2021
DRC 21/02/03
Updated September 2021

Abstract

Lipophilic bioactive compounds such as curcumin, polyphenols, etc. are often encapsulated before adding into various foods. The food matrix and its structural reorganizations under the influence of gastric and intestinal conditions affect their release, and uptake and utilization by the human body. Understanding the digestion behaviour of different food matrices is mandatory to modulate the release kinetics of bioactive ingredients. However, the information about the fortified food matrices post consumption is very limited. Fundamental knowledge of how the fortified bioactive compounds interact with the food component in the matrix during processing and further during gastrointestinal digestion is critical. Initial studies also suggest that the breakdown of food matrices in the gastrointestinal tract significantly influence on the delivery of nutrients. This area of research needs to be intensively investigated before the knowledge can be applied to rational design of functional foods that could modulate the rate of digestion and the bioaccessibility/bioavailability of fortified bioactive compounds.

This thesis focuses on understanding how microstructural rearrangement of the dairy and starch-based foods during gastric digestion influences the bio-accessibility of curcumin. Initially a curcumin nanoemulsion (CNE) was optimized with high encapsulation efficiency (~ 94%) along with acceptable shelf stability. Further, these CNEs were incorporated into milk, milk gels or corn starch gels. Using the human gastric simulator (HGS), these food systems were digested before being subjected to intestinal digestion in a static in vitro intestinal model.

The results showed that milks reconstituted from low-heat, medium-heat, and high-heat skim milk powders exhibited significantly distinct curd structures and disintegration behaviours in the stomach due to the varying degrees of casein/whey protein interactions that occurred during milk powder manufacture. The reconstituted milk made using high-heat milk powder formed soft curd under dynamic gastric conditions, resulting in a faster outflow of

proteins and entrapped curcumin nanoemulsion droplets. Thus, the changes in the gastric digesta profiles influenced both the rate of lipid hydrolysis and the bioaccessibility of curcumin during intestinal digestion.

Milk gels were formed using rennet enzyme or acid with similar rheological and compositional profiles. The gastric emptying was significantly impacted by the way these gels disintegrated during dynamic gastric digestion. The curd particles from the acid- gel were digested much faster than that from the rennet gel. The composition of the digesta was affected by these changes to the curd structures and stomach emptying rates during the gastric phase, which altered how the oil droplets were released from the stomach. This in turn affected the related lipophilic curcumin's bioaccessibility during the intestinal phase.

Furthermore, the digestion behaviour of corn starch gels made from waxy, native, and high amylose corn starches with added CNE were investigated. The physicochemical properties of the gels were drastically altered by the addition of curcumin nanoemulsion. Because of the waxy gel's adhesive character, most of the oil droplets were held inside the gel fragments throughout the dynamic gastric phase. This resulted in the delayed breakdown and emptying of gels from the stomach. This variation in the compositional and structural characteristics of the gastric digesta was further connected to the varying rates of starch hydrolysis, the release of free fatty acids, and the associated proportion of bioaccessible curcumin.

These findings in this thesis highlight how the release of health-promoting bioactive compounds from food matrix can be manipulated by understanding the complex dynamic processing behaviour of the food materials within the gastrointestinal tract. This can further help in designing novel functional foods for various populations.

Acknowledgements

All praise belongs to Allah, and may He bestow His peace and blessings upon all His messengers, and His Final messenger Prophet Muhammad Peace be Upon Them all, until the day of Judgement.

For me, pursuing this PhD has been a rewarding and life-changing experience. I could not have finished my doctoral dissertation without the incredible help of many wonderful people. As a result, I'd like to take this opportunity to express my heartfelt gratitude to each and every one of them.

I want to start by expressing my gratitude and admiration to my supervisory panel, which consists of Professor Aiqian Ye, Dr. Alejandra Acevedo-Fani, and Dist. Prof. Harjinder Singh. It is such a privilege to be advised by eminent researchers like them, and I couldn't have asked for a better supervisory panel; you've all been incredible academic role models for me!

I would like to start by sincerely thanking my chief supervisor, Prof. Aiqian Ye, for his mentoring and all the fruitful conversations, especially throughout the beginning and end of my PhD. You've allowed me a lot of leeway to choose my own research course, and I really appreciate that. My PhD journey was made easier by his persistence, encouragement, and, most importantly, his bright outlook and nice nature. Throughout my study, especially when I was writing, his insightful remarks and thorough writing abilities were helpful. I could not have imagined having a better advisor for my doctoral studies. I would like to express my sincere gratitude to my co-supervisor, Dr. Alejandra Acevedo-Fani for her encouragement, assistance, and technical support. My profound gratitude and respect are due to Distinguished Professor Harjinder Singh, my co-supervisor. It has been an immense honour to get guidance from your expertise and knowledge. Many thanks for the support as well as the insightful comments and

suggestions. My supervisory team has been incredibly kind and encouraging during my PhD studies, especially during the COVID period when I was stuck abroad for more than a year.

My gratitude also goes to Associate Prof. Jaspreet Singh, Dr. Ali Rashidinejad, Dr Anant Dave, Dr. Parthasarathi Subramanian and Dr. Teresa Wegrzyn for their great support and guidance about my project. Many thanks to the staff members who assisted me with my PhD. I like to thank Dr. Lovedeep Kaur as well for her suggestions at my confirmation. For the equipment training, lab management, and assistance with my work, I would like to thank Maggie Zou, Chris Hall, Michelle Tamehana, Jack Cui, Dr. Peter Zhu and Steve Glasgow. I would like to express my gratitude to the Riddet Institute management team, which includes Mr. John Henley-King, Mrs. Terri Palmer, Mrs. Ansley Te Hiwi, Dr. Sarah Golding, Michelle Heayns and Ms. Meg Wedlock. I also appreciate Dr. Claire Woodhall's excellent editorial guidance on the publications resulting from this research.

I wish to acknowledge the financial support provided by the HEC (Higher Education Commission of Pakistan) and Riddet Institute, in the form of Scholarship and travel grant for attending international conference in Ireland.

For advice and encouragement throughout my studies, I am grateful to my Massey University coworkers and friends, in particular Patrick Tai, Alex Kanon, Joanna Nadia, Davide Fraccascia, Giovanna Castillo-Fernandez, Laura Payling, Xin Wang, Saman Sabet, Roy, Natasha Nayak, Siqi Li, Aylin Şen, Muhammad Rehan, Muhammad Uzair, Nabil Parker, Saad Ghafoor, Taimoor Khan. Thank you for all of your fascinating corridor chats, lunch breaks, surprise parties, and general good times over the last four years.

I would also like to acknowledge all my colleagues and seniors from the University of Veterinary and Animal Sciences, Lahore, Pakistan who were the first to inspire me to start a

PhD, helped me to make right decision and have supported me while I was stuck in Pakistan during COVID Pandemic.

My big thanks to my wife Nida Fakhar, my daughters Anayah and Fatima and my son Ibrahim, who were with me in New Zealand and supported me to achieve this milestone. They suffered a lot because of my busy schedule during the PhD programme.

Finally, my wholehearted gratitude goes to my beloved Mother (Rubina), Mother-in-Law (Shameem) and Father (Qazi Jamshaid). Without them and their prayers, I would not have had the courage to embark on this PhD journey in the first place. Thank you for teaching me that all good things are always possible! You are always right! Yes, I did it and thus I dedicate my PhD dissertation to you!

Haroon Jamshaid Qazi

April 2023

Table of contents

List of figures

List of tables

List of Abbreviations

AG	Acid gel
ANOVA	Analysis of variance
CNE	Curcumin nanoemulsion
FFA	Free fatty acids
HACS	High amylose corn starch
HGS	Human gastric simulator
MHH	Milk high heated
MLH	Milk low heated
MMH	Milk medium heated
NCS	Normal corn starch
RG	Rennet gel
SD	Standard deviation
SE	Standard error
SGF	Simulated gastric fluid
SIF	Simulated intestinal fluid
SSF	Simulated salivary fluid
SEM	Scanning electron microscopy
WCS	Waxy corn starch
w/w	weight per weigh
w/v	weight per volume

Peer-reviewed publications, conference presentations and awards

Publications

Qazi, H. J., A. Ye, A. Acevedo-Fani, and H. Singh. 2021. In vitro digestion of curcumin-nanoemulsion-enriched dairy protein matrices: impact of the type of gel structure on the bioaccessibility of curcumin. *Food Hydrocolloids*, 117:106692.

Qazi, H. J., A. Ye, A. Acevedo-Fani, and H. Singh. 2022. Impact of recombined milk systems on gastrointestinal fate of curcumin nanoemulsion. *Frontiers in Nutrition*, 9:890876.

Qazi, H. J., A. Ye, A. Acevedo-Fani, and H. Singh. 2023. Impact of differently structured starch gels on gastrointestinal fate of curcumin-containing nanoemulsions. *Food & Function*, 14(17), 7924-7937.

Manuscript submitted and in preparation

Qazi, H. J., A. Ye, A. Acevedo-Fani, and H. Singh. 2023. Modulating delivery of encapsulated bioactive compounds through food matrix design: recent trends and future perspectives. [Manuscript in preparation].

Additional publication

Sabet, S., Rashidinejad, A., **Qazi, H. J.,** & McGillivray, D. J. (2021). An efficient small intestine-targeted curcumin delivery system based on the positive-negative-negative colloidal interactions. *Food Hydrocolloids*, 111, 106375.

Conference Presentations and awards

Qazi, H. J., Ye, A., Acevedo-Fani, A., & Singh, H. Gastric digestion of dairy protein matrices: Impact on delivery of the curcumin loaded nanoemulsions to the intestine. Food Structure, Digestion, and Health Conference. Rotorua, New Zealand, 1st– 3rd October 2019. (Poster presentation)

Qazi, H. J., Ye, A., Acevedo-Fani, A., & Singh, H. Impact of dairy gels structure on gastrointestinal fate of curcumin nanoemulsion. 12th NIZO Dairy Online Conference – Innovations in Dairy Ingredients, 5 – 7 October 2021. (Poster presentation)

Qazi, H. J., Ye, A., Acevedo-Fani, A., & Singh, H. Impact of fortified milk systems on gastrointestinal fate of curcumin nanoemulsion. Food Structures, Digestion & Health 6th International Virtual Conference, 16th –19th November 2021. (Oral presentation)

Qazi, H. J., Ye, A., Acevedo-Fani, A., & Singh, H. Impact of the fortified dairy gel structure on the bioaccessibility of curcumin nanoemulsion. Nutrition Society of New Zealand 2021 Virtual Conference 2nd -3rd December 2021. (Oral presentation)

Qazi, H. J., Ye, A., Acevedo-Fani, A., & Singh, H. Impact of milk matrices on gastrointestinal fate of curcumin nanoemulsion. New Zealand Institute of Food Science and Technology Annual Conference, Rotorua, New Zealand 5th – 7th July 2022. (Poster presentation – awarded Best Poster PhD Presentation)

Qazi, H. J., Ye, A., Acevedo-Fani, A., & Singh, H. Impact of fortified milk systems on gastrointestinal fate of curcumin nanoemulsion. 5th Food Structure and Functionality Symposium, Cork, Ireland 18th – 21st September 2022. (Oral Presentation)

Qazi, H. J., Ye, A., Acevedo-Fani, A., & Singh, H. In-vitro digestion of differently structured starch gels: Impact on the bioaccessibility of curcumin. Riddet Institute Conference, Napier, New Zealand 14th – 16th November 2022. (Oral Presentation)

Qazi, H. J., Ye, A., Acevedo-Fani, A., & Singh, H. In-vitro digestion of differently structured starch gels: Impact on the bioaccessibility of curcumin. New Zealand Institute of Food Science and Technology Annual Conference, Dunedin, New Zealand 3rd – 5th July 2023. (Oral Presentation)

Key oral presentations locally in New Zealand

Nano-carriers for delivery of bioactive compounds in food systems. Riddet Institute Visualise Your Thesis Competition 2019. 22nd July 2019, Palmerston North, New Zealand.

The Food Maze. Massey University Three Minute Thesis (3MT) competition 14th September 2022, Palmerston North, New Zealand. (Won people choice award).

Digestion of complex food systems containing health-promoting compounds. Manawatū Branch of the Royal Society Te Apārangi, 18th April, 2023, Palmerston North, New Zealand.

Chapter 1: Introduction and project overview

1.1 Background

The concept of "food matrix" is mostly used in literature to denote the large continuous medium formed naturally or produced during processing that chemically or physically embed all microstructural elements in foods (Aguilera, 2018; Donhowe, Flores, Kerr, Wicker, & Kong, 2014). Scientific research has shown that foods' ability to promote health is not simply dependent on their nutrient content but also depends on the matrix that surrounds them (Acevedo-Fani & Singh, 2021; Fardet, Dupont, Rioux, & Turgeon, 2018; H. Singh & Gallier, 2014). The natural state of foods i.e. liquid, semi-solid or solid as well as structural association and organization of macro, micronutrients and other non-nutritional components may affect the bioavailability of nutrients (Capuano, Oliviero, Fogliano, & Pellegrini, 2018; Shen, Apriani, Weerakkody, Sanguansri, & Augustin, 2011). In fact, two meals with similar compositions (nutrients and calories) but with different matrix structures that arise from either different mechanical processes or different stages of disintegration in the gut may result in different health effects (Acevedo-Fani & Singh, 2021; Dupont et al., 2015; H. Singh & Acevedo-Fani, 2022).

Scientific recognition of the potential benefits of the bioactive food components has stimulated consumers preferences towards natural products with additional health-promoting effect (Betoret, Betoret, Vidal, & Fito, 2011; Delfanian & Sahari, 2020; Mollet & Rowland, 2002). Many fruits, vegetables and some sources from animal origin contain hydrophilic and lipophilic bioactive compounds such as carotenoids, polyphenols, phytosterols, and omega-3 fatty acids that differ in their physiochemical properties as well as in their bio-functionality, including antioxidant, antimicrobial, anti-cancerous, anti-ageing and anti-inflammatory properties (B. Chen, McClements, & Decker, 2013; Espín, García-Conesa, & Tomás-Barberán,

2007; Raikos & Ranawana, 2017; Ubbink & Krüger, 2006). However, these compounds generally have low oral bioavailability if consumed from its native food source. Therefore, concentrated extract of isolated forms are often utilised in fortification of food products as a tool to tackle nutritional deficiencies, and also, to increase the therapeutic effect of bioactive compounds (de Lourdes Samaniego-Vaesken, Alonso-Aperte, & Varela-Moreiras, 2012; Prior et al., 2010; H. Singh, 2016). Significant challenges need to be overcome while fortifying foods with bioactive compounds because these substances have their own inherited characteristics (e.g. strong odour, taste, color, volatility), which may affect quality attributes of the final product, or make their incorporation into foods rather complicated (El Sohaimy, 2012; Topolska, Florkiewicz, & Filipiak-Florkiewicz, 2021; Ubbink, 2012). Such opportunities and challenges have led the food industry to develop functional foods that may promote health, and have good acceptance among consumers (Guo, Ye, Bellissimo, Singh, & Rousseau, 2017; David Julian McClements & Grossmann, 2021; Shahidi, 2009).

Curcumin is an orange-yellow colored natural polyphenolic bioactive constituent, extracted from the rhizome. It is a lipophilic compound and has a higher solubility in medium chain triglyceride compared to long chain triglycerides and can be increased by increasing the temperature (Zou et al., 2016). Similarly, it is sensitive to light and loses its biological activity when it is exposed to alkaline pH, higher temperature and under GIT conditions resulting in lower bioavailability (Araiza-Calahorra et al., 2018; Prasad et al., 2014; Shaikh, Ankola, Beniwal, Singh, & Kumar, 2009; Zou et al., 2016). Scientist have tried using different strategies to improve the stability and bioavailability of curcumin. Compounds such as piperine is commercially being used along with curcumin as an absorption enhance. Piperine have been testified through clinical studies on human subjects to inhibit curcumin metabolizing enzymes that circumventing thereby making it more bioavailable (Shoba et al., 1998). However, use of piperine cannot enhance the application of curcumin in various foods, as they require a suitable

delivery system. To overcome these hurdles, curcumin can be encapsulated utilizing a carefully designed food-based colloidal delivery system. These delivery systems not only conserve their biological form but also has been reported to enhance curcumin bioavailability without compromising sensory and chemical stability of food (McClements & Jafari, 2018; Sessa et al., 2015; Silva et al., 2018).

In this context, encapsulation has emerged as a promising technique with the possibility of developing new food products with added lipophilic bioactive compounds with enhanced stability. However, the implementation of encapsulation technology in the food industry has been relatively slow due to a combination of limiting factors, such as strict regulations regarding food-grade ingredients selection, processing and storage parameters, interaction with complex food systems, low profit margins (Francesco Donsì, 2018; F. Donsì, Sessa, & Ferrari, 2013; P. N. Ezhilarasi, Indrani, Jena, & Anandharamakrishnan, 2014). Nanoemulsions have been used for addressing some of these food fortification limitations. Their nanosized structures ($d < 500$ nm) make them stable to flocculation, coalescence, gravitational separation as compared to conventional emulsions (Chang, McLandsborough, & McClements, 2012; Kumar et al., 2016; Patel, Patra, Shah, & Khedkar, 2018). Additionally, nanoemulsions protects the compound of interest to withstand food processing and their unique small size makes them highly bioavailable i.e. crossing the epithelial barriers in the gastrointestinal tract and releasing the bioactive compound at the targeted tissues (Galanakis, 2017; Martinez-Ballesta, Gil-Izquierdo, Garcia-Viguera, & Dominguez-Perles, 2018; Qazi, Majeed, Safdar, Antoniou, & Fang, 2015; Rein, Renouf, Cruz-Hernandez, et al., 2013; Salvia-Trujillo, Qian, Martín-Belloso, & McClements, 2013). Despite all these favourable properties of nanoemulsions, additional studies are required to understand how the bioactive compounds contained within the nanoemulsions behave as a part of the whole food matrix. Foods are non-equilibrium

assemblies that change over time and in response to external environmental conditions, which may occur during production or during eating and digestion.

The gastrointestinal behaviour and release of encapsulated bioactive compounds from different food systems are different and so far, a few in vitro and in vivo studies have been reported. For example, dairy products based on food structures can be classified into three main categories; i.e., liquid (milk and fermented milk products), semisolids (yogurt and few varieties of soft cheeses) and solid (mostly cheeses). Ye and co-workers investigated structural changes in unheated and heated skimmed milk (90°C for 20 min) during gastric digestion, using human gastric simulator (Ye, Cui, Dalgleish, & Singh, 2016). Both milks formed a clot with different structures in the gastric environment. The clot formed by the heated milk was loose with larger spaces while unheated milk clot had a tightly knitted structure that hindered the penetration of pepsin that consequently slowed the rate of protein hydrolysis.

In the same way, semi-solid milk gel structures impact the release of nutrient during digestion. An in-vivo study investigating the digestion kinetics of acid and rennet gels on the bioavailability of amino acids was conducted by Barbé et al. (2014). Effluents from small intestine and plasma samples were collected from six mini pigs fed at different time points during 7 h post meal ingestion. Results showed that rennet gels took longer time to digest compared to acid gel. Extending their work, Floury and co-workers (2018) developed a time-lapse synchrotron deep-UV microscopy methodology to monitor in situ microstructural changes in acid and rennet gels. Their results confirmed that rennet gel formed protein aggregates in stomach due to low pH, which slowed down the proteolysis by reducing the enzyme accessibility to the substrate.

Apart from the dairy matrices, the digestibility of starch-based foods during gastrointestinal digestion is markedly influenced both by the composition of the starch (i.e.

amylose content, amylose chain length and amylose to amylopectin ratio) and by texture and viscosity of the post-processing food matrix (Magallanes-Cruz, Flores-Silva, & Bello-Perez, 2017; Pletsch & Hamaker, 2018; J. Singh, Kaur, & Singh, 2013). The susceptibility of starch to in vitro or in vivo digestion is linked with the rate of glucose release from the matrix and its absorption into the bloodstream. In a recent study, M. Zheng, Ye, Singh, and Zhang (2021) looked at how different corn starch gel structures with varying amylose contents affected their disintegration during gastrointestinal digestion. They found that during the oral-gastric phase, starch hydrolysis in the gels was more dependent on the gel structure than on the molecular characteristics of the starch, whereas during the intestinal phase, the composition of the starch was more important.

This project aimed to understand intrinsic characteristics of selected food systems (dairy and starch-based) containing added curcumin in the form of nanoemulsion. The focus was to understand the dynamics of structural modifications in the gastric environment (using HGS), and the release kinetics of curcumin and macronutrients.

1.2 Research objective

Specific research objectives of this project were as follows:

1. To examine physicochemical and structural changes in curcumin nanoemulsion (CNE) enriched recombined milks in the gastric environment using the dynamic HGS and the release of curcumin during the intestinal transit.
2. To examine the behaviour of the CNE supplemented dairy protein gelled structures i.e. acid and rennet gels, during the gastric phase and its effect on the subsequent lipolysis and the bioaccessibility of curcumin in the small intestine.

3. To investigate the effect of CNE on the rheological properties of the starch gels manufactured using waxy (WCS), normal (NCS) or high amylose (HACS) corn starch and their consequent impact on digestion of lipids and starches as well as the bioaccessibility of curcumin during the in vitro gastrointestinal digestion.

1.3 Organization of the thesis

The research objectives in the Section 1.2 were completed through three in vitro studies using dynamic gastric model (Human Gastric Simulator). A literature review on the effect of food matrix on the delivery of encapsulated bioactive compounds (Chapter 2) provides the background information of the experiments. This thesis includes four experimental chapters (Chapters 3–5) derived from three in vitro gastrointestinal studies of CNE added to reconstituted milk, acid and rennet coagulated milk gels, and corn starch gels formed using starches with varying amylose contents. The findings from the experimental chapters are summarised and discussed in Chapter 6, which also includes conclusions and recommendations for further research.

Statement of contribution (DCR 16 forms)

MASSEY UNIVERSITY
TE KUNENGA KI PŪREHUROA
UNIVERSITY OF NEW ZEALAND

GRADUATE RESEARCH SCHOOL

STATEMENT OF CONTRIBUTION DOCTORATE WITH PUBLICATIONS/MANUSCRIPTS

We, the student and the student's main supervisor, certify that all co-authors have consented to their work being included in the thesis and they have accepted the student's contribution as indicated below in the Statement of Originality.

Student name:	Haroon Jamshaid Qazi
Name and title of main supervisor:	Aiqian Ye / Professor
In which chapter is the manuscript/published work?	Chapter 2

Describe the contribution that the student and members of the supervisory team have made to the manuscript/published work:[1]

Haroon Jamshaid Qazi: Writing – original draft, editing, artwork design
Aiqian Ye: Conceptualization, funding acquisition, writing – original draft, writing – review, Supervision.
Alejandra Acevedo-Fani: Writing – review & editing, Supervision.
Harjinder Singh: Conceptualization, Writing – review & editing, Supervision.

Please select one of the following three options:

- ○ The manuscript/published work is published or in press
  Please provide the full reference of the research output:
- ○ The manuscript is currently under review for publication
  Please provide the name of the journal:
- ◉ It is intended that the manuscript will be published, but it has not yet been submitted to a journal

Student's signature:	Haroon Jamshaid Qazi — Digitally signed by Haroon Jamshaid Qazi DN: cn=Haroon Jamshaid Qazi, c=NZ, ou=Riddet Institute, email=h.j.qazi@massey.ac.nz Date: 2023.06.20 10:57:30 +12'00'	Main supervisor's signature:	Aiqian Ye — Digitally signed by Aiqian Ye DN: cn=Aiqian Ye, c=NZ, o=Massey University, ou=SF&AT, email=a.m.ye@massey.ac.nz Date: 2023.06.20 12:10:57 +12'00'

This form should be placed at the beginning of each relevant thesis chapter.

[1] Refer to the Massey University Publishing and Authorship guidelines (OneMassey for staff, Stream for students) and/ or Contributor Roles Taxonomy (CRediT) guidelines for guidance.

Chapter 2: Literature Review

2.1 Abstract

The process of encapsulation has produced encouraging results in terms of improving the stability and the targeted delivery of isolated bioactive substances. The next stage is to integrate these encapsulated bioactive compounds into real food systems and to confirm how the food matrix influences their delivery. In this context, physicochemical interactions between the food matrix and the encapsulated bioactive compounds occur initially during processing and further during their disintegration during digestion. This review focuses mainly on understanding the intricate connection between the structure/matrix of different food systems and added encapsulated bioactive compounds and how this can be used to design functional foods for optimum bioavailability without affecting the quality of the product.

2.2 Introduction

Bioactive compounds are biologically active substances that are extracted from animal- or plant-based sources and have pharmacological or physiological effects that can promote human health. In general, these compounds are produced as secondary metabolites in small quantities and can modulate metabolic processes (Graebin, Ribeiro, Rogério, & Kümmerle, 2019; Khaw, Parat, Shaw, & Falconer, 2017; Yang et al., 2016). They are extremely heterogeneous (polyphenols, carotenoids, tocopherols, phytosterols, organosulfur compounds, and peptides) with antimicrobial, antioxidant, anti-inflammatory, anticancer, and antidiabetic properties (Eggersdorfer & Wyss, 2018; Oyenihi & Smith, 2019; Prasad et al., 2022; Ruhee, Roberts, Ma, & Suzuki, 2020; Szewczyk, Chojnacka, & Górnicka, 2021; Tornesello, Borrelli, Buonaguro, Buonaguro, & Tornesello, 2020). In natural foods, these bioactive compounds are entrapped in the complex matrices of lipids, proteins, and carbohydrates, which interfere with their release during digestion. Moreover, their low naturally low levels in various foods,

possible chemical interactions with other food constituents, and losses during processing have led to the isolation of these compounds and their fortification in other commonly consumed foods (Moreno & Ilic, 2018; Shahidi, 2009). Because of the stringent regulations in the food industry with respect to ingredients, processing methods, and storage conditions, it is critical that the incorporated bioactive ingredient does not affect the sensory attributes, freshness, or appearance of the food. However, active substances in food products are susceptible to a variety of physical and chemical conditions, which can result in the loss of biological functionality, chemical degradation, or an early or partial release during digestion. Therefore, well-designed delivery systems that are specifically designed for the target food application are frequently required (Carbonell-Capella, Buniowska, Barba, Esteve, & Frígola, 2014; Francesco Donsì, 2018; Galanakis, 2017).

The most common approach for adding bioactive compounds to foods is the use of encapsulation systems for protection or controlled release. The functionality of the encapsulated bioactive compound is associated with a specific formulation that involves combining the appropriate ratios of carrier materials, functional substances, and one or more biopolymeric emulsifier layers with the right hydrophilic–lipophilic balance values (Bao et al., 2019; Francesco Donsì, 2018; Đorđević et al., 2015; David Julian McClements, 2018; Qazi et al., 2015; Zhu, 2017). The encapsulation technique entraps the bioactive compound into the dispersed phase of an emulsion or adsorbs it on to the interface; it is a useful tool that influences the release of the compound and its incorporation into micelles for subsequent absorption (Donhowe et al., 2014; Jiang, Liao, & Charcosset, 2020).

In the food industry, the encapsulation process is applied during the manufacture of the appropriate therapeutic/functional food system, which can encapsulate the bioactive molecules, protect them from the peripheral environments, decrease volatility and toxicity, enhance

bioactivity, regulate their release at a controlled rate over prolonged periods, and improve consumer compliance and convenience (Nedovic, Kalusevic, Manojlovic, Levic, & Bugarski, 2011; Rezvankhah, Emam-Djomeh, & Askari, 2020; Rodríguez, Martín, Ruiz, & Clares, 2016). However, despite the growing interest in functional foods, few attempts to integrate delivery methods into model and actual food systems have been made, and little in vitro and in vivo research to assess how well they perform after being taken orally has been carried out (Augustin & Sanguansri, 2015). To date, the published studies have focused only on the characterization of delivery systems and their influence on the release of the bioactive compound in the gastrointestinal tract and have neglected their behavior within the food product. Although the encapsulation approach has shown to improve the solubility, stability, taste, bioaccessibility, and bioavailability of various bioactive compounds, the behviour of encapsulated bioactive compounds in different food matrices particularly during processing and consumption remains unknown. Hence, this is the main focus of the review.

2.3 Effect of food matrix on encapsulated bioactive compounds

The food matrix is a part of the microstructure of foods, usually corresponding to a physical and spatial domain, that contains, interacts directly and/or gives a particular functionality to a constituent or element of the food (Aguilera, 2018). This cellular- or colloidal-based dissipative organization is often categorized as soft matter, as its functionality is driven mainly by its internal (i.e., physicochemical and biochemical reactions) and external (i.e., enzymes, pH, thermal fluctuations, and microorganisms) perturbations (Aguilera, 2019; Alongi & Anese, 2021). The complexity of self-assembled structures in animal- or plant-based foods and structures generated in processed foods revolves around their structural orientation and their chemical composition (Aguilera, 2005; Capuano et al., 2018; Flores & Kong, 2017; Parada & Aguilera, 2007; Ubbink, 2012). The rigid and intact structures of native foods, such

as plant- and animal-tissue-based fibrous structures, plant-based fleshy materials, and encapsulated plant embryos, not only impact on functionality and digestibility but also significantly impact on the release of nutrients and the entrapped bioactive compounds (Acevedo-Fani, Dave, & Singh, 2020; Cifelli, 2021). The processing of these foods affects several physical, chemical, and nutritional attributes via the changes their structural arrangements. Processing can be used to develop, from basic raw materials, more complex structures in foods; for example, yogurt, cheese, and ice cream are all milk-based products with distinctive structures and properties (Dima, Assadpour, Dima, & Jafari, 2020). Moreover, the processed food is sometimes structurally modified to such an extent that its biological origin is not readily apparent, e.g., the conversion of liquid milk to solid cheese or the transformation of hard grain to fluffy bread. In addition, structural changes continue either during or after processing.Most foods never attain thermodynamic equilibrium, e.g., the softening and loss of crunchiness in fruits as they go through an physical transformation that leads to undesirable product quality by simultaneously changing the composition (Agarwal et al., 2019; Joardder, Kumar, & Karim, 2017). Thus, an understanding of the structural properties of food materials is important for proper control of food processing operations as well as for improvement in the quality of the final product (Karim, Rahman, Pham, & Fawzia, 2018; Lamothe, Rémillard, Tremblay, & Britten, 2017; Parada & Aguilera, 2007).

Fig. 2.1 depicts the interactions between the food matrix and the encapsulated bioactive compounds during processing and digestion. These interactions are discussed in more detail in subsequent sections.

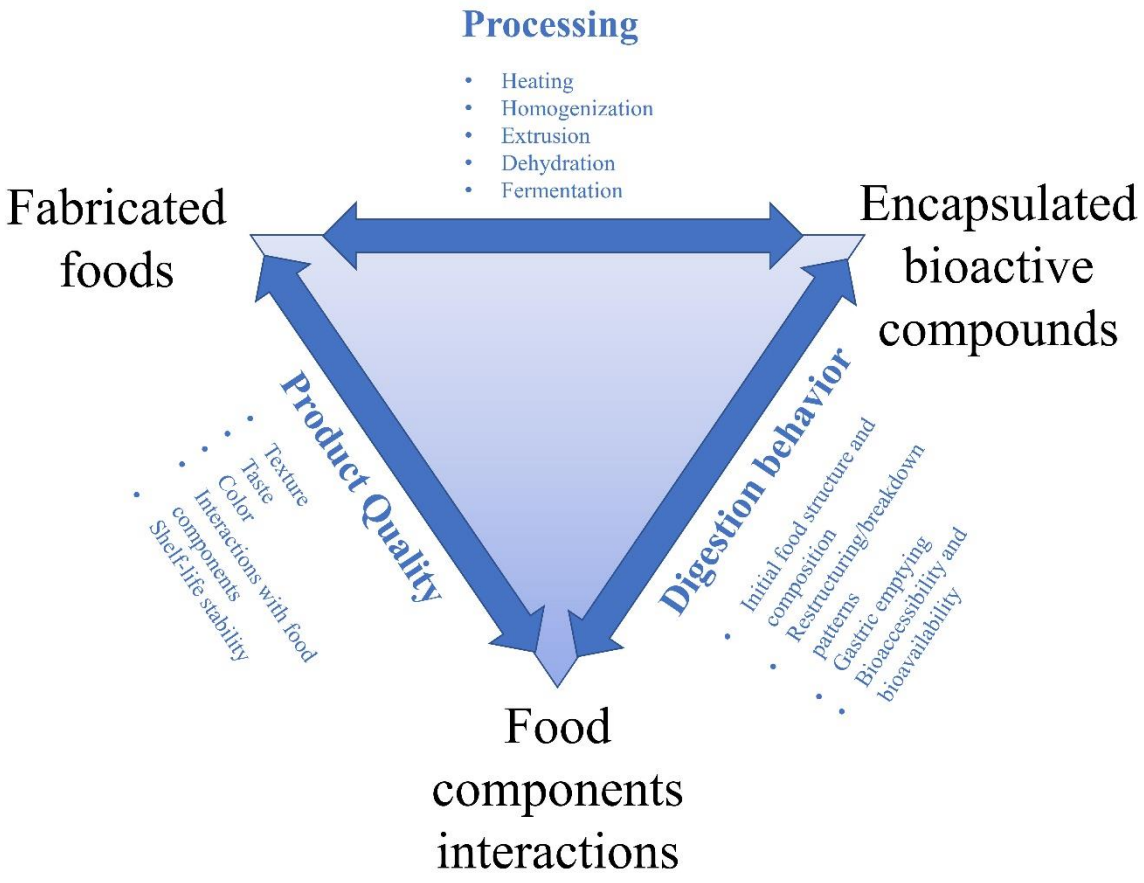

Fig. 2. 1 Interactions between fortified food matrices and effects of various factors on the delivery and bioaccessibility of loaded bioactive compounds.

2.3.1 In-product behavior

Encapsulated bioactive compounds can alter the sensory, physicochemical, and biological properties of food products (Dima et al., 2020; Khan, Grigor, Winger, & Win, 2013; H. Singh, 2016; Zhu, 2017). The compatibility, reactivity, and interactions of the encapsulated bioactive compounds with other food components, and the stringent processing and preservation conditions all have an impact on how these compounds behave within food products (Acevedo-Fani et al., 2020; Alongi & Anese, 2021; Francesco Donsì, 2018).

Recent research has evaluated the biological and functional effects of encapsulated bioactive compounds in a range of food product formulations. The findings of some of these studies are summarized in Table 1 and are addressed in the sections that follow.

Table 2. 1 Previous investigations on the relationship between the encapsulated bioactive compound and the fortified food matrix.

Encapsulated bioactive compound	Fortified food matrix	Size	Fortification level	Emulsifier	Outcomes	Reference
Epigallo-catechin gallate (EGCG)	Fruit nectar	270 and 220 μm	0.1 g	Alginate and chitosan	The chitosan-encapsulated EGCG in the fruit nectar was found to be more stable than the alginate-coated microparticles, which was attributed to alginate interactions with the phospholipid bilayer.	(Istenič, Cerc Korošec, & Poklar Ulrih, 2016)
Echinacea extract	Acidic beverage	190 nm	0.25%	Phospholipid	Encapsulation not only preserved the bioactive compounds against degradation under external conditions provided by the acidic beverage but also enhanced the bioavailability.	(Molaveisi, Shahidi Noghabi, Parastouei, & Taheri, 2021)
Steppogenin	Apple juice	> 35 nm	1 mL per 9 mL of apple juice	Tween 80 and PEG 400	Compared with enhanced juice with free steppogenin and regular apple juice, nanoencapsulated steppogenin had superior physicochemical and organoleptic qualities and showed effective antibrowning capabilities.	(Tao et al., 2017)
Cinnamon extract	Chocolate beverage	162 nm	60 mL of colloidal cinnamon nanoparticles and distilled water mixture	Shellac and xanthan gum	Despite the incorporation of nanoparticles significantly improving the suspension stability of chocolate beverages, the stabilization effect of the nanoparticles appeared to be significantly influenced by the characteristics of the beverage raw material.	(Muhammad et al., 2019)
Curcumin	Low-fat milk	63–126 nm	30.18 mL of milk and 12.82 mL of CNE containing 15 mg of curcumin	Tween 20	Fortified milk had significantly lower lipid oxidation than the control.	(Joung et al., 2016)
Fish oil	Fermented probiotic milk	37 nm	0.3 g of omega-3 fatty acid per 240 mL	Gum arabic and Tween 80	Nanoencapsulated-fish-oil-fortified samples had higher eicosapentaenoic acid and docosahexaenoic acid content, greater survival of probiotic bacteria, and greater overall acceptibility.	(Moghadam, Pourahmad, Mortazavi, Davoodi, & Azizinezhad, 2019)
Arjuna phenolics	Chocolate vanilla dairy drink	–	0.3%	Gum arabic and maltodextrin	Addition of encapsulated arjuna phenolics markedly affected the physicochemical attributes of the fortified matrix during prolonged storage.	(Sawale, Patil, Hussain, Singh, & Singh, 2017)

Fish oil	Milk, yogurt, and salad dressing	1.2 µm	2% milk, 2% yogurt, and 20% salad dressing	Potassium sorbate and denatured whey protein	Fish oil emulsion was more stable in milk than in yogurt and salad dressing and this difference was attributed to possible interactions or interchange between the food system and the delivery system.	(Let, Jacobsen, & Meyer, 2007)
Gac oil	Milk, yogurt, and cake mix	< 30 µm	20 g in milk and yogurt and 160 g per 414 g of dry cake mix	Whey protein concentrates and gum arabic	Encapsulated gac oil showed better retention of color, β-carotene, and lycopene and low peroxide value during storage.	(Kha, Nguyen, Roach, & Stathopoulos, 2015)
Fish oil/ ɣ-oryzanol	Yogurt	152 nm	3%/0.1%		Fish oil/γ-oryzanol incorporated as a nanoemulsion into yogurt showed closer sensory attribute scores to those of plain yogurt.	(Zhong, Yang, Cao, Liu, & Qin, 2018)
Zeaxanthin	Yogurt	184 and 150 nm	12.5% (v/v)	Tween 80	Zeaxanthin nanoparticles and nanoemulsion incorporation resulted in decreased firmness and viscosity.	(de Campo et al., 2019)
β-Carotene	Yogurt	148.65–162.45 µm	2.5 and 5 g/100 g	Sodium alginate	Carotenoids that were encapsulated greatly increased the yogurt's antioxidant capacity.	(Šeregelj et al., 2021)
Olive fruit polyphenols	Greek and European-style yogurt	–	500 ppm of 20% (w/w) encapsulated polyphenol powder in 10 kg of yogurt	Modified starch	Encapsulated polyphenols did not develop a color change during storage, which was evident in the yogurt with plain polyphenols.	(Petrotos, 2012)
Date palm pollen	Yogurt	–	0.75% (w/v) of milk	Sodium caseinate and soy lecithin	In comparison with other fortified varieties and the control, yogurt enhanced with nanoencapsulated date palm pollen displayed the best texture and stronger radical inhibition.	(El-Kholy, Soliman, & Darwish, 2019)
Rubus ulmifolius Schott flowers phenolics	Yogurt	14 and 88 µm	70 mg of lyophilized microspheres per 125 g of yogurt matrix	Calcium alginate	The encapsulation protected the antiangiogenic ability of the polphenols in the acidic environment of the yogurts compared with free extracts.	(Oliveira et al., 2017)
Echium oil and phytosterols	Yogurt	42 µm	2% (w/w)	Gelatin–arabic gum and gelatin–cashew gum	Compared with yogurt without encapsulated bioactive components, yogurt with microcapsules had better physicochemical properties and increased oxidative stability.	(Comunian et al., 2017)
Agaricus bisporus extracts	Yogurt	11.34 and 13.42 µm	2.5 mg/50 g	Maltodextrin crosslinked with citric acid	Phenolics encapsulated with maltodextrin contributed to the preservation of antiradical activity and overall nutritional properties in yogurt during storage.	(Francisco et al., 2018)
Tocotrienol	Yogurt	–	0.1% (w/v)	Chitosan and alginate	The addition of microcapsules to yogurt reduced changes in texture, color, and viscosity but was	(Tan et al., 2018)

					ineffective in protecting the encapsulated tocotrienols during storage.	
Sour cherry phenolics	Yogurt	276 nm	5% (w/w)	Maltodextrin, lecithin, and chitosan	Liposomal-encapsulated phenolics were protected in the yogurt matrix during storage and especially the spray-dried capsules led to increased total dry solids and reduced syneresis.	(Akgün et al., 2020)
Polyphenols and anthocyanins	Yogurt	–	0.5 g of encapsulated powder in 50 g of yogurt	Maltodextrin	The bioactive compounds encapsulated in yogurt behaved similarly to those not encapsulated in juice.	(Robert et al., 2010)
Rubus ulmifolius hydroalcoholic extract	Yogurt	79–380 μm	40 mg per 20 g	Sodium alginate	Compared with plain yogurt and yogurt with free polyphenols, fortified yogurt with the encapsulated phenolics displayed somewhat increased antioxidant activity over time.	(Martins et al., 2014)
β-Carotene	Fat-free tapioca pudding and yogurt	10.5 μm	0.528 mg of encapsulated β-carotene per 8 g of pudding	Maltodextrin and sodium alginate–chitosan	Both fortified pudding and yogurt matrices significantly decreased the release and micelle incorporation compared with water-dispersible β-carotene.	(Donhowe et al., 2014)
Fish oil	Cream cheese	< 21.2 μm	1.3% (70% fish oil emulsion)	Sodium caseinate, whey protein, milk protein + phospholipids	Addition of fish oil through delivery emulsions changed the microstructure of the cream cheeses and the choice of emulsifier impacted the oxidative stability of the product.	(Horn et al., 2012)
Curcumin	Soft cheese	14 nm	5 %	Tween 20	The cheese with curcumin nanoemulsion showed a better sensory evaluation and uniform distribution of popsity compared to the control.	(Bagale et al. 2023)
Saffron extract	Ricotta cheese	190 nm	0%, 0.125%, 1%, and 2% (w/v)	Soy lecithin	Compared with the control cheese, the cheeses containing encapsulated saffron extract had significantly higher levels of hardness and chewiness.	(Siyar, Motamedzadegan, Mohammadzadeh Milani, & Rashidinejad, 2021)
Polyphenols	Cheese	> 100 μm	–	Gum arabic, mesquite gum, and maltodextrin	Addition of encapsulated and unencapsulated polyphenols showed a significant difference in cheese microstructure, moisture, and ash content.	(Pimentel-González et al., 2015)

Green tea catechins	Low-fat hard cheese	133 nm	0.25% (w/v) of cheese	Soy lecithin	The interaction of catechins with food matrix components was protected by the encapsulation technique, which also protected against degradation and loss of antioxidant activity.	(Ali Rashidinejad, Birch, Sun-Waterhouse, & Everett, 2014)
Fish oil	Processed cheese	0.21 µm	5% of the final product	Sodium caseinate	The incorporation of encapsulated fish oil into processed cheese during processing reduced oxidation of omega-3 long-chain polyunsaturated fatty acids while maintaining the rheological properties of the processed cheese.	(A. Ye, Cui, Taneja, Zhu, & Singh, 2009)
Curcumin	Ice cream	334 nm	0.24% of the final product	Sodium caseinate	CNE incorporated into ice cream withstood the processing conditions, showing an encapsulation efficiency of 93.7%.	(Kumar et al., 2016)
Anthocyanins	Margarine	–	–	Maltodextrin	When compared with margarine containing free anthocyanins, margarine containing encapsulated anthocyanins had higher oxidative stability and melting completion temperature with lower onset crystallization temperature.	(Zaidel, Sahat, Jusoh, & Muhamad, 2014)
Polyphenols	Mayonnaise	90.76–95.35 nm	500 mg per 1 kg	Soy lecithin	Encapsulated polyphenols demonstrated improved phenolic content retention, increased lipid oxidative stability, and reduced changes to the color and sensory properties of mayonnaise.	(Rafiee, Barzegar, Sahari, & Maherani, 2018)
Curcumin	Bread	13.35 nm	20.75 g per 1 kg	Tween 80	CNE incorporated into the bread formulation as the replacement for margarine showed an increase in the total strain and the elasticity of the bread crumb compared with the control bread.	(Bagale et al., 2022)
Oleic acid and garlic phenolics	Bread	110–140 nm	0.65 mL/100 g of dough	Phosphatidyl-choline	When compared with pure garlic phenolics, nanocapsules in the bread formulation retarded liposomal thermal decomposition.	(Pinilla, Thys, & Brandelli, 2019)
Green tea extract	Bread	8–141 µm	2 g per 100 g of wheat flour	Maltodextrin and β-cyclodextrin	The volume and the crumb firmness of the encapsulated green-tea-polyphenols-enriched bread were almost identical to those of the control but had better sensory attributes.	(Pasrija, Ezhilarasi, Indrani, & Anandharamakrishnan, 2015)

Garcinia fruit extract	Bread	20–100 μm	2 g in 100 g of wheat flour	Maltodextrin and whey protein isolate (WPI)	Breads containing microencapsulates had significantly better qualitative characteristics than breads containing water extract. Because of the efficient encapsulation of WPI, bread with WPI encapsulates had significantly higher volume, softer crumb texture, and highly desirable sensory attributes.	(P. Ezhilarasi, Indrani, Jena, & Anandharamakrishnan, 2013)
Green tea extract	Biscuits	500 and 780 nm	2 g/100 g flour	Gelatin and zein	Microparticles proved to be very effective in stabilizing the catechins during thermal treatment.	(Gomez-Estaca, Balaguer, Gavara, & Hernandez-Munoz, 2012)
Beetroot pomace phenolics	Biscuit	–	10.8% of dry matter	Soy protein isolate	Pomace phenolics enhanced some nutritional properties and changed the color of baked goods, particularly when used as encapsulates.	(Hidalgo, Brandolini, Čanadanović-Brunet, Ćetković, & Tumbas Šaponjac, 2018)
Cocoa hull polyphenols	Biscuit	6.4 μm	0.32%	Gum arabic and maltodextrin	The use of maltodextrin for encapsulation resulted in the most stable powder with a total phenolic content that was unaffected by the baking process.	(Valentina A. Papillo et al., 2019)
Polyphenols	Cookies	–	10, 15, 20%	Pumpkin protein isolate	Hardness, color, and sensory attributes of the cookies were significantly impacted by different levels of the fortified encapsulated bioactive compounds.	(Čakarević et al., 2021)
Olive leaf extract	Meat system	0.3–20 μm	100 mg oleuropein/kg	Polyglycerol ester of polyricinoleic acid and sodium caseinate	Improvement of binding properties and texture of the meat system.	(Robert et al., 2019)
Fish oil	Beef burger	–	15% of the fat	–	Increasing encapsulated fish oil inclusions did reduce cooking loss but resulted in greater texture modification compared with controls.	(Keenan et al., 2015)
Cinnamon extract	White and milk chocolate	191 nm	0.5, 1, 1.5, 2% (w/w)	Shellac and xanthan gum	Cinnamon-extract-nanoparticle-containing chocolates showed minor differences in moisture content, hardness, color, and flow behavior, but not in particle size or melting properties.	(Muhammad, Saputro, Rottiers, Van de Walle, & Dewettinck, 2018)
Fish oil + brown seaweed extracts	Granola bars	0.9 μm	5% of the final product	Sodium caseinate and chitosan	The coating material repelled the pro-oxidative ions in the water phase, reducing the interaction with the interface and thus resulting in higher oxidation stability of oils in baked granola bars.	(Hermund et al., 2016)

Fish oil	Energy bars	–	5% of the final product	Sodium caseinate	The caseinate protective layer around fish oil increased the distance between pro-oxidants in the surrounding matrix, which enhanced the oxidative stability of the energy bars.	(Nielsen & Jacobsen, 2009)
Betanin	Gummy candy	36 nm	10% (w/w)	Lecithin	The betanin nanoliposomes reinforced the gel matrix by reducing water activity and enhancing the interaction between gelatin chains, which led to an improvement in the texture of gummy candies in terms of hardness, gumminess, and chewiness.	(Amjadi, Ghorbani, Hamishehkar, & Roufegarinejad, 2018)

2.3.1.1 Beverages

Encapsulation has improved the sensory characteristics of functional beverages, including improved flavor,, better shelf stability, and prolonged or fast flavor release. In addition, the incorporated bioactive ingredients serve to improve the health-promoting properties of the beverages (Ozdal, Yolci-Omeroglu, & Tamer, 2020). Tao et al. (2017) encapsulated steppogenin, a natural flavanone, in a microemulsion to increase its solubility and stability in aqueous liquids and to further investigate its capacity to prevent the oxidation in fresh apple juice. The microemulsion not only enhanced steppogenin's solubility to up to 3000-fold higher than that in water but also significantly inhibited the browning of fresh apple juice. In another investigation, (Istenič et al., 2016) conducted a storage test of free epigallocatechin gallate, and epigallocatechin gallate encapsulated in liposomes, and alginate and chitosan microparticles reinforced with liposomes to investigate the stability of epigallocatechin gallate in a fruit nectar. Compared with the unencapsulated form, both encapsulation techniques had the ability to stabilize epigallocatechin gallate in food products during storage.

2.3.1.2 Dairy-based products

Dairy-product-based food structures can be classified into three main categories: liquid (milk and fermented milk products), semi-solid (yogurt and a few varieties of soft cheese), and solid (mostly cheeses). Since ancient times, they have been the primary source of nutrients such as protein, fat, vitamins, and minerals, making them the most popular and highly consumed products worldwide (Eržen, Kač, & Pravst, 2014; Pereira, 2014; Scholz-Ahrens, Ahrens, & Barth, 2020). This also makes them appropriate vehicles for the addition or modification of a variety of nutrients and health-improving substances. However, the stability and the effective integration of pure bioactive compounds have a detrimental impact on sensory attributes and preservation. Additionally, heat, light, oxygen, an acidic or basic pH, and water can make these bioactive chemicals vulnerable, which leads to undesirable changes in the products (Augustin

& Sanguansri, 2015; Bao et al., 2019; Cifelli, 2021; Raikos & Ranawana, 2017). Encapsulation with a properly chosen coating material can overcome these challenges, with little to no impact on the physicochemical and organoleptic qualities of the product. For example, Moghadam et al. (2019) incorporated nanoencapsulated fish oil consisting of omega-3 fatty acids into a probiotic fermented milk. The nanoencapsulated fish oil not only increased the probiotic bacterial count but also decreased the oxidation of eicosapentaenoic acid and docosahexaenoic acid without negatively affecting the sensory properties of the final product. Similarly, Joung et al. (2016) assessed the radical scavenging activity of a CNE in a low-fat milk. The radical scavenging activity was not significantly affected by the water content, but was significantly increased by the surfactant concentration, indicating that a high surfactant concentration might make it easier for curcumin to dissolve in the oil phase, which would then increase the antioxidant activity. In a different study, the inclusion of both free and encapsulated arjuna herb phenolics had a significant impact on the physicochemical characteristics of the fortified matrix during long-term storage. However, changes in quality characteristics occurred less frequently in the sample containing encapsulated arjuna phenolics than in the other samples, indicating that the encapsulated form was successful in improving the storage stability of dairy drinks (Sawale et al., 2017).

The fundamental steps in the production of fermented dairy products (i.e., cheese and yogurt) include coagulation or gelation of milk proteins. Caseins and whey proteins, the two primary proteins found in milk, can be destabilized by enzymes such as rennet to coagulate the caseins, heat to denature the whey proteins, and acid to coagulate the caseins as well denatured whey proteins. These gelation processes are irreversible because milk protein undergoes rearrangements, fusion, and syneresis during and after gelation (Fagan, O'Callaghan, Mateo, & Dejmek, 2017; Lucey, 2008; Panthi et al., 2019). These structures in a coagulated protein system entrap milk fat as well as related nutrients and bioactive compounds. Tan et al. (2018)

investigated the impact of storage and the yogurt matrix on the stability of tocotrienols encapsulated in chitosan–alginate microcapsules. The texture, color, and viscosity of the yogurt matrix were not significantly altered by the addition of tocotrienol microcapsules, and the tocotrienol microcapsules demonstrated greater resistance to oxidation during heat treatment than the unencapsulated tocotrienols. However, both the heat treatment and the acidity of the yogurt caused the rapid loss of α-tocotrienol in the fabricated microcapsules. Another study used yogurt as a delivery system for liposomal powdered phenolics from sour cherries. Compared with the control yogurt, the spray-dried liposomal powder resulted in an increased total dry solids and an increased water-holding capacity, which reduced syneresis in the fortified yogurt. Moreover, physicochemical stability, which was measured via the total phenolic content, was found to be highest in the yogurt samples that incorporated encapsulated sour cherry phenolics (Akgün et al., 2020). A. A. Ye et al. (2009) evaluated the lipid oxidation, sensory stability, and microstructure of processed cheese enriched with fish oil emulsion. The addition of emulsified fish oil substantially changed the microstructure of the processed cheese, and it was hypothesized that this change in microstructure and the choice of emulsifier for preparing the delivery emulsions contributed to the oxidative stability of the processed cheese.

Green tea catechins and epigallocatechin gallate that were encapsulated in soy lecithin based liposomes were added to low-fat hard cheese (Rashidinejad et al. 2014). During cheese processing, the loaded liposomes were retained in the curd rather than partitioning into the whey. However, the interaction of the catechins with the components of the cheese matrix was protected by the encapsulation, which also protected them against degradation and loss of antioxidant activity. Similarly, grape polyphenols that were encapsulated by multiple emulsions and added to Chihuahua cheese were structurally and physicochemically compared with the control cheese and cheese with free grape polyphenols (Pimentel-González et al., 2015). Even though the inclusion of encapsulated polyphenols had an impact on the

cohesiveness, moisture content, and ash content of the cheese, the encapsulation proved to be more effective at protecting the polyphenols and the cheese displayed physicochemical traits that were comparable with those of traditional cheese.

2.3.1.3 Starch-based foods

Starch is composed of two types of molecule: linear glucose polymer (amylose) and branched polymer (amylopectin) (J. Singh, Dartois, & Kaur, 2010; S. Wang & Copeland, 2013). Different ratios of these two molecules and their orientation within the granules provide starch with considerable variability in functional properties, such as water absorption, swelling, pasting, gelation behavior, and vulnerability to enzymatic degradation (J. Singh et al., 2013; Zhu, 2017).

The starch matrix has been shown to better protect hydrophilic and hydrophobic food ingredients from degradation under high temperature processing compared with lipid and protein food matrices, which undergo degradation (Fathi, Martín, & McClements, 2014; Zhu, 2017); however, the direct addition of bioactive compounds to cooked foods is still not possible, because of their easy thermal degradation/oxidation (Valentina A. Papillo et al., 2019). Additionally, in a complex food system, the manner in which proteins and lipids interact with starch throughout the processing and digestion of meals might alter the quantities of glucose and active ingredients that are released (Y. Lu, Mao, Hou, Miao, & Gao, 2019; J. Singh et al., 2010). To overcome the environmental influence, the encapsulation has shown promising results in protecting the payload. Papillo et al. (2019b) added microencapsulated cocoa husk polyphenols to model biscuits to increase their stability during baking. After baking, the antioxidant activity of all the biscuits was decreased considerably compared with that of the equivalent powder at 0 min. The biscuits containing polyphenol microencapsulated with maltodextrin, which served as a stabilizing agent in preventing the heat-liable polyphenols from

degradation, had the highest total phenolic content and the highest antioxidant activity. In contrast, the biscuits containing extract that was not microencapsulated had little stability. In a different study, the oxidative stability of granola bars supplemented with a multilayered fish oil emulsion was examined in the presence of novel brown-seaweed-based antioxidants. The bars made with the secondary emulsion method produced fewer oxidation products, which could probably be attributed to the thicker interfacial layer, which would act as a barrier to the penetration and diffusion of molecular species that support oxidation in lipids during the baking of granola bars (Hermund et al., 2016).

The integration of bioactive compounds has been proven to have an impact on the structural characteristics of the finished product in addition to the protective effect of encapsulation on the fortified bioactive compound (Delfanian & Sahari, 2020; Tolve, Bianchi, Lomuscio, Sportiello, & Simonato, 2023). For instance, the presence of gluten protein during bread baking gives distinctive viscoelastic properties to the dough, allowing the dough to expand during fermentation while also retaining the majority of the gas inside the dough structure. However, the direct addition of organic acids to the dough can significantly reduce the mixing time and make the dough weaker (X. Lu et al., 2021; Su et al., 2019). P. N. Ezhilarasi et al. (2014) studied the effect of both unencapsulated and microencapsulated Garcinia fruit extract on the quality of bread. The direct addition of the Garcinia fruit extract significantly lowered the volume of the bread because of the presence of hydrooxycitric acid, which directly affected the dough development and ultimately resulted in the poor bread volume. In contrast, microencapsulation improved the resistance of the dough to the effects of acid and assisted in maintaining the volume of the dough at a specific level, producing a bread with a softer crumb texture and better sensory attributes. Even though there is a wealth of information on the use of starch-based delivery methods for bioactive substances, a thorough approach examining the interactions between the starch matrix and the encapsulated bioactive

ingredients is still required. With the appropriate physicochemical properties and controlled release applications, it will be possible to build superior functional products.

2.3.1.4 Meat

The meat industry is paying increased attention to the incorporation of bioactive compounds in order to create various meat products that are both nutritious and of high quality. As well as the successful replacement of synthetic antioxidants and antimicrobials in recent years, meat products incorporating bioactive-loaded oil-in-water emulsions have also demonstrated an improvement in the fat content to fulfil consumer demand (Domínguez, Pateiro, Munekata, McClements, & Lorenzo, 2021; Keenan et al., 2015; Robert et al., 2019). The partial substitution of native saturated animal fat with bioactive-loaded emulsions containing healthier unsaturated fats/lipids from other sources is arguably a healthier option but creates considerable hurdles in terms of texture, lubricity, and mouthfeel in comminuted products (Nacak, Öztürk-Kerimoğlu, Yıldız, Çağındı, & Serdaroğlu, 2021; Nieto & Lorenzo, 2021; Serdaroğlu, Öztürk, & Urgu, 2016). Robert et al. (2019) encapsulated olive leaf extract in a double emulsion and introduced it into a meat system as a fat replacer. Because of the enhanced double emulsion dispersion within the meat matrix, the substitution of pork backfat with the double emulsion greatly improved the binding and textural qualities of the meat system. Additionally, encapsulated olive leaf extract also enhanced the oxidative stability and oleuropein degradation, resulting in meat systems with reduced concentrations of thiobarbituric acid reactive substances and lower peroxide values compared with the control. Another study compared the effects of using encapsulated and unencapsulated fish oil to partially replace the fat in beef burger patties (Keenan et al., 2015). In addition to altering the fatty acid profile, the inclusion of encapsulated fish oil resulted in greater texture modification with reduced cooking loss compared with the control. Despite these published studies, this area of meat-based foods with added encapsulated bioactive compounds has not been extensively investigated. Thus,

further research to explore the in-product interactions of the bioactive compounds with the other elements of the surrounding matrix is required, as this will aid in the development of meat products that are have better consumer acceptance.

2.3.1.5 Lipid/fat-based foods

Lipid/fat-based foods are complex colloidal systems (water-in-oil emulsions) consisting of highly organized, self-assembled microstructures that can generally be affected by various factors such as water content, processing conditions, fat/lipid composition, and storage conditions. These foods have been used as an important template for the delivery of poorly water-soluble bioactive compounds. However, most of the studies to date have focused on the direct fortification of these isolated health-promoting compounds, which undergo various transformations during processing and storage. Encapsulation is an effective method for protecting these chemicals from degradation while also improving their stability in the matrix and ensuring end-product functionality. Zaidel et al. (2014) investigated the storage and stability characteristics of margarine, i.e., a water-in-oil emulsion, containing both nonencapsulated and encapsulated anthocyanins from roselle and red cabbage. When compared with nonencapsulated anthocyanins, margarines containing encapsulated anthocyanins had superior attributes, as evidenced by their high melting completion temperature, low onset crystallization temperature, and higher stability during storage. In another study, (Rafiee et al., 2018) evaluated the effect of phenolic compounds containing nanoliposomes on the oxidative stability, microbial spoilage, and sensory properties of mayonnaise samples during storage. In addition to improving the phenolic component retention, the slower, more gradual release of the polyphenols from the nanoliposomes resulted in significantly fewer alterations in color metrics and sensory characteristics than did the free phenolic compounds.

2.3.2 Behaviour of encapsulated bioactive compounds during digestion

The process of the disintegration and consequent absorption of nutrients in the human gut is directly affected by the microstructural arrangement of the food (Aguilera, 2019; F. Kong & Singh, 2008; Rein, Renouf, Cruz-Hernandez, et al., 2013). The complex structure of the meal is disrupted throughout the digestion process, reducing its particle size by comminution and trituration. Thus, for the design and production of innovative foods with particular targeted behaviors within the body, it is crucial to understand the relative relevance of the gut disintegration processes in relation to the composition and structure of the foods (Acevedo-Fani et al., 2020; Somaratne et al., 2020).

The structural breakdown of foods takes place in the mouth, stomach, and small intestine – the three primary parts of the digestive system. Depending on their physiology/anatomy and the structure of the ingested food, each of these digestive organs contributes differently to the breakdown process. All the fragments of the ingested food, regardless of their texture, and size, are processed in a specific way and vary a lot from one person to another. These variations in fragmentation are influenced by the individual person's behavior and masticatory system, i.e., total ocular area ≈ 214.7 cm^2, including lips, cheeks, palate, tongue, and teeth, number of teeth and chewing cycles, bite force applied by jaw muscular activity, amount of saliva produced to bind the masticated food into a coherent and slippery bolus, and the different phases of the foods including solids, semi-solids, or even liquids (Dengyong Liu, Deng, Sha, Abul Hashem, & Gai, 2017; van der Bilt, 2009). Additionally, factors such as age, gender, ethnic groups, and oral health may vary the process of chewing (J. Chen, 2009). During the chewing process, saliva moistens the food particles and converts them into a slippery bolus that can pass easily down the alimentary canal. Unlike solid foods, liquid foods do not undergo a large amount of chewing and mastication and have comparatively very short residence times in the oral cavity (Minekus et al., 2014). Additionally, the nature of the liquid, i.e., viscosity because of dispersed

particles, the ratio of water to fat, and rheological attributes of emulsions mixed with salivary proteins, significantly influences the structural properties of the bolus (Dengyong Liu et al., 2017; van der Bilt, 2009).

The heterogeneous particles of the bolus are further hydrolyzed by the gastric secretions, which convert the dispersed nutrients into more readily bioavailable forms (Fanbin Kong & Singh, 2009). The rate of digestion of the bolus is determined by the time required for the gastric secretions to reach the walls of the surrounding matrix and free the bioactive compound from the matrix (Fig. 2.2) (Bornhorst & Singh, 2014; Guo, Ye, Singh, & Rousseau, 2020; Lentle & Janssen, 2011). Depending on the starting pH and buffering ability of the food, the pH in the stomach steadily decreases and may vary from one food to another (Acevedo-Fani, Ochoa-Grimaldo, Loveday, & Singh, 2021; Luo, Ye, Wolber, & Singh, 2021; Qazi, Ye, Acevedo-Fani, & Singh, 2021, 2022). Similarly, gastric emptying depends upon the properties of the meal consumed, such as viscosity, density, and particle size. Both propulsion and retropulsion processes, along with the gastric juice, attempt to reduce the size of the food to fine particles and to empty them into the first part of the small intestine, i.e., the duodenum. Additionally, in vivo studies (Egger et al., 2017; Miranda & Pelissier, 1981; Ye et al., 2019) and a dynamic in vitro human gastric simulator (HGS) have shown that the stomach juice and the mechanical grinding can cause liquids such as milk to coagulate, which prolongs their digestion rate and their duration within the stomach (Mulet-Cabero, Mackie, Wilde, Fenelon, & Brodkorb, 2019; Ye, 2021).

Following gastric digestion of the food, its digestion is continued in the small intestine, where the macromolecules are predominantly broken down and water and nutrients are absorbed (Campbell, Berry, & Liang, 2019; C. Li, Yu, Wu, & Chen, 2020). The segmentation and peristaltic movement patterns in the small intestine help to mix the chyme and increase its

interaction with the villous surfaces (Feher, 2017; Nadia, Bronlund, Singh, Singh, & Bornhorst, 2021).

Pancreatic and bile secretions play a pivotal role in the digestion in the small intestine, firstly, by drastically changing the pH of the gastric chyme with bicarbonate ions to pH ≈ 5–7 (N'Goma, Amara, Dridi, Jannin, & Carrière, 2012), and secondly, by enzymatically (i.e., amylase, proteases, peptidases, lipases, and esterase) cleaving the protein, starch, and lipids that remained unhydrolyzed during the gastric phase (H. Singh & Gallier, 2014). Pancreatic proteases are divided into trypsin, chymotrypsin, elastase, and carboxypeptidases A and B. Pancreatic lipase is the major contributor to the digestion of lipids and fats in food (MacFarlane, 2018; Minekus et al., 2014). The pancreatic lipase, colipases, cholesterol esterase, phospholipase, etc. catalyze the mono- or diglycerides, fatty acids, and cholesterol. Similarly, pancreatic α-amylase hydrolyzes the 1-4 α linkages in starch (Nadia et al., 2021; Patricia & Dhamoon, 2019). Another major factor in intestinal digestion is the bile salts produced by the liver and stored in the gall bladder. They are rigid, biological surfactants that are synthesized from cholesterol. Their major function is to reduce the surface tension and to conjugate with the products of lipolysis, i.e., phospholipids and monoglycerides, resulting in emulsification, the formation of a cylindrical disk called a micelle, and its transportation across the brush border membrane (Salvia-Trujillo et al., 2017; Sarkar, Ye, & Singh, 2016; Vítek & Haluzík, 2016). Following digestion in the small intestine, the undigested material, such as dietary fiber, enters the colon, where it is fermented by the residing microbiota (Wong et al. 2012). Thus, the unique pattern of the disintegration of food during digestion and the release of fortified or enriched bioactive compounds deserves special attention in order to understand and design a therapeutic food matrix that may contribute maximum health benefits. Table 2.2 lists the in vitro digestion studies of several encapsulated bioactive compounds that were enriched into

real/model food matrices. In the following sections, we give more detail about a few of these examples.

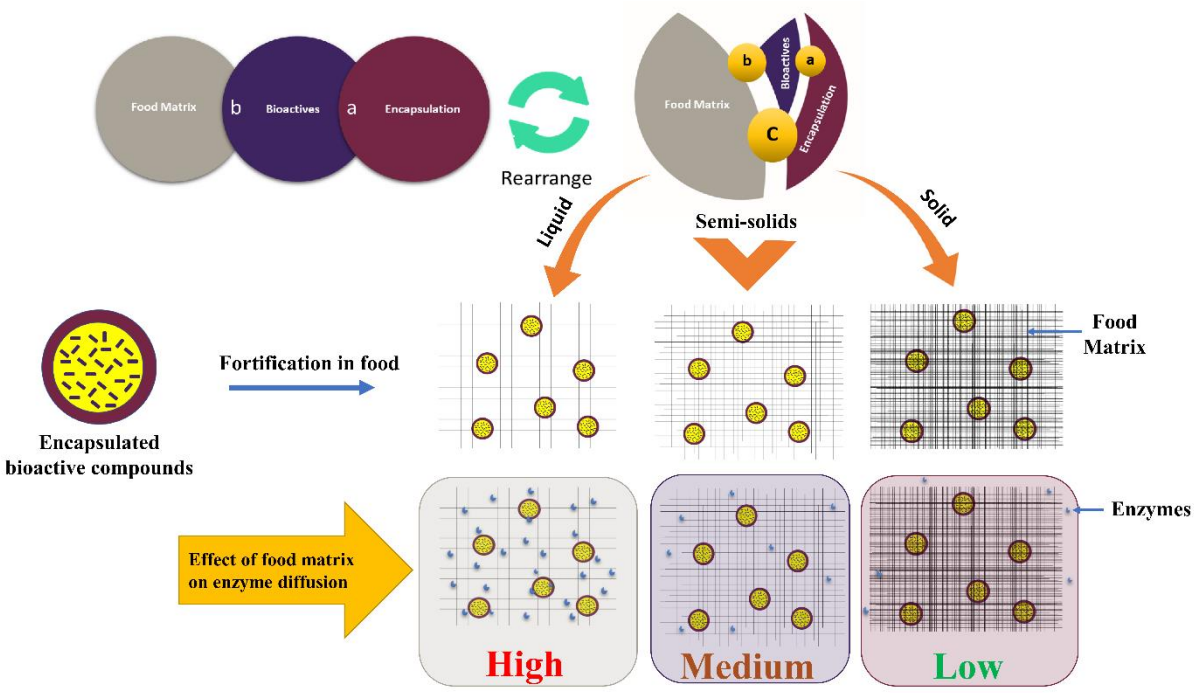

Fig. 2. 2 Effect of different types of food matrix on the penetration of digestive enzymes.

Table 2. 2 Summary of in vitro digestion studies of different encapsulated bioactive compounds that were fortified into real/model food matrices.

Encapsulated bioactive compound	Fortified food matrix	Size	Fortification level	Emulsifier	Outcomes	Reference
Isoflavones	Isotonic drink	2–10 μm	250 mg	Inulin and maltodextrin	Isoflavone levels in all samples were found to have significantly decreased during the gastric phase and were dependent on the food matrix and the pH prevailing in the process.	(Wyspiańska, Kucharska, Sokół-Łętowska, & Kolniak-Ostek, 2019)
Curcumin	Model beverage	150 nm	38 μg/mL	Lecithin and Tween 80	When compared with beverages with free curcumin, the integration of lipid-based nanodelivery systems increased curcumin's bioaccessibility while showing that the components present in the beverage affected lipid digestion and mixed micelle formation.	(Gonçalves, Vicente, & Pinheiro, 2023)
Mangiferin	Milk	135 nm	2%, 4%, 6%, and 8%	β-Lactoglobulin and chitosan	Addition of mangiferin nanoparticles slowed the glycemic index of milk because of suggested hydrophobic bonds between mangiferin and carbohydrates and proteins.	(Samadarsi, Mishra, & Dutta, 2020)
Curcumin	Milk systems	187 nm	0.03% of lipid fraction	Sodium caseinate	High-heated milk showed faster disintegration in the gastric phase and higher curcumin release and bioaccessibility compared with medium- and low-heated curcumin-nanoemulsion-fortified milk systems.	(Qazi et al., 2022)
Coenzyme Q10	High protein beverage	≈ 200 nm	1250 g of nanoemulsion per 5 kg batch	Whey protein isolate, lecithin, or modified starch	In comparison with a coenzyme Q10 nanoemulsion and coenzyme Q10 dissolved in oil, a high-protein beverage as a food system increased the lipolytic activity, which improved the absorption of an enriched coenzyme-Q10-loaded nanoemulsion.	(Niu et al., 2020)
β-Carotene	Fat-free yogurt	10.5 μm	0.528 mg encapsulated β-carotene per 8 g of yogurt	Maltodextrin and sodium alginate–chitosan	The fortified yogurt matrix and the encapsulation method significantly decreased the release and micelle incorporation.	(Donhowe et al. 2014)

Zeaxanthin	Yogurt	184 and 150 nm	12.5% (v/v)	Tween 80	The zeaxanthin bioaccessibility was found to be lower in both fortified with zeaxanthin nanoparticle and nanoemulsion, and this was connected to the wall material and the food matrix.	de Campo et al. (2019)
Curcumin	Yogurt	64–102 µm	1.6 mg per 100 mL of yogurt	Whey protein isolate	The yogurt matrix slowed down the release of curcumin, which was linked with the composition, pH profile, and viscosity of the emptying digesta.	(Q. Ye et al., 2021)
Cinnamon leaf extract	Yogurt	–	0.8% (w/v)	Agar	The beneficial compounds that can stop protein denaturation were unable to stabilize the proteins before the yogurt was digested because of the physical entrapment of cinnamon leaf extract in the agar and yogurt matrix.	(Tang, Cham, Hou, & Deng, 2022)
Rutin	Yogurt	–	2.5 mg/g	Sodium caseinate	The strong interaction between the encapsulated rutin and the yogurt matrix protected the rutin during gastrointestinal digestion and increased its solubility in the small intestine.	(Acevedo-Fani et al., 2021)
Algae oil	Strawberry yogurt	258 nm	4.29 g of nanoemulsion per 100 g of yogurt	Soy lecithin	Yogurt enriched with a nanoemulsion of algae oil offered an enhanced rate and extent of absorption for omega-3, the bulk oil.	(Lane et al. 2014)
β-Carotene	Whole milk, oat meal, and whole milk–oatmeal	560 nm	0.1%	Tween 80	Microstructural changes in the meal matrices because of macromolecule interactions influenced the lipid emptying rate, which was further linked with the retention of β-carotene during gastrointestinal digestion.	(Molet-Rodríguez, Torcello-Gómez, Salvia-Trujillo, Martín-Belloso, & Mackie, 2023)
Capsaicinoids	Whey protein emulsion gels	0.5 µm	0.02 wt%	Whey protein isolates	The matrices of the gels affected the characteristics of the gastric digesta, which in turn influnced the lipolysis in the intestinal digestion and the bioaccessibility of the incorporated capsaicinoid.	(Luo et al., 2021)

Curcumin	Yogurt and cheese gels	187 nm	0.03% of lipid fraction	Sodium caseinate	The yogurt-like gel had a higher bioaccessibliity than the cheese-like gel and this change was linked with the structural changes of the gels in the stomach affecting the composition of the gastric digesta, which changed the free fatty acid release and the curcumin bioaccessibility in the small intestine.	(Qazi et al., 2021)
Curcuminoids	Yogurt and rice	1–15 μm	0.05%	Gum arabic and maltodextrin	Fortified rice showed higher curcuminoid bioaccessibility than yogurt and was also 2- and 1.5-times more bioaccessible than the ingredient alone.	(Valentina Azzurra Papillo et al., 2019)
Tuna oil	Orange juice, yogurt, cereal bar	–	0.8 g of microcapsules (25% oil loaded) per 38.2 g of yogurt	Sodium caseinate, glucose, and hylon VII	Microencapsulated-tuna-oil-fortifed cereal bars had higher digestion of polyunsaturated fatty acids because of the presence of higher dietary fiber content compared with the other two food matrices.	(Shen et al., 2011)
β-Carotene	Almond butter	–	1.8 mg/g	Whey protein isolate, sodium alginate, and chitosan	Despite the higher recovery of β-carotene in the small intestine, the incorporation into the micelle fraction was much lower for the encapsulated system in the food matrix, which was associated with the influence of the coating material.	(Roman, Burri, & Singh, 2012)
β-Carotene	Murumuru butter	35 nm	0.06 g/100 g	Span 80 and Cremophor RH40	The amount of fatty acid release as a result of lipolysis in each gut compartment was linked with the bioaccessibility of β-carotene.	(Gomes et al., 2019)
Green tea catechins	Hard low-fat cheese	165 nm	125, 250, and 500 mg/kg	Soy lecithin	Catechin recovery was much higher for the 500 mg/kg catechin-enriched cheese than for the other two fortified cheeses. The increased breakdown of the protein–catechin association by digestive enzymes in the cheese containing 500 mg/kg of enriched catechin resulted in more unbound catechin available under the same digestion conditions.	(A. Rashidinejad, Birch, Sun-Waterhouse, & Everett, 2015)

Curcumin	Starch gels	187 nm	0.03% of lipid fraction	Sodium caseinate	The initial structures of the starch gels and further changes in the stomach significantly impacted the release of entrapped CNE into the intestine.	(Qazi et al. 2022)
β-Carotene	Rice starch hydrogels	0.26 μm	0.3% (w/w) of lipid fraction	Whey protein isolate	Emulsion-filled hydrogels had faster digestion of lipid droplets than conventional emulsions, which subsequently resulted in higher bioaccessibility of β-carotene.	(Mun, Kim, & McClements, 2015)
Beetroot juice polyphenols	Cookies	–	10, 15, 20%	Pumpkin protein isolate	The gastrointestinal digestion produced novel peptides that improved the bioactive properties of enriched products via synergistic action with active compounds from beetroot juice.	(Čakarević et al., 2021)
Curcuminoids	Bread	–	3.0 mmol per portion	Ethocel 100 and hydrogenated vegetable oil	The bread matrix lowered the concentration of curcuminoids in the serum despite the encapsulation preventing the biotransformation of curcuminoids.	(Vitaglione et al., 2012)
Curcumin	Gellified fish product	0.5 μm	0.5 g/100 g of mince	Gelatin	Curcumin bioaccessibility in fish gels incorporated with curcumin–gelatin microparticles was comparable with that of commercial curcumin-loaded fish gels; however, complexation of free curcumin with water-soluble protein in the fish gel decreased the antioxidant activity.	(Gómez-Estaca, Gavara, & Hernández-Muñoz, 2015)

2.3.2.1 Digestion of liquid foods

Healthy dairy- and plant-based beverages, sports and energy drinks, fermented beverages, and many more comparable items are always in high demand from consumers. To cater for the increasing consumer demand for healthier beverages, food industry is continually developing various fortified beverages that are stable, have good shelf life, and are appealing to consumers (Ahmad & Ahmed, 2019; Ansari & Kumar, 2012; Puiggròs et al., 2017).

As liquid foods generally lack structures that need to be broken down, they empty from the stomach exponentially without a lag phase, thus resulting in a minimum matrix effect (Siegel et al., 1988; Ye, 2021). The alterations in liquid foods are mostly brought about by interactions between the constituent parts of the food and bodily fluids, or between the constituent parts when they are in a gastrointestinal environment (David Julian McClements, Decker, Park, & Weiss, 2008; H. Singh & Acevedo-Fani, 2022). A simple liquid matrix, such as isotonic beverages, has a set of easily digestible carbohydrates and a well-balanced mineral composition, is a suitable carrier for supplementing functional ingredients. Wyspiańska et al. (2019) designed an isotonic drink that was fortified with inulin- or maltodextrin-microencapsulated soybean isoflavone to investigate the impact of the microencapsulation process on the stability and antioxidant activity of isoflavones during a simulated in vitro gastrointestinal digestion. The isotonic beverage had no matrix effect on the delivery of the microcapsules. Although using inulin as a carrier resulted in capsules with a superior surface structure and better storage stability, the isoflavone levels in all samples were found to be significantly affected by the acidic and basic environments in the gut. To circumvent environmental impacts that such fortified beverages experience during digestion, a number of delivery methods have been suggested. To evaluate the release behavior, a model beverage was prepared by combining various curcumin-loaded lipid-based nanodelivery systems. The CNE showed increased instability immediately after incorporation into the beverage, whereas the

beverage stability relative to the pH remained unaffected in the presence of solid lipid nanoparticles and nanostructured lipid carriers. Furthermore, the beverage containing solid lipid nanoparticles had higher curcumin bioaccessibility than the other beverages, implying that lipid digestion products from liquid lipids bound with the salts in the beverage, preventing the formation of mixed micelles (Gonçalves et al., 2023).

In contrast, because of their instability under gastric conditions, e.g., creaming of oil/fat, protein aggregation, and the high viscosity of carbohydrates, some fortified liquid foods can remain in the stomach for longer periods of time (Araiza-Calahorra, Glover, Akhtar, & Sarkar, 2020; Dian Liu, Parker, Curcic, Kozerke, & Steingoetter, 2016; Niu et al., 2020; Steingoetter et al., 2017; X. Wang, Ye, Dave, & Singh, 2021; Ye, 2021). Liquid food such as milk have unique digestion kinetics because of their protein content, with completely distinctive properties. The coagulation of caseins in the stomach, driven by pepsin, and the acidic environment lead to a protracted gastric digestion, resulting in slower release of the fortified ingredients (Hodgkinson, Wallace, Boggs, Broadhurst, & Prosser, 2018; Mudgil & Barak, 2019; Qazi et al., 2022). In contrast, whey proteins are digested and absorbed in the intestine more quickly. Recent research has demonstrated that altering the processing conditions, i.e., homogenization, heating, etc., can vary the interactions between the milk proteins and the other constituents, hence changing the kinetics of milk digestion (Egger et al., 2017; Huppertz & Chia, 2021; Mulet-Cabero, Mackie, Brodkorb, & Wilde, 2020; Mulet-Cabero et al., 2019; Ye, Cui, Dalgleish, & Singh, 2017; Ye et al., 2019). The gastrointestinal digestion of recombined milk systems fortified with CNE was investigated using an HGS (Qazi et al., 2022). The milk systems reconstituted from low-heat, medium-heat, and high-heat skim milk powders had significantly different disintegration behaviors in the stomach because of the different degrees of casein/whey protein complexes formed during the processing of the milk. In contrast to the low-heat and medium-heat milk proteins, the high-heat-treated milk proteins produced a loose

and soft curd under dynamic gastric conditions, which led to a quicker outflow of the curd fragments and entrapped CNE. Thus, both the release of free fatty acids and the bioaccessibility of curcumin during intestinal digestion were affected by these variations in the gastric digesta profiles. Milk proteins have high surface activity and can partially or completely displace low-surface-active emulsifiers from the surface of emulsion droplets, making oil droplets in the beverage more susceptible to lipase action, which can accelerate the formation of mixed micelles in the small intestine. Niu et al. (2020) showed that, when used as a food system, a high-protein beverage improved the absorption of an enriched coenzyme-Q10-loaded nanoemulsion by boosting the lipolytic activity, in comparison with a coenzyme-Q10 nanoemulsion and coenzyme Q10 dissolved in oil. Whey protein and milk protein concentrates were effective in replacing the modified starch used to encapsulate the coenzyme-Q10, making them more susceptible to lipolysis, resulting in increased free fatty acid release and mixed micelle formation during the intestinal phase. Likewise, beverages made by structurally modifying milk proteins during fermentation, such as drinking yogurt, have been shown to alter the digestion kinetics and the release of entrapped phenolics in the gastrointestinal tract (Altin, Gültekin-Özgüven, & Ozcelik, 2018).

In recent years, there has been a surge in consumer interest in replacing dairy milk with plant-based milks in the diet, demonstrating several health benefits to health-conscious consumers (Fructuoso et al., 2021; David Julian McClements & Grossmann, 2021; Sethi, Tyagi, & Anurag, 2016). Typically, plant-based milks are produced utilizing size-reduction techniques that entail mechanical, chemical, or enzymatic breakdown of the original plant tissue structure (David Julian McClements & Grossmann, 2021; Reyes-Jurado et al., 2021). However, they differ greatly from dairy-based milk systems in terms of their protein structures and interactions with fortified bioactive chemicals during processing and digestion (Fructuoso et al., 2021). Very few studies that have evaluated fortified plant-based milk systems are

available. B. Zheng, Zhang, Peng, & McClements (2019) compared the efficacy of curcumin crystals dispersed in water (control) with three delivery systems produced using the pH-shift method: curcumin nanocrystals; curcumin-loaded nanoemulsions; and curcumin-loaded soy oil bodies (commercial soymilk). The curcumin-loaded nanoemulsion and the soymilk had a homogeneous appearance and good stability. However, there were noticeable differences in terms of aggregation during the gastrointestinal digestion. In particular, the soymilk was considerably more prone to aggregation in the stomach than the nanoemulsions, which appeared to be more prone to aggregation in the mouth. However, by the end of the digestion, both systems produced curcumin that was relatively stable and bioaccessible. In contrast, curcumin nanocrystals had low bioaccessibility because there were fewer mixed micelles to solubilize the curcumin molecules. Similarly, B. Zheng, Zhou, and McClements (2021) encapsulated curcumin in the oil bodies of plant-based milk analogs (coconut, cashew, almond, and oat milks) using the same pH-driven method. Overall, the lipids in the plant-based milk were digested reasonably quickly during the first 20 min of the intestinal phase but more slowly thereafter. These differences were attributed to the different compositions and structures of the lipids. Furthermore, the concentration of curcumin in the mixed micelle phase was much higher in the plant-based milks than in the control. It is interesting to note that, regardless of the lipid makeup of the oil bodies, the bioaccessibility of the curcumin was very consistent across all the plant-based milks. Recent research utilizing the dynamic gastric model, i.e., the HGS, has demonstrated that different plant-based milk systems go through various physicochemical changes in the gastric compartment (X. Wang et al., 2021; X. Wang, Ye, Dave, & Singh, 2022; X. Wang, Ye, & Singh, 2020). These changes have been shown to have a significant impact on the gastric emptying of nutrients in the small intestine, which can further influence the bioaccessibility of fortified bioactive compounds. The two studies that were presented earlier used a static approach to in-vitro digestion, ignoring the dynamism that occurs in the actual

gut. Therefore, in the future, thorough in vitro and in vivo studies will be needed to understand how plant-based milk matrices affect bioactive delivery.

2.3.2.2 Digestion of fortified semi-solid food matrices

The viscoelastic behavior of semi-solid matrices is substantially greater than that of liquid matrices, and semi-solid matrices contain a sophisticated biopolymer network that can hold a lot of water (Aguilera, 2019; Alsanei, Chen, & Ding, 2015; Devezeaux de Lavergne, van de Velde, van Boekel, & Stieger, 2015). Assemblies made during processing frequently contain fortified elements, which must be released during digestion for them to be further absorbed in the gut (Augustin & Sanguansri, 2015; Dupont et al., 2015; Parada & Aguilera, 2007). Additionally, these food structures, defined during processing, undergo further structural reorganization during digestion, which impacts on the release of fortified bioactive compounds from the food matrix (Mao, Roos, Biliaderis, & Miao, 2017; Qazi et al., 2021). Semi-solid foods, as opposed to liquid foods, spend a longer time in the oral cavity, where they first undergo transformation during mastication and salivation. Increased surface exposure during mastication as a result of increased mouth fragmentation increases the likelihood that bioactive substances that were previously contained will be released. Meanwhile, the salivary secretion also lubricates and wets the food after it has been chewed, creating a cohesive bolus that is ready for swallowing (J. Chen, 2009; Minekus et al., 2014; Mun & McClements, 2017). Apart from its role in bolus formation, saliva contains various proteins, enzymes, and electrolytes, which play a significant role in the emulsification and disintegration of food assemblies. Both in vitro and in vivo trials to understand the oral breakdown of semi-solid foods into small particles have been conducted. Luo, Ye, Wolber, and Singh (2019) investigated the breakdown behavior in the mouth of capsaicinoid-containing whey protein emulsion gel structures; 18 human subjects chewed the gels, i.e., soft/elastic gel, semi-solid gel, and hard/brittle gel. The bioactive diffusivity was higher in the soft and semi-solid gels, as they went through a greater

degree of fragmentation because of their loose structures. (Luo et al., 2021) extended this work by subjecting the whey protein soft and hard emulsion gels to in vitro gastrointestinal digestion to evaluate the influence of the gel structures on the bioaccessibility of capsaicinoids. The hard gel had lower levels of lipid digestion and disintegrated more slowly than the soft gel because of the larger gastric particles and oil droplet sizes and the increased fat content in the digesta. It was found that the degree of lipid digestion was positively linked with the bioaccessibility of the capsaicinoids.

As previously discussed, liquid milk undergoes significant modifications during the gastric phase by forming a curd, which influences the release of fortified bioactive compounds; however, semi-solid dairy gel matrices such as yogurt and cheese, which are formed by the acid and rennet coagulation of milk proteins during processing, can alter the digestion kinetics and nutrient release in the gastrointestinal cavity. Our recent study investigated the in vitro digestion of yogurt- and cheese-like model gels that were fortified with CNE (Qazi et al., 2021). Although these gels had similar rheological and compositional profiles, their disintegration behaviors during dynamic gastric digestion had a significant impact on gastric emptying. After 240 min, all the curd particles from the acid-coagulated gel had disintegrated and none remained inside the gastric chamber. In contrast, the curd particles from the rennet-coagulated gel were rebuilt into a dense protein network under the influence of the gastric fluids and the gastric chamber was filled with numerous compact structured clots by 240 min (Fig. 2.3). These alterations in the curd structures and gastric emptying rates during the gastric phase had an effect on the compositional profile of the digesta, which changed how the oil droplets were delivered and digested. This, in turn, had an effect on the bioaccessibility of the associated lipophilic curcumin during the intestinal phase.

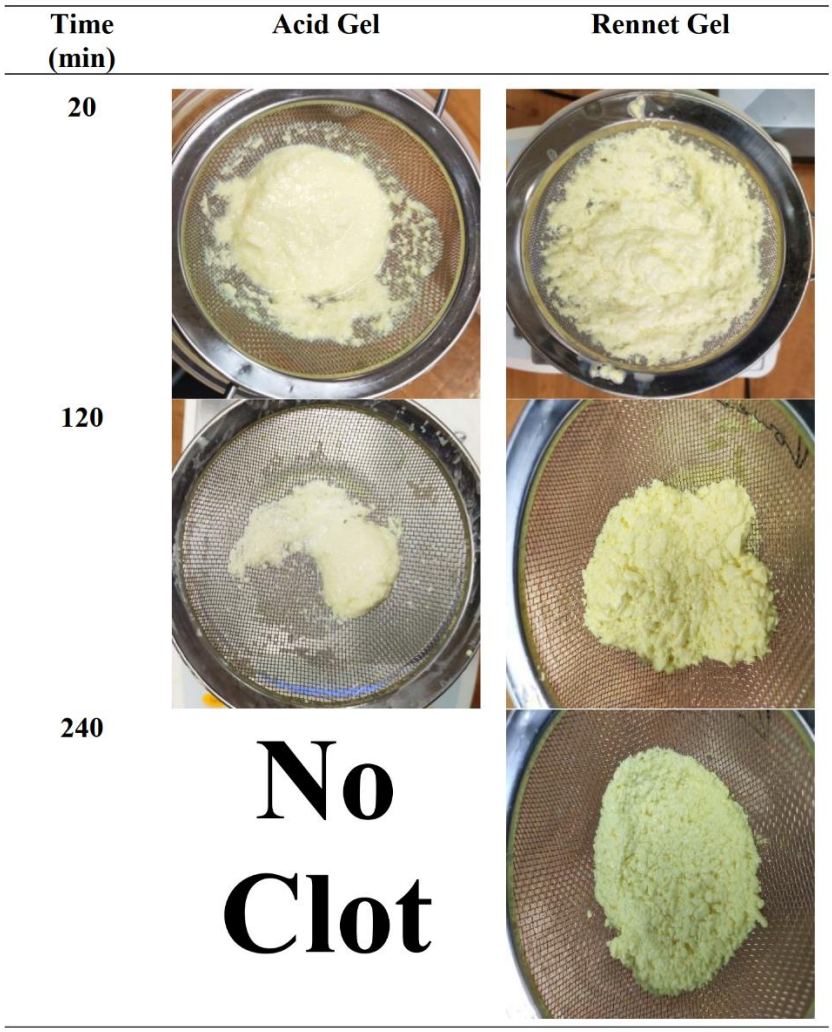

Fig. 2. 3 Images of curds formed by acid and rennet gels within the gastric chamber at selected time points [adapted from Qazi et al. (2021)].

The release and delivery of these bioactive compounds can also be changed by fortifying them in various food matrices. Using a protein-rich food (yogurt) and a carbohydrate-rich food (rice), Papillo et al. (2019a) studied the gastrointestinal absorption of microencapsulated curcuminoids coated with gum arabic/maltodextrin. The gastric degradation of curcuminoids in yogurt was less than that in rice, but the bioaccessible fraction of curcuminoids was much higher in the presence of the rice matrix compared with the yogurt matrix. Similarly, by combining two or more food elements, these food matrices can be made more complex. Another study investigated the digestion dynamics of a stirred yoghurt matrix enriched with

the flavonoid rutin, as well as how interactions between the food matrix and rutin influenced the flavonoid's release and bioaccessibility throughout digestion (Acevedo-Fani et al., 2021). The results showed in comparison to co-digestion of an unfortified yoghurt with a rutin vegetable capsule, fortification of the yoghurt with a casein–rutin co-precipitate improved rutin protection and solubility during gastrointestinal digestion. Molet-Rodríguez et al. (2023) investigated the effects of whole milk, oatmeal, and whole milk–oatmeal containing β-carotene emulsions on the rate at which the stomach emptied, the digestibility of the lipids, and the retention of β-carotene. Changes in the microstructure of the meal matrices brought on by interactions between macromolecules had an impact on the rate of lipid emptying. Both the whole milk–oatmeal and the oatmeal had delayed lipid emptying, which was probably caused by the presence of β-glucan, which increases viscosity. Both the amount of fat emptied at each time point and the retention of β-carotene were linked by the in vitro small intestinal digestion. Furthermore, the introduction of oil-in-water emulsions into the complex meals enhanced the retention of β-carotene during the in vitro small intestinal digestion, leading to speculation that milk and oat flake components may prevent β-carotene from degrading during transit in the gut.

Vegetable butters as a potential matrix for the delivery of encapsulated bioactive compounds have also been explored. Roman et al. (2012) used in vitro digestion models, i.e. a static shaking water bath and an HGS, to study the release and bioaccessibility of β-carotene from fortified almond butter. β-Carotene oil (oil) and whey protein isolate–alginate–chitosan capsules (capsule) containing β-carotene oil were studied. In comparison with the shaking water bath model, peristalsis in the HGS model resulted in a greater release of β-carotene from the almond butter enriched with oil. In contrast, during intestinal digestion, more β-carotene was released from the almond butter enriched with capsules. However, more β-carotene was found in the micelle fraction of the almond butter that had been fortified with oil, pointing to

the potential role of the coating material in preventing the β-carotene in the fortified almond butter from being absorbed into the body.

Despite several studies, many untested semi-solid food matrices must be investigated in the future if they are to be potentially employed for the delivery of these bioactive compounds.

2.3.2.3 Digestion of fortified solid food matrices

Natural and processed solid foods vary greatly in their structure and texture and these properties have a significant impact on the release of nutrients and active ingredients in the gut. Solid food matrices are usually low-moisture, semi-crystalline or crystalline structures. It is thought that the rate at which nutrients can dissolve into a solution for absorption is determined by how quickly the solid food matrices undergo disintegration, when the food particulates break into small fragments, allowing the nutrients that are held therein to dissolve into the gastric fluids (F. Kong & Singh, 2008). Solid food begins to break down in the mouth during mastication, when saliva containing amylase is combined with the food to create a swallowable bolus that is then transported into the stomach by the esophagus. Compared with oral mastication, the gastric phase has greater complexity because of influencing factors such as fed/fast state, gastric acid, enzymatic reactions, and hydrodynamic and mechanical forces. These factors have been shown to significantly affect the restructuring of the food matrix, which further plays a major role in the release and bioavailability of active ingredients from food in the small intestine (Acevedo-Fani et al., 2020; Acevedo-Fani & Singh, 2021; Somaratne et al., 2020; Ye et al., 2019).

Čakarević et al. (2021) assessed the physicochemical and sensory properties of cookies fortified with pumpkin-protein-isolate-encapsulated beetroot juice polyphenols at three different levels, i.e., 10%, 15%, and 20%. The addition of the encapsulate increased the overall phenolic and betalain content and significantly improved the stability during storage. After

gastrointestinal digestion, new peptides were created, which, in combination with the active ingredients in the beetroot juice, improved the bioactive properties of the enriched products. Mun, Kim, and McClements (2015) investigated the influence of rice starch hydrogels on the bioaccessibility of emulsified-lipid-solubilized β-carotene. To evaluate the bioaccessibility of β-carotene, the rice starch hydrogels loaded with β-carotene emulsion were compared with unencapsulated β-carotene-loaded starch gels and emulsions. Their study showed greater bioaccessibility of encapsulated β-carotene in the hydrogels compared with the other two systems, which was attributed to the protective effect provided by the surrounding hydrogels against aggregation of the lipid droplets during digestion. However, the composition of these gels could have altered the release behavior, ultimately altering the lipid digestibility. Mun et al. (2016) extended this work by studying the influence of methylcellulose (0–0.2%) on the digestion of rice starch hydrogels loaded with encapsulated β-carotene. In this case, the lipid digestion and the bioaccessibility of β-carotene decreased with increasing concentration of the indigestible polysaccharide (methylcellulose). It is interesting to note that most of the research carried out on the digestion of starch gels has been conducted using static models of in vitro digestion, which do not provide detailed information regarding the behavior of the gels in the stomach and how this affects the bioaccessibility of the bioactive compounds. In a recent study, curcumin-nanoemulsion-loaded corn starch gels made from waxy, native, and high amylose corn starches were examined in detail for their microstructure, physicochemical characteristics, and in vitro gastrointestinal digestion (Qazi et al. 2023). The addition of CNE to the gels significantly changed their initial physicochemical characteristics. In the dynamic gastric phase, the breakdown and the emptying from the stomach of the waxy gel were slowed down, despite its higher amylopectin content, because of its higher adhesive nature, which trapped the majority of the nanoemulsified oil droplets inside the gel fragments. The different rates of starch hydrolysis, the release of free fatty acids, and the related bioaccessible percentage of

curcumin were further linked to this heterogeneity in the compositional and structural profiles of the gastric digesta. In another study, Gómez-Estaca et al. (2015) investigated the bioaccessibility of curcumin after subjecting fish gels containing encapsulated curcumin microparticles to an in vitro gastrointestinal digestion. When applied to a gelatinized fish product, the bioaccessibility and the antioxidant activity of the gelatin-encapsulated curcumin were reduced, indicating that curcumin may be able to form more stable complexes with some digested water-insoluble fish proteins that would lower these characteristics.

2.4. Conclusions and future outlook

Consumer interest in functional foods is increasing because they offer supplement-level concentrations of health-promoting substances. However, despite this increasing interest, few efforts have been made to integrate encapsulated bioactive compounds into actual or model food systems; little in vitro and in vivo research has been carried out to assess their effectiveness after oral administration. The food matrix is a key component that, in most cases, not only relates to a spatial physical domain that holds, interacts with, or confers specific functionalities to supplemented bioactive compounds during processing, but also controls their release in the gastrointestinal system. The intricate processing and preservation procedures can affect not only where bioactive chemicals are absorbed but also how well they interact physicochemically with other dietary components. These modifications to these matrices cause distinctive disintegration patterns under dynamic digestion conditions, which eventually affect how fortified bioactive compounds are released and absorbed in the gut. Several types of food matrix, such as dairy- and starch-based food systems, have been shown to have a longer residence time in the stomach, which alters the composition and the emptying pattern of the gastric digesta into the small intestine. The microstructure and the composition of the digesta

that is expelled from the stomach is linked to the release of nutrients and bioactive substances. Therefore, in order to properly regulate the release of and eventually increase the bioavailability of the bioactive compounds, it is crucial that future studies concentrate on creating functional foods with precise engineering of food structures in real foods.

Statement of contribution (DCR 16 forms)

MASSEY UNIVERSITY
TE KUNENGA KI PŪREHUROA
UNIVERSITY OF NEW ZEALAND

GRADUATE RESEARCH SCHOOL

STATEMENT OF CONTRIBUTION
DOCTORATE WITH PUBLICATIONS/MANUSCRIPTS

We, the student and the student's main supervisor, certify that all co-authors have consented to their work being included in the thesis and they have accepted the student's contribution as indicated below in the Statement of Originality.

Student name:	Haroon Jamshaid Qazi
Name and title of main supervisor:	Aiqian Ye / Professor
In which chapter is the manuscript/published work?	Chapter 3

Describe the contribution that the student and members of the supervisory team have made to the manuscript/published work:[1]

Haroon Jamshaid Qazi: Conceptualization, Methodology, Validation, Investigation, Formal analysis, Data curation, Writing – original draft, Visualization.
Aiqian Ye: Conceptualization, Methodology, Resources, Writing – review & editing, Project administration, Supervision, Funding acquisition.
Alejandra Acevedo-Fani: Writing – review & editing, Supervision.
Harjinder Singh: Conceptualization, Writing – review & editing, Supervision.

Please select one of the following three options:

- (●) The manuscript/published work is published or in press

  Please provide the full reference of the research output:

  Qazi, H. J., Ye, A., Acevedo-Fani, A., & Singh, H. (2022). Impact of Recombined Milk Systems on Gastrointestinal Fate of Curcumin Nanoemulsion. Frontiers in Nutrition, 9.

- ( ) The manuscript is currently under review for publication

  Please provide the name of the journal:

- ( ) It is intended that the manuscript will be published, but it has not yet been submitted to a journal

Student's signature:	Haroon Jamshaid Qazi — Digitally signed by Haroon Jamshaid Qazi, DN: cn=Haroon Jamshaid Qazi, c=NZ, ou=Riddet Institute, email=h.j.qazi@massey.ac.nz, Date: 2023.06.20 11:10:29 +12'00'	Main supervisor's signature:	Aiqian Ye — Digitally signed by Aiqian Ye, DN: cn=Aiqian Ye, c=NZ, o=Massey University, ou=SF&AT, email=a.m.ye@massey.ac.nz, Date: 2023.06.20 12:12:08 +12'00'

This form should be placed at the beginning of each relevant thesis chapter.

[1] Refer to the Massey University Publishing and Authorship guidelines (OneMassey for staff, Stream for students) and/ or Contributor Roles Taxonomy (CRediT) guidelines for guidance.

Chapter 3: Impact of recombined milk systems on gastrointestinal fate of curcumin nanoemulsion

3.1 Abstract

Milk powder is an important ingredient in various foods and paediatric formulations. The textural and digestion properties of the formulations depend on the preheat treatment of the milk powder during manufacture. Thus, it is interesting to know how these modifications can influence on the release of fortified bioactive compounds during digestion with a milk matrix. In this study, a CNE was incorporated into milks reconstituted from low-heat, medium-heat and high-heat skim milk powders and the milks were subjected to semi dynamic in vitro digestion. All the recombined milk systems formed a curd under gastric conditions, which reduced the gastric emptying of protein and curcumin-loaded oil droplets. Because of the formation of heat-induced casein/whey protein complexes, the open fragmented curd formed by the high-heat-treated reconstituted powder resulted in higher protein and oil droplet emptying to the intestine and higher curcumin bioaccessibility. This study provides better understanding on how protein ingredients can govern the fate of added health-promoting compounds during digestion.

3.2 Introduction

Defatted dry milk, also known as skim milk powder (SMP), is a major trade item in the food industry because of its ease of transportation, handling and processing, its long shelf life (18–24 months) and its use in a wide range of products (Martin, Williams, & Dunstan, 2007; Sharma, Jana, & Chavan, 2012; H. Singh, 2007). The manufacture of SMP involves the following steps: fat separation, preheat treatment, concentration and spray drying. The desirable functional properties, such as flavour, colour, gelling, foaming etc., that are required for different food formulations are largely dependent on the state of the milk proteins.

Milk proteins are highly influenced by the nature of the preheat treatment applied during powder manufacture and, based on the extent of the heat treatment, SMPs are commonly classified as low heat (MLH), medium heat (MMH) or high heat (MHH) (Patel, Anema, Holroyd, Singh, & Creamer, 2007). The typical preheat treatments that are used to produce MLH, MMH and MHH are 70 °C/15 s, 85–105 °C/60–30 s and 90–120 °C/1–2 min respectively. This preheating step denatures the whey proteins, i.e. β-lactoglobulin (β-LG) and α-lactalbumin (α-LA), forming aggregates that further associate with the casein micelles, and specifically with κ-casein (Havea, 2006; H. Singh, 2007). These modified casein micelle/denatured whey protein complexes largely determine the functionalities and applications of SMPs. For example, MLH is preferred for recombined pasteurized milk and cheese making, MMH is preferred for ice cream and chocolate confectionery and MHH is preferred for bakery products and sweetened condensed milk (Er, Sert, & Mercan, 2019; Patel et al., 2007; Sharma et al., 2012).

Recent studies have shown that the heat treatment not only leads to changes in the physicochemical properties of milk but also may have a far greater impact on the gastrointestinal digestion behaviour (Tunick et al., 2016; Wada & Lönnerdal, 2014; Ye et al., 2019). Our previous in vitro study using a human gastric simulator (HGS) showed that liquid milk without any heat treatment, i.e. raw/unheated milk, formed a close-knit dense clot in the stomach. In contrast, the curds formed by heated and UHT milks were fragmented and crumbled in appearance, with large voids (Ye et al., 2016). Similar behaviour of these liquid milks was also observed in an in vivo study in rats (Ye et al., 2019).

Milk-based formulations have been the most preferred delivery vehicles for vitamin and mineral fortification and the addition of lipophilic drugs and bioactive compounds to promote health (Boyd et al., 2018; Elzoghby, Abo El-Fotoh, & Elgindy, 2011; Niu et al., 2020). Among

various bioactive compounds curcumin is well-known for its health benefits. However, due to its limited water solubility, biochemical/structural breakdown, and poor bioavailability, its application has been difficult (Almeida et al., 2018; Joung et al., 2016). As a result, numerous studies are focusing on employing lipid-based nanosystems to encapsulate curcumin, particularly nanoemulsions, to overcome these constraints (Araiza-Calahorra, Akhtar, & Sarkar, 2018; Qazi et al., 2021; Sabet, Rashidinejad, Qazi, & McGillivray, 2021). However, their physicochemical interactions with milk proteins and other food components during processing and digestion within the gastrointestinal tract play a significant role in the recreation of the food structure and matrix (Q. Ye et al., 2021). In general, food structure influences the rates of nutrient digestion and absorption, primarily through the kinetics of digestion and the rate at which nutrients are transmitted from one digestive organ to the next in the gastrointestinal tract.

Our recent study investigated the in vitro digestion of acid and rennet gels that were fortified with CNE (Qazi et al., 2021). Despite the fact that these gels had similar rheological and compositional profiles, but their disintegration behaviour during dynamic gastric digestion showed a significant impact on the gastric emptying of the oil droplets and, as a result, on the bioaccessibility of the associated lipophilic curcumin during the intestinal phase (Qazi et al., 2021). Similarly, in another study, Niu et al. (2020) showed that a high-protein beverage as a food system enhanced the absorption of an enriched coenzyme-Q10-loaded nanoemulsion by increasing the lipolytic activity compared with a coenzyme Q10 nanoemulsion and coenzyme Q10 dissolved in oil. Thus, the nature of the restructuring that occurs in the stomach and the potential interaction of nanoemulsified bioactive compounds with natural food materials have a significant impact on the composition of the food chyme that exits the stomach at different times.

Building on previous work done on heated liquid milk systems, this study sought to evaluate the gastrointestinal digestion profile of recombined milk systems enriched with CNE. Different SMPs, i.e. MLH, MMH and MHH, were reconstituted with a CNE and water to achieve an equivalent fat-to-protein ratio. The aim of this study was to evaluate the impact of physicochemical changes in the morphology of the emptied gastric digesta and the clot produced using the dynamic HGS on lipolysis and the release of curcumin during intestinal transit. This research will further our knowledge of the digestion and release of lipophilic bioactive compounds from differently processed recombined milks, as well as the development of dietary food supplements produced from these milk powders.

3.3 Materials and methods

3.3.1 Chemicals and ingredients

MLH, MMH and MHH SMPs (whey protein nitrogen indices of ≥ 6, 3.3 and 0.3 respectively) and sodium caseinate were purchased from Fonterra Co-operative Group, Auckland, New Zealand. Curcumin (purity ≥ 95%) was purchased from Xi'an Lukee Bio-Tech Co. Ltd, Xi'an, China. Soybean oil (Essenté) was purchased from Davis Trading Company, Palmerston North, New Zealand, and was used without further purification. The following chemicals were purchased from Sigma-Aldrich (St. Louis, MO, USA): pepsin from porcine gastric mucosa (EC 3.4.23.1; product no. P7125), pancreatin (EC 232.468.9; P7545) from porcine pancreas (8×USP specifications) and bile bovine (EC 232.369.0; B3883). All other chemical reagents and solvents were of analytical grade. Milli-Q water (Millipore Corp., Bedford, MA, USA) was used to prepare all solutions.

3.3.2 Preparation of recombined milk systems loaded with CNE

A curcumin-loaded oil-in-water nanoemulsion, with an average size of 187 ± 11 nm and containing 20% soybean oil, 0.03% curcumin and sodium caseinate as an emulsifier, was manufactured according to a previous method (Qazi et al., 2021). Briefly, both oil and aqueous phases were homogenized (Ultra-Turrax) for 2 min at ambient temperature, which was further passed through double-stage high-pressure homogenizer (APV 2000, Albertslund, Denmark) for 4 cycles at 350/50 bar pressure, to obtain fine nanoemulsion. This CNE was further mixed with the SMPs, i.e. MLH, MMH and MHH, followed by dilution with Milli-Q water to achieve final protein and oil contents of 3.7 and 5% respectively. The final solutions were then stirred for 2 h at room temperature to allow complete dissolution and were immediately stored at 4 °C overnight before being subjected to digestion.

3.3.3 Dynamic in vitro gastric digestion

A dynamic gastric model – the HGS designed by Fanbin Kong and Singh (2010) – was used for the in vitro gastric digestion of all milk samples. The method described in Qazi et al. (2021) was used in the present study with a slight modification. Briefly, 200 g of prewarmed milk sample at 37 °C was mixed with 31.3 mL of simulated salivary fluid (SSF) and kept in a water bath for 2 min at 37 °C. Before gastric digestion, 28 mL of simulated gastric fluid (SGF) containing pepsin was mixed with the sample to mimic the fasting state of the human stomach. After the food mix had been transferred into the latex stomach chamber, the titration pumps that dosed the SGF and the pepsin separately at a controlled rate of 2.5 mL/min (2.0 mL/min of the 1.25x concentrated SGF and 0.5 mL/min of pepsin solution) were switched on (Ye et al., 2019). The rollers installed in the HGS contracted three times per minute to simulate the actual peristaltic contraction of the stomach. A 50 mL sample of gastric digesta was emptied after every 20 min and, to mimic human gastric sieving, the emptied gastric digesta was passed through a stainless-steel sieve (pore size approximately 1 mm). The maximum digestion time

was 240 min; however, to analysis the changes in the structure of the curd within the stomach and in the emptied gastric digesta, the whole digestion process was terminated at selected timepoints, i.e. 20, 60, 120, 180 and 240 min. Gastric curds collected at these timepoints were freeze-dried and pulverised into powder for further investigation. The pH of the gastric digesta emptied at every 20-min interval was immediately recorded and was assumed to be similar to the pH within the HGS. Further, to stop the activity of pepsin, the pH of the digesta samples was adjusted to 7 by 1 M NaOH and/or 1 M HCl and were stored at 4 °C for further compositional analysis.

3.3.4 Physicochemical analyses of emptied digesta and gastric clot

The emptied digesta samples collected at selected timepoints were further chemically analysed for dry matter and oil content according to the method described in the previous study (Qazi et al., 2021). Similarly, to analyse the changes in the weight of the curd, the gastric digestion was terminated at 20, 60, 120, 180 and 240 min for all recombined milk systems. The contents of the HGS were collected and passed through the 1-mm sieve to separate the solid curd and the liquid gastric digesta. The clot was weighed immediately before being subjected to microscopy to analyse microstructural changes.

3.3.5 Protein profile of gastric clot and emptied digesta

The time-dependent hydrolysis of the proteins in the initial and digested samples (gastric curd and emptied digesta) of MLH, MMH and MHH in the HGS was determined by analysing the protein composition of the samples as a function of the digestion time using sodium dodecyl sulphate polyacrylamide gel electrophoresis (SDS-PAGE) as described in Qazi et al. (2021). Briefly, initial and emptied digesta samples from selected timepoints were diluted five times with Milli-Q water. These samples were then mixed with sample buffer at a ratio 1:1, and 7 µL of each mixture was loaded into each well. For solid curd samples, 4.5 mg of freeze-dried

sample was mixed with sample buffer and 10 μL was loaded into each well. The electrophoresis analysis was conducted at 120 V for approximately 90 min. After staining and destaining, these gels were scanned using a Molecular Imager Gel Doc XR system (Bio-Rad Laboratories, Hercules, CA, USA).

3.3.6 Microstructure of curds and gastric digesta

The microstructural changes in the milk systems, i.e. MLH, MMH and MHH, were observed using a confocal laser scanning microscope (Leica SP5 DM6000B; Leica Microsystems, Heidelberg, Germany). A 50 μL aliquot of Nile Red [0.1% (w/v), acetone-dissolved] and a 50 μL aliquot of Fast Green (1.0%, dissolved in water) were added into 500 μL of sample (original and gastric digesta samples) to stain the lipid and protein respectively. However, the solid curd samples were stained by submerging them into both dyes for 10 min to facilitate the diffusion of the dyes into the samples. An appropriate amount of stained sample was placed on the concave surface of a confocal microscope slide (Sail; Sailing Medical-Lab Industries Co. Ltd, Suzhou, China), covered with a coverslip and examined under a ×63 oil immersion lens. An argon laser with an excitation wavelength at 488 nm was used for Nile Red and a He–Ne laser with an excitation wavelength at 633 nm was used for Fast Green. The images of the oil and protein microstructures were obtained directly from the supporting microscope software (Leica) and were stored with 1024 × 1024 pixel resolution.

3.3.7 In vitro intestinal digestion

The gastric digesta emptied at 20, 120 and 240 min were further submitted to in vitro intestinal digestion. The INFOGEST in vitro digestion technique was used to imitate in vitro intestinal digestion under static conditions (Brodkorb et al., 2019). To reach a final ratio of 1:1, 20 mL of simulated intestinal fluid containing 10 mM bile and pancreatin (trypsin activity 100 U/mL) was mixed with a gastric digestion sample in a digestion flask. The digestion was

carried out at 37 °C for 2 h, and the pH of the mixture was constantly checked and corrected to 7 using 0.1 M and 1 M NaOH.

The release of FFAs during lipid digestion was detected using a pH-stat technique and calculated using the following equation:

$$\frac{\mu\text{mol}_{fatty\ acid}}{mL_{gastric\ digesta}} = \frac{[V_{NaOH}(t) - V_{NaOH}(a)] - C_{NaOH} \times 1000}{V_{gastric\ digesta}}$$

Here, $V_{NaOH}(t)$ is the volume of NaOH used at neutralize total acid released at digestion time t, $V_{NaOH}(a)$ is the volume of NaOH used to neutralize acid released as amino acids during digestion time t µmol, C_{NaOH} is the concentration of the NaOH solution used to titrate the acid released in 2 h, i.e. 0.05 M, and $V_{gastric\ digesta}$ is the volume of the gastric digesta, i.e. 20 mL.

3.3.8 Particle and oil droplet sizes of gastrointestinal digesta

The mean particle sizes of the gastrointestinal digesta after collection were determined using a Mastersizer 2000 (Malvern Instruments Ltd, Malvern, Worcestershire, UK). The powders were diluted in water to achieve a saturation between 14 and 16% (concentration of ~0.001%). An emptied digesta sample at a selected timepoint was immediately added to an automated small volume sample dispersion unit (Hydro2000S) prefilled with distilled water until an obscuration between 10 and 15% had been reached. Similarly, the impact of the gastric digestion on the oil droplet size was analysed by mixing the emptied gastric digesta sample with a mixture of 2% SDS and 50 mM EDTA at a ratio of 1:2. The mixture was then gently mixed for an hour to dissociate the clusters of protein stabilizing the oil droplets. This dissolved mixture was then used to measure the oil droplet size using polydisperse analysis and the droplet size was recorded as the surface-weighted diameter ($D_{3,2}$). All measurements were conducted at room temperature and the average particle and droplet diameters of the emptied gastric digesta were measured in triplicate.

3.3.9 Curcumin bioaccessibility

After the small intestinal phase, the samples were separated into two portions: a micelle sample and a total digest sample. To isolate the mixed micelle fraction containing solubilized curcumin, a 20 mL aliquot of the entire digesta was centrifuged (38200 *g* and 20 °C for 30 min) using a T-865 rotor (Sorvall WX Ultra 100; Thermo Scientific, Asheville, NC, USA) and the clear supernatant was collected. To separate hydrophobic curcumin, the mixed micelle fraction and the whole digest fraction were dispersed in chloroform, vortexed and centrifuged for 60 min at 3800 *g*. The curcumin concentration was quantified using the standard curve (Annexure 1). The following equation was used to calculate the bioaccessibility of curcumin:

$$\text{Bioaccessibility (\%)} = 100 \times \frac{C_{micelle}}{C_{digesta}}$$

In this formula, the measured curcumin concentration in the micelle phase is represented by $C_{micelle}$, and the actual curcumin concentration in the intestinal digesta is represented by $C_{digesta}$.

3.3.10 Statistical analysis

Data plotting and statistical analysis (one-way analysis of variance and Tukey's multiple comparison test) were performed using Minitab software (Minitab version 16; Minitab, Inc., State College, PA, USA). The results were expressed as the mean ± standard deviation of at least two replicates. Differences were considered to be statistically significant at a level of $p < 0.05$.

3.4 Results and discussion

3.4.1 Gastric phase

3.4.1.1 Coagulation behaviour of recombined milks in the HGS

The formation of curd in all three recombined milk systems in the HGS was seen visually; however, the structures of the curds formed during the first 20 min of digestion were different for all three systems [(Fig. 3.1 (A)]. The curd formed by MLH at 20 min was fragmented and had a crumbled texture. This curd appeared to be similar to the curd formed during the gastric digestion of pasteurized milk (Roy, Ye, Moughan, & Singh, 2021). The curds formed by MMH and MHH were soft with loose structures. The differences among the nature of the clots formed may have been due to the degree of preheat treatment applied to these milk systems before spray drying. The high heat treatment of milk results in greater denaturation of the whey proteins and their interactions with the casein micelles, which then results in the formation of a softer curd during digestion (Ye et al., 2019).

The size of the curd fragments of MLH reduced gradually with increasing digestion time. After 240 min, these curd pieces were less integrated and separated into smaller pieces. The soft curds formed at 20 min by MMH and MHH, which had similar appearances, transformed into two distinct shaped curds by the end of the gastric phase. The amount of MHH curd decreased markedly and the curd formed gave the appearance of breadcrumbs that shrunk to a smaller size at longer digestion times. This curd was similar to the images of the curd obtained during the dynamic in vitro gastric digestion of sheep milk that was homogenized and heated to 95 °C (Pan et al., 2021). However, for MMH, the initial soft curd transformed into numerous compact curd fragments over time [Fig. 3.1 (A)]. The differences in these curd structures may have been due to the level of whey protein associated with the casein micelles (H. Singh, 2007; Ye et al., 2019).

The weight of the curd formed inside the HGS was also recorded after the curd had been passed through a 1-mm sieve. MHH disintegrated more rapidly in the gastric chamber than MMH and MLH [Fig. 3.1 (B)], which is consistent with previous work demonstrating decreased curd retention in the stomach with an increase in the amount of heat applied to the milk (Mulet-Cabero et al., 2019; Ye et al., 2019).

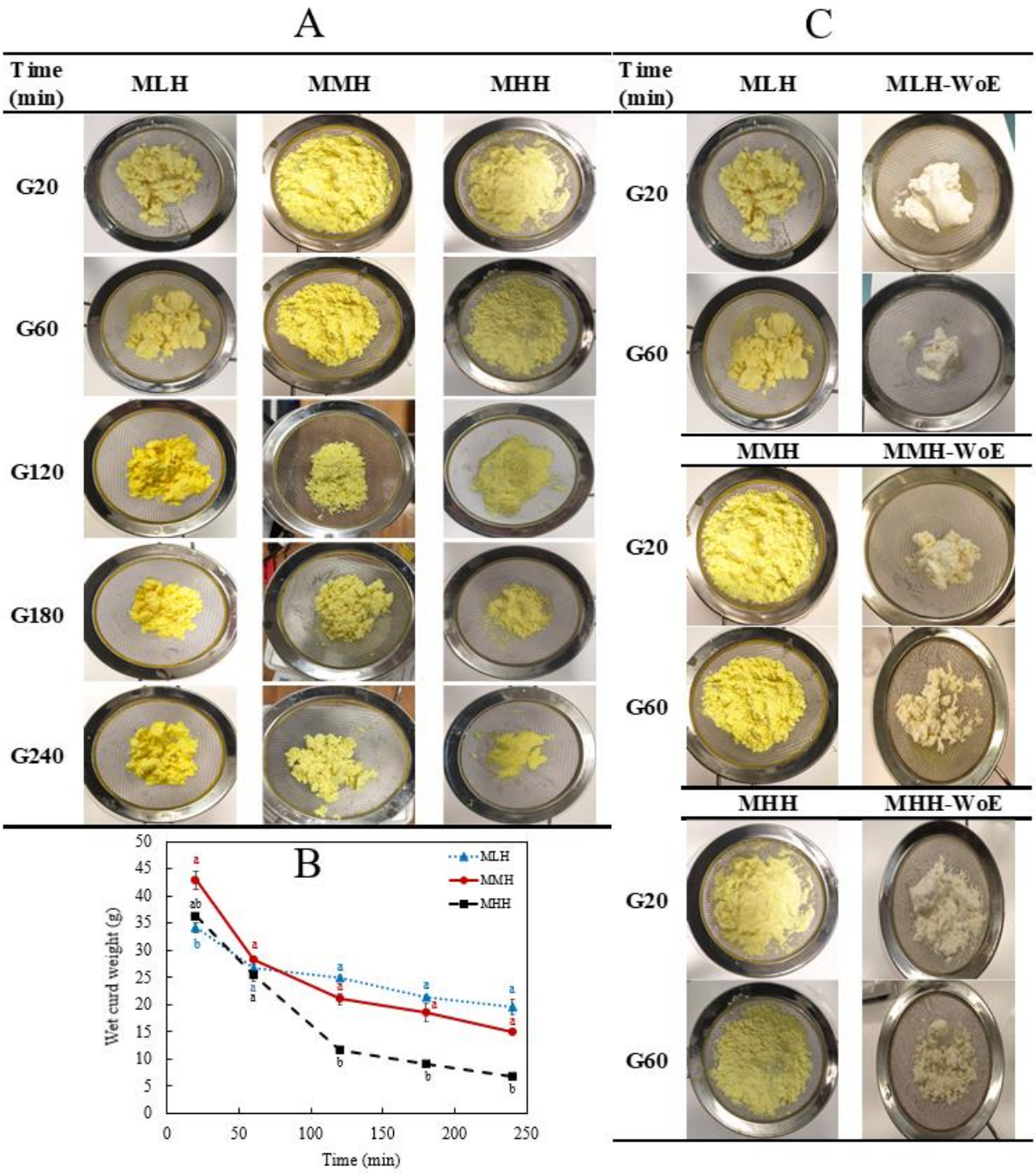

Fig. 3. 1(A) Images and (B) wet weights of the curds formed during the gastric digestion (simulated gastric fluid with pepsin) of 200 g of recombined milks with added CNE, i.e. low heat (MLH), medium heat (MMH) and high heat (MHH), at 20, 60, 120, 180 and 240 min of gastric digestion. (C) comparison of the structures of the curds formed with and without CNE (WoE) at 20 and 60 min of gastric digestion.

To determine the influence of the CNE on the structure of the curds formed in the stomach, all recombined milks without the addition of nanoemulsion (i.e. reconstituted skim

milks) were subjected to gastric digestion for 1 h. The reconstituted skim milks formed compact structured clots at both 20 and 60 min of digestion; they were significantly different from the clots containing CNE [Fig. 3.1 (C)]. This may have been due to the entrapment of a large number of emulsified curcumin-loaded oil droplets within the curds, which prevented close contact among the coagulating casein particles. A previous study found that the homogenization of whole milk resulted in the coating of the fat globules with casein/whey protein, which then became embedded into the coagulum, leading to changes in the structure of the curd (Ye et al., 2017). Similarly, sodium-caseinate-stabilized nanoemulsion oil droplets may have interacted with the casein/whey protein aggregates, leading to alterations in the structure of the protein curd.

3.4.1.2 Microstructures of gastric curd and emptied digesta

The microstructural variations in the curds formed by the recombined milk systems in the HGS were investigated using a confocal laser scanning microscope [Fig. 3.2 (Curd)]. Before digestion, emulsified oil droplets were uniformly distributed in the protein aqueous phase in all three recombined milk systems. At an early stage of digestion (20 min), a close-knit network of protein was observed for MLH and MMH, whereas the curd formed by MHH had a more open network with numerous irregular dark intermittent holes; this structure was similar to that seen in UHT milk during gastric digestion (Ye et al., 2019). The protein matrix appeared to shrink as the digestion time increased, and the structure of the curds became considerably more open, with blocks of aggregated proteins [Fig. 3.2 (240 min)]. A portion of the oil droplets in the casein network or the surrounding pores of the casein network appeared to be physically trapped. Previous studies investigating the gastric colloidal behaviour of milk proteins in different dairy products have shown that the oil droplet/fat globule size increases with increasing digestion time (Guo, Ye, Lad, Dalgleish, & Singh, 2016; Roy et al., 2021; Ye et al., 2019). In our study, because the initial average size of the oil droplets was so small (<

200 nm), most of the oil droplets that were embedded within the protein microstructure remained invisible under the microscope. Although the droplet size data showed a small increase in size towards the end of digestion, i.e. approximately 300 nm [Fig. 3.1 (C)], it was not noticeable under the microscope. The more open microstructure of the MHH curd generated by the gastric digestion showed these stained nanosized oil droplets as red zones inside the protein matrix, whereas these zones were less noticeable in the MLH and MMH curds. Conversely, the larger droplets observed in the curd micrographs could represent a limited degree of oil droplet coalescence within the curd matrix.

In contrast, in the stomach environment, the emptied digesta of all three systems revealed a constant disintegration of the associated protein networks [Fig. 3.2 (Liquid Digesta). Initially at 20 min, the digesta samples contained numerous small-sized curd particles with evenly distributed oil droplets. Within the first hour of digestion, these small curd particles grew in size and became flake-like, before gradually shrinking in size until the end of digestion.

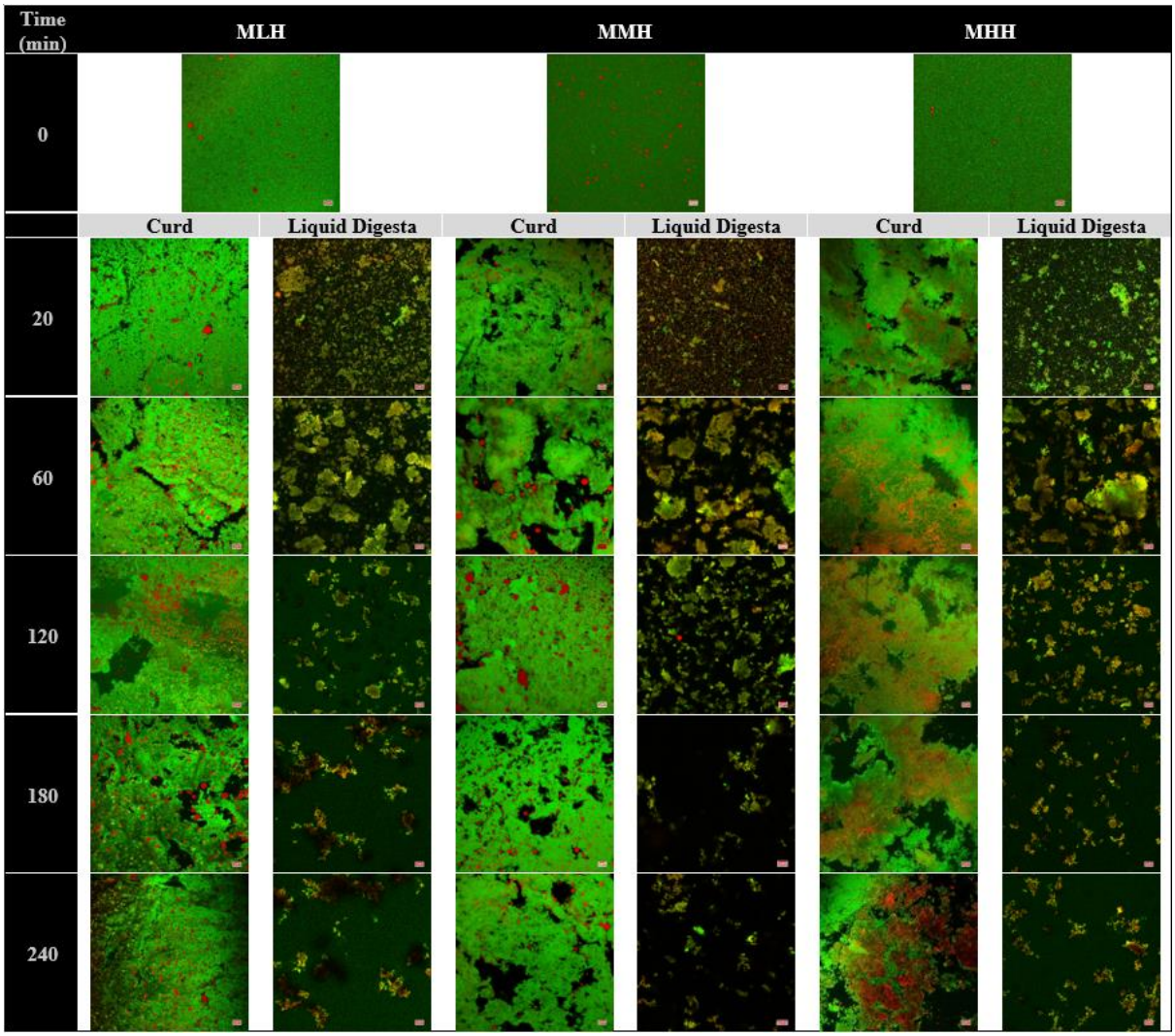

Fig. 3. 2 Confocal microscopy images of gastric curd and liquid digesta formed at 0, 20, 60, 120, 180 and 240 min of gastric digestion of low-heat (MLH), medium-heat (MMH) and high-heat (MHH) recombined milk systems. Red shows the oil droplets and green shows the milk protein. The scale bar corresponds to 10 µm for all micrographs.

3.4.1.3 Physicochemical changes in emptied liquid digesta

The pHs of the recombined milk samples during gastric digestion were recorded every 20 min for up to 240 min [Fig. 3.3 (A)]. The initial pHs of the samples in the stomach (before mixing with the SSF and 28 mL of SGF) were 6.64, 6.58 and 6.54 for MLH, MMH and MHH respectively. With the gradual addition of SGF during digestion, the pH of the emptied digesta decreased gradually over time to about pH 2.29 by the end of 240 min. Throughout the 240

min of digestion, MHH had a significantly slower decrease in pH, followed by MMH and MLH. These results are in agreement with those reported by Ye et al. (2019), in which UHT milk demonstrated a greater pH buffering capacity than unheated and pasteurized milk during the gastric phase. The higher buffering capacity of the heated milk system was possibly due to changes in the structure and composition of the casein micelles during heat treatment. The different preheat treatments applied during the manufacture of SMPs result in different extents of whey protein denaturation. These denatured whey proteins further interact with κ-casein, forming complexes with κ-casein on the surface of the casein micelles (Douglas Jr, Greenberg, Farrell Jr, & Edmondson, 1981). The higher level of whey protein association in MHH resulted in a more fragmented structure of the curd in the stomach [Fig. 3.3 (A)], which could affect the rate of pH decrease during gastric digestion.

The variations in the weight-to-volume diameter ($D_{4,3}$) of the emptied digesta during gastric digestion were significantly different in all three recombined milk systems [Fig. 3.3 (B)]. The $D_{4,3}$ values of the MMH and MHH digesta samples increased rapidly between 20 and 60 min from 58 and 52 µm to 111 and 91 µm respectively. In the MHH digesta sample, this particle size reached 154 µm at 120 min, before dropping to 84 µm at the end of the digestion. In contrast, there was no discernible change in the particle size of the MMH digesta beyond 60 min of digestion. In comparison with the MMH and MHH digesta, the $D_{4,3}$ of the MLH digesta increased slightly to 35 and 41 µm after 20 and 60 min respectively, before dropping to 9 µm at 180 min. Interestingly, during the last hour of digestion, there was a substantial increase in the particle size, bringing it close to the $D_{4,3}$ values of the MMH and MHH digesta. During the gastric digestion, the sizes of the emulsion droplets embedded within the curd particles were observed to be less affected [Fig. 3.3 (C)], which is similar to the behaviour observed for CNE that were enriched within dairy gels (Qazi et al., 2021). This demonstrated that the

nanoemulsion embedded within the curd particles had greater stability to the structural transformations during the gastric phase.

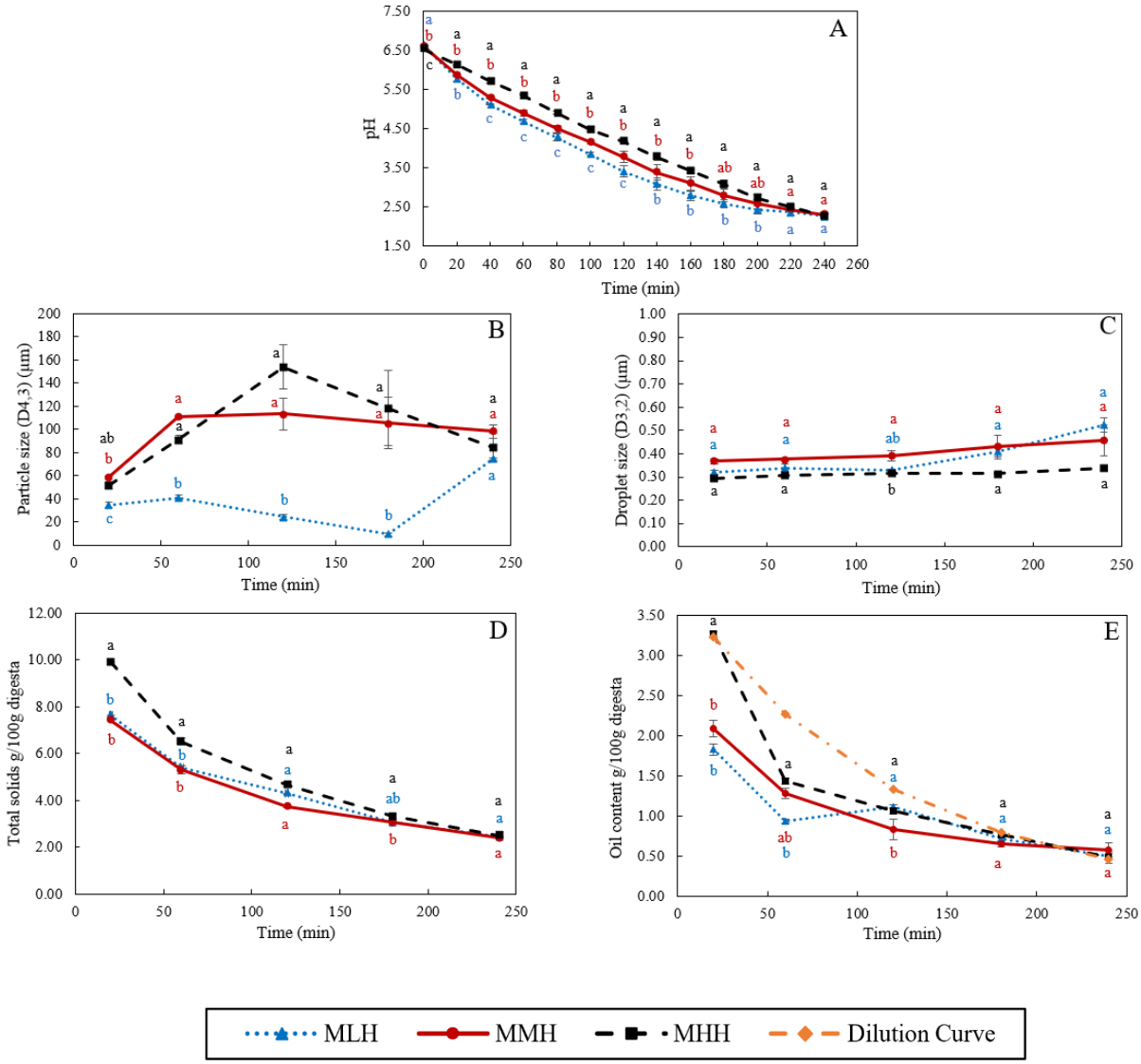

Fig. 3. 3 Effect of dynamic in vitro gastric digestion of different recombined milk systems on changes in (A) pH, (B) particle size ($D_{4,3}$), (C) oil droplet size ($D_{3,2}$), (D) total solids and (E) oil content of the emptied gastric digesta. The standard error is indicated by error bars.

During the first 120 min of gastric digestion, MHH showed a significantly ($p < 0.05$) faster emptying of total solids than MLH and MMH [Fig. 3.3 (D)]. These results are in agreement with the gastric curd images [(Fig. 3.1 (A)] and the wet weights of the curds [Fig. 3.1 (B)], showing faster disintegration of the MHH samples. The curds formed by the other

two recombined milk systems retained the maximum total solids, while allowing a small fraction to pass through to the liquid digesta. This difference became less pronounced as the digestion progressed and, at the end of the process, the total solids contents of the MLH, MMH and MHH digesta were almost identical.

The oil contents emptied in the gastric digesta at different digestion times from the different recombined milk systems were also analysed [Fig. 3.3 (E)]. The MHH digesta sample emptied at 20 min had significantly higher emptying of oil content, i.e. approximately 3.27%, than the MMH and MLH gastric digesta samples, i.e. approximately 2.09 and 1.83% respectively. The oil content in the MHH digesta sample at 20 min was similar to the hypothetically calculated oil value (i.e. the dilution curve), based on dilution of the digesta because of the gradual addition of SGF at different timepoints. The more open microstructure of the curd formed by MHH clearly allowed more oil droplets to be released into the digesta compared with the other two recombined milk systems, which entrapped them within the curd. With the progression of digestion, the oil content in the digesta samples of all three recombined milk systems gradually decreased with no significant differences at digestion durations of longer than 120 min. Overall, the oil content of the MHH digesta remained significantly higher than those of the MLH and MMH digesta, indicating that it disintegrated more rapidly in the HGS, as explained in Section 3.1.1.

3.4.1.4 Kinetics of milk protein disintegration during gastric phase

The protein fraction of the gastric curd and emptied digesta samples of all three milk systems were characterised by sodium dodecyl sulfate-polyacrylamide gel electrophoresis (SDS-PAGE) under reducing conditions (Fig. 3.4). Fig. 3.4 (A-C), (B-C) and (C-C) depicts the protein hydrolysis by pepsin in the curd samples recovered from the stomach at selected timepoints. The changes during the digestion were then compared with the protein profile of

the native samples (lane M). Overall, MHH had faster protein hydrolysis in the curd than MLH and MMH. With increasing digestion time, the intensities of the α_s-casein and β-casein bands reduced; several peptide bands with varied molecular weights (from 10 to 20 kDa) were clearly evident from 60 min onwards in the MHH curd samples (Fig. 4 C-C). In contrast, MLH and MMH did not show any notable drop in intensity over time for casein bands other than κ-casein [Fig. 3.4 (A-C) and (B-C)]. The only trend that all three systems had in common was the disappearance of the κ-casein bands during the first 20 min of digestion as a result of pepsin hydrolysis, which led to the formation of a para-κ-casein band with a molecular weight of 15 kDa (Ye et al., 2016). The β-LG and α-LA bands were more prominent in the MHH curd samples, compared with the other samples, and decreased gradually as the digestion progressed [Fig. 3.4 (C-C)]. This confirmed that the whey proteins were involved in the formation of the MHH curd structure because of the association of whey proteins (β-LG and α-LA) with the casein micelles during powder manufacture. For MLH and MMH, very faint whey proteins bands were seen at 20 min of digestion; they then disappeared [Fig. 3.4 (A-C) and (B-C)].

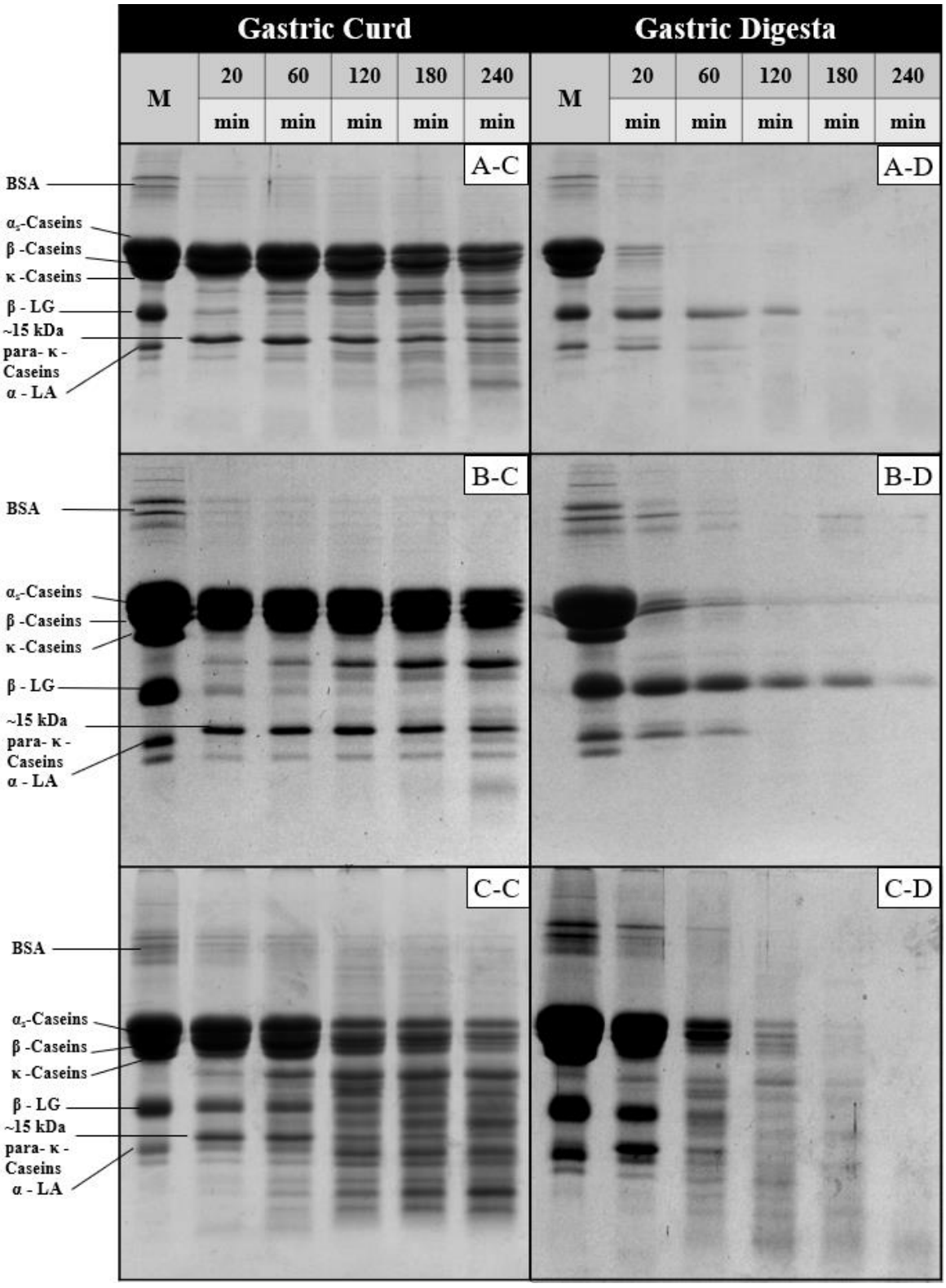

Fig. 3. 4 SDS-PAGE patterns (under reducing conditions) of freeze-dried gastric curd (C) and liquid digesta (D) samples obtained at selected timepoints of gastric digestion of MLH (A), MMH (B) and MHH (C). M stands for the original samples before digestion and all other samples are labelled appropriately in the figure.

In contrast, for MLH, MMH and MHH, the casein bands on the SDS-PAGE gels of the digesta samples disappeared after 20, 60 and 120 min of digestion respectively [Fig. 3.4 (A-D), (B-D) and (C-D)]. Casein was emptied into the gastric digesta in a pattern that was comparable with but opposite to that of the curds retained in the gastric chamber. That is, the greater was the amount of curd that was retained in the stomach, the lesser was the amount of casein that was discharged into the digesta. MHH also had greater peptide release into the digesta. The higher rate of protein digestion in heated milk has been attributed to the loose structure of the curd (Ye et al., 2017; Ye et al., 2019). This creates a larger surface area for pepsin diffusion into the curd, resulting in faster protein breakdown and a higher rate of curd particle (1 mm) emptying into the digesta. The presence of intact β-LG and α-LA in the digesta during the early stages of MLH and MMH digestion was attributed to the fact that β-LG is not hydrolysed by pepsin in its native state. However, after 60 min of digestion, the α-LA band disappeared, but the β-LG band faded steadily as the digestion progressed. In contrast, these whey protein bands disappeared and peptide bands appeared in the MHH digesta samples after 60 min.

3.4.2 Intestinal phase

3.4.2.1 Particle size

The gastric digesta emptied at 20, 120 and 240 min were further subjected to a static in vitro intestinal digestion. During the intestinal phase, portions of the digesta were removed at 1, 10, 30, 60 and 120 min and immediately analysed for changes in particle size distribution (Fig 3.5). The MLH and MMH gastric digesta emptied at 20, 120 and 240 min had trimodal size distributions whereas the MHH gastric digesta had a bimodal distribution at 20 and 120 min and a trimodal distribution at 240 min. Within 1 min of intestinal digestion, the particle size, initially falling under the peak in the range 1–100 μm, distributed into two distinct peaks: a narrow peak between 0.1 and 1 μm and multimodal peaks between 10 and 1000 μm. This

initial breakdown of particles within the first minute of digestion was consistent across all gastric digesta of the recombined milk systems that were emptied at selected timepoints. As the digestion progressed, the area under the multimodal peaks, representing undigested particles, decreased continuously until 120 min of intestinal digestion, indicating disintegration of the larger curd fragments. In contrast, the unimodal peak, representing small, digested particles, became narrower and the volume of particles with size between 0.1 and 1 μm increased steadily. This continuous increase in newly generated small particles over time can be connected to the mixed micelles generated from the hydrolysis products of lipids and bile salts, which play a key role in enhancing the bioaccessibility of lipophilic bioactive substances (Rein, Renouf, Cruz-Hernandez, et al., 2013; Salvia-Trujillo et al., 2017).

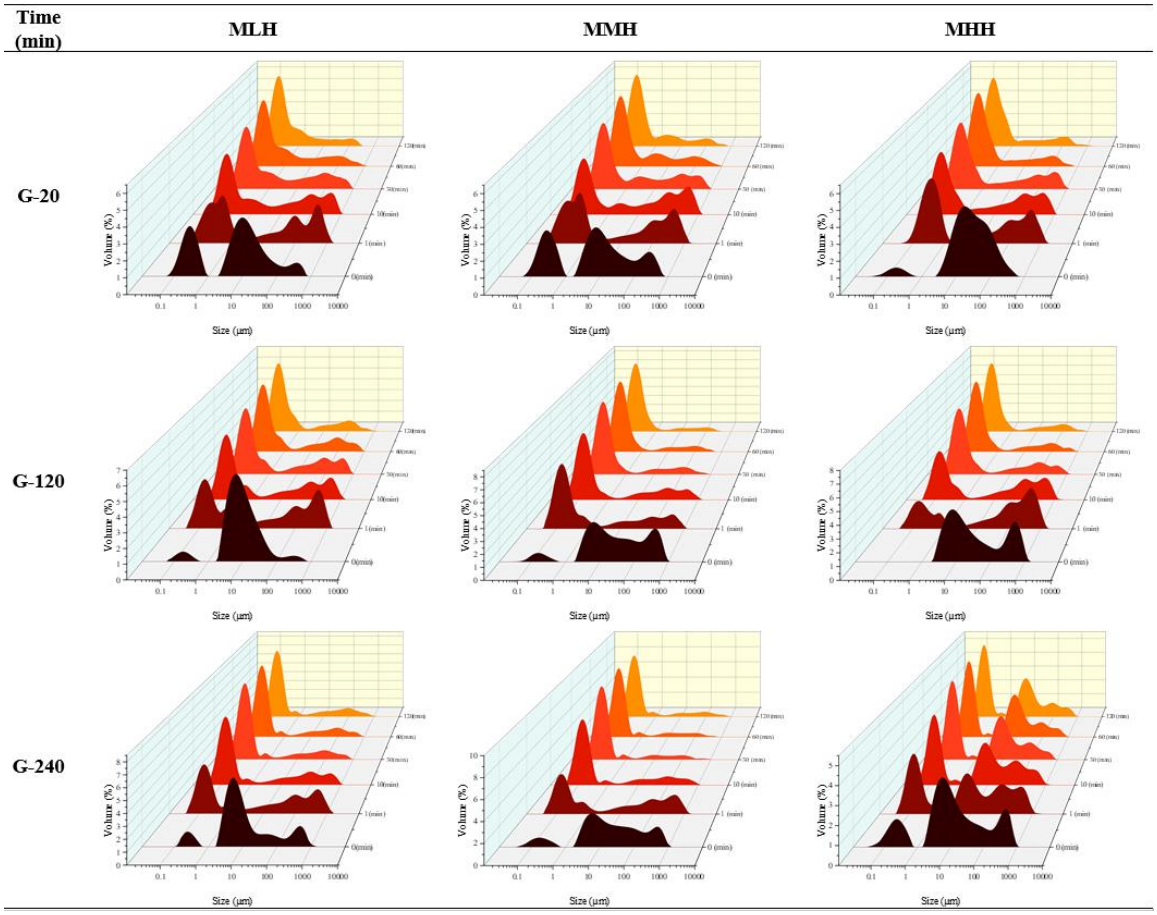

Fig. 3. 5 Changes in particle size distribution of emptied gastric digesta (20, 120 and 240 min) before (0 min) and during the intestinal digestion of MLH, MMH and MHH at different times (1, 10, 30, 60 and 120 min).

3.4.2.2 FFA release

[Fig. 3.6 (A)] shows the FFA release profiles per millilitre of digesta sample emptied after 20, 120 and 240 min of gastric digestion throughout 120 min of intestinal digestion. The FFA concentration reached a plateau during the first 10 min of intestinal digestion, indicating that most of the lipid in the digesta samples had been digested. This behaviour has been observed previously in the gastrointestinal digestion of a high-protein beverage incorporating a coenzyme Q10 nanoemulsion system (Niu et al., 2020) and in dairy gels loaded with CNE (Qazi et al., 2021). Beyond 10 min, the moderate and more sustained FFA release with the

progression of the intestinal digestion can be associated with multiple factors, i.e. enzyme-to-oil ratio, agglomeration of the digestion products generated as a result of lipolysis at the oil droplet interface and characteristics of the oil, which include their type, droplet size and nature of the emulsifier stabilizing them (Giang et al., 2016; Guo, Ye, Lad, Dalgleish, & Singh, 2016; Luo et al., 2021; Qazi et al., 2021). For all recombined milk systems during the intestinal phase, the gastric digesta emptied at 20 min released significantly more FFAs than the digesta emptied at 120 and 240 min. Moreover, the release of FFAs was significantly ($p < 0.05$) greater in the MHH gastric digesta at 20 and 120 min than in the MLH and MMH digesta at the same timepoints. This followed the same pattern as that of the emptying of the oil content into the digesta, namely G-20 > G-120 > G-240 [Fig. 3.3 (E)], and comparable behaviours were also observed during the gastrointestinal digestion of dairy gels (Qazi et al., 2021).

However, when the amount of FFAs released was calculated per gram of fat as a function of time, the trend changed for all recombined milk systems [Fig. 3.6 (B)]. The gastric digesta emptied at 240 min had the highest rate of lipolysis, followed by the gastric digesta emptied at 120 min, and finally the gastric digesta emptied at 20 min in all recombined milk systems. Similar behaviour was observed by Guo et al. (2016) when they evaluated FFA release during the intestinal digestion of whey protein emulsion gels. They explained these changes as a result of the changes in the gel structure or the colloidal structure of gel fragments during intestinal digestion, which may have impacted the hydrolysis of the oil droplets incorporated within the protein matrix. This appears to be the most likely mechanism regulating lipid release during the intestinal digestion of milk systems, but additional research is needed to fully comprehend lipid/protein interactions and their behaviour inside the gastric and intestinal chambers.

3.4.2.3 Bioaccessibility of curcumin

The bioaccessibility of curcumin was found to be significantly ($p < 0.05$) higher in the MHH digesta samples than the MMH and MLH digesta samples for all three selected timepoints [Fig. 3.6 (C)]. These differences can be related to the microstructural changes occurring in the stomach, which influenced the nature of the curd fragments emptied in the digesta. Similar behaviour was observed in our previous study, in which an acid milk gel, with softer gel fragments and an open microstructure, resulted in a significantly higher fraction of bioaccessible curcumin than a rennet gel (Qazi et al., 2021). For all three recombined milk systems, there was no noticeable difference in the fraction of bioaccessible curcumin in the gastric digesta emptied at 20, 120 and 240 min. In our study, the high bioaccessibility of curcumin (> 70%) for all recombined milk systems can be attributed to the fortification of curcumin as a nanoemulsion; because of its smaller droplet size and larger surface area, the incorporation of curcumin into the mixed micelles was enhanced (Wooster et al., 2017; Zhang & McClements, 2018). These mixed micelles, having a hydrophilic surface with a nanometric size, are able to disperse in digestive fluids, boosting the likelihood of them passing through

the mucus layers and reaching the intestinal epithelium for absorption (Rein, Renouf, Cruz-Hernandez, et al., 2013; Salvia-Trujillo et al., 2017).

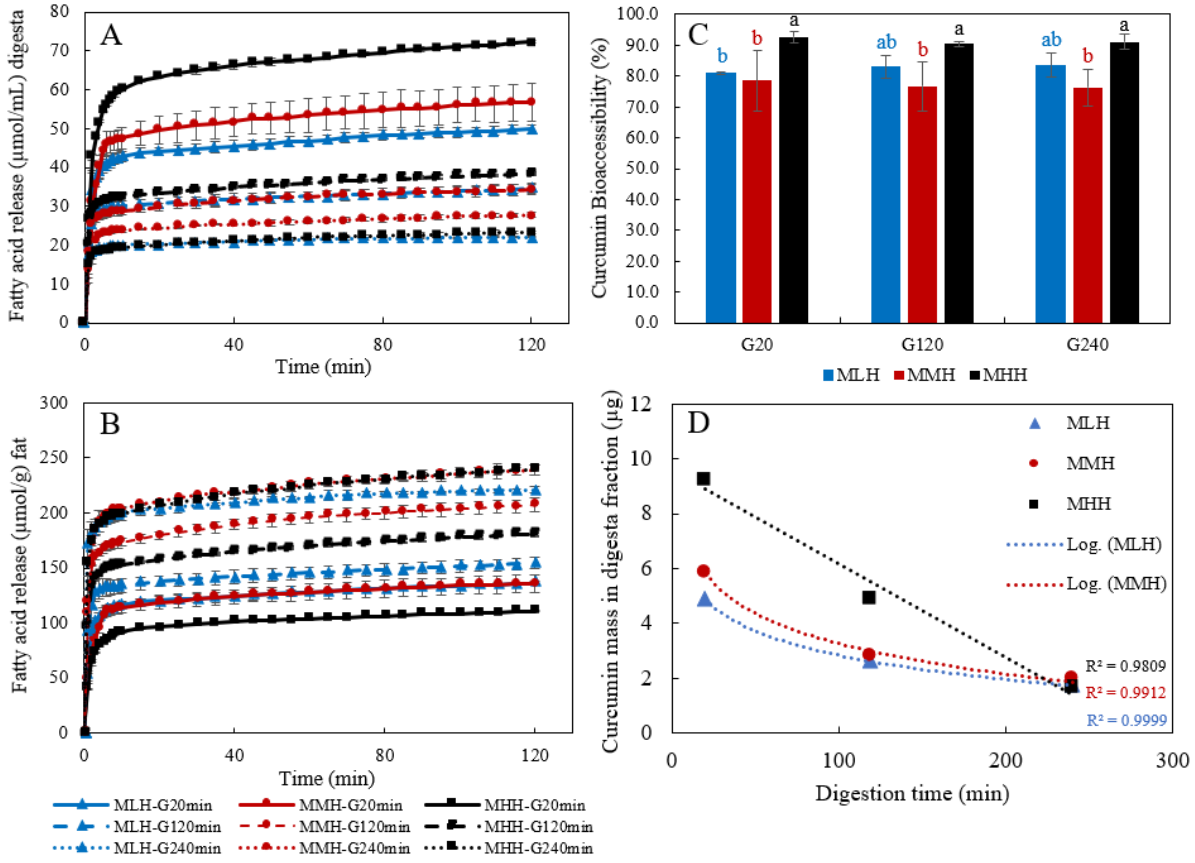

Fig. 3. 6 Free fatty acid release profile (A) per millilitre of gastric digesta and (B) per gram of fat, (C) bioaccessibility of curcumin and (D) curcumin mass in digesta fractions after in vitro gastrointestinal digestion.

In contrast, when the curcumin masses in these digesta fractions were analysed [Fig. 3.6 (D)], the gastric digesta emptied at 20 min showed a higher release of curcumin, which was followed by the gastric digesta emptied at 120 and 240 min. This is also in accordance with the concentration of oil droplets in the gastric digesta and the amount of FFA release. However, it is interesting to note that the fraction of curcumin in the MHH digesta samples showed a linear decreasing pattern whereas those in the MMH and MLH digesta samples followed a logarithmic decreasing trend. This logarithmic trend shows that the structural changes in MLH

and MMH had a greater impact on the release of the curcumin fraction in the digesta than those in MHH. Moreover, positive correlations, i.e. MLH (r = 0.983), MMH (r = 0.999) and MHH (r = 0.983), between the concentration of curcumin recovered from the intestinal digesta and the amount of FFAs released were observed. This behaviour has also been observed when carotenoids form part of oil-in-water emulsions (Mutsokoti et al., 2017), curcumin forms part of dairy gels (Qazi et al., 2021) and capsaicinoids form part of whey protein emulsion gels (Luo et al., 2021).

3.5 Conclusions

This work demonstrated the impact of the gastrointestinal digestion of recombined milks on the bioaccessibility of curcumin, highlighting the effect of the process-induced changes in the milks on the composition of the emptied gastric digesta. Both the nature of the preheat treatment used during SMP manufacture and the CNE supplementation modified the structure and consistency of the gastric curds. Under dynamic gastric conditions, the high-heat-treated milk proteins in MHH formed a loose and soft curd that resulted in faster outflow of the curd fragments along with entrapped CNE, compared with MLH and MMH. These differences in the gastric digesta profiles resulted in differences in the release of FFAs and the bioaccessibility of curcumin during intestinal digestion. In conclusion, the findings demonstrate the gastrointestinal bioaccessibility curcumin was better from MHH than from MLH and MMH and was dependent on the microstructural and compositional changes during the digestion of milk systems.

.

Statement of contribution (DCR 16 forms)

MASSEY UNIVERSITY
TE KUNENGA KI PŪREHUROA
UNIVERSITY OF NEW ZEALAND

GRADUATE RESEARCH SCHOOL

STATEMENT OF CONTRIBUTION
DOCTORATE WITH PUBLICATIONS/MANUSCRIPTS

We, the student and the student's main supervisor, certify that all co-authors have consented to their work being included in the thesis and they have accepted the student's contribution as indicated below in the Statement of Originality.

Student name:	Haroon Jamshaid Qazi
Name and title of main supervisor:	Aiqian Ye / Professor
In which chapter is the manuscript/published work?	Chapter 4

Describe the contribution that the student and members of the supervisory team have made to the manuscript/published work:[1]

Haroon Jamshaid Qazi: Methodology, Validation, Investigation, Formal analysis, Data curation, Writing - original draft, Visualization.
Aiqian Ye: Conceptualization, Methodology, Resources, Writing - review & editing, Project administration, Supervision, Funding acquisition.
Alejandra Acevedo-Fani: Writing - review & editing, Supervision.
Harjinder Singh: Conceptualization, Methodology, Writing - review & editing, Supervision.

Please select one of the following three options:

- (●) **The manuscript/published work is published or in press**

  Please provide the full reference of the research output:

  Qazi, H. J., Ye, A., Acevedo-Fani, A., & Singh, H. (2021). In vitro digestion of curcumin-nanoemulsion-enriched dairy protein matrices: Impact of the type of gel structure on the bioaccessibility of curcumin. Food Hydrocolloids, 117, 106692.

- ( ) **The manuscript is currently under review for publication**

  Please provide the name of the journal:

- ( ) **It is intended that the manuscript will be published, but it has not yet been submitted to a journal**

Student's signature:	Haroon Jamshaid Qazi — Digitally signed by Haroon Jamshaid Qazi, DN: cn=Haroon Jamshaid Qazi, c=NZ, ou=Riddet Institute, email=h.j.qazi@massey.ac.nz, Date: 2023.06.20 11:08:15 +12'00'	Main supervisor's signature:	Aiqian Ye — Digitally signed by Aiqian Ye, DN: cn=Aiqian Ye, c=NZ, o=Massey University, ou=SF&AT, email=a.m.ye@massey.ac.nz, Date: 2023.06.20 12:12:34 +12'00'

This form should be placed at the beginning of each relevant thesis chapter.

[1] Refer to the Massey University Publishing and Authorship guidelines (OneMassey for staff, Stream for students) and/ or Contributor Roles Taxonomy (CRediT) guidelines for guidance.

Chapter 4: In vitro digestion of curcumin-nanoemulsion-enriched dairy protein matrices: impact of the type of gel structure on the bioaccessibility of curcumin

4.1 Abstract

This study examined the impact of the dynamic gastric digestion of two iso-caloric dairy gels containing CNE (D3,2 = 0.187 μm) on the intestinal lipid digestion and the bioaccessibility of curcumin. The residence time in the stomach and the release of oil together with solubilized curcumin were influenced by the type of gel structure. The rennet gel restructured and became denser because of the action of pepsin and the low pH, thus slowing the outflow of both protein and oil from the gel. In contrast, the acid gel experienced rapid protein disintegration under gastric conditions and most of the chyme was emptied out of the stomach within 2 h. Similarly, the content of curcumin-enriched oil in the digesta of the acid gel was higher than that in the digesta of the rennet gel, in which the oil droplets appeared to be embedded in the gelled particles. The size of the oil droplets within the emptied gastric digesta of both gels was not significantly impacted during digestion. The rate of free fatty acid release and the concentration of curcumin during intestinal digestion were linked with the compositional profile of the gastric digesta, whereas the bioaccessibility of curcumin (85–91%) was influenced by the gel type and the gastric disintegration of the gels. This study demonstrates the influence of different gel structures on the bioaccessibility of curcumin, which could be further used to design therapeutic dairy products with health benefits.

4.2 Introduction

Curcumin is the most abundant polyphenolic bioactive compound in turmeric. It has been widely studied and is recognized for its significance in human health, such as its antioxidant,

antimicrobial, anticancer and anti-inflammatory activities (Esatbeyoglu, Ulbrich, Rehberg, Rohn, & Rimbach, 2015; Jamwal, 2018; Rauf, Imran, Orhan, & Bawazeer, 2018). However, its natural pigmentation, low water solubility and high sensitivity to processing conditions limit its direct utilization within food products. In addition, curcumin has low bioavailability after oral intake and digestion (Anand, Kunnumakkara, Newman, & Aggarwal, 2007; Araiza-Calahorra et al., 2018; B. Zheng et al., 2019). Previous studies have shown how colloidal-based delivery systems, i.e. nanoemulsions, can overcome some of these limiting factors and improve the functionality of curcumin (Jiang et al., 2020; Kumar et al., 2016; Park, Garcia, Shin, & Kim, 2018). In particular, nanoemulsions have been found to increase the physical stability of curcumin and facilitate its transfer from the lipophilic interior of lipid droplets into the micellar phase during digestion (Araiza-Calahorra et al., 2018; B. Zheng, Peng, Zhang, & McClements, 2018).

To meet the increased interest of consumers in therapeutic foods, there has been a strong focus on developing new strategies to fortify foods so that they contain a biologically active and stable form of curcumin without a change in their sensory attributes (Joung et al., 2016). Nanoemulsions have been used to incorporate hydrophobic bioactive compounds in different food products, e.g. milk, cheese, yoghurt and ice cream (Kumar et al., 2016; Marcolino, Zanin, Durrant, Benassi, & Matioli, 2011; Park et al., 2019). However, there is insufficient information on how these different food structures can affect the delivery of bioactive compounds such as curcumin and, consequently, the bioaccessibility and bioavailability of these compounds (Rein, Renouf, Cruz-Hernandez, et al., 2013; H. Singh & Gallier, 2014).

In the literature, the concept of “food matrix” is used mainly to denote the large continuous medium that is formed naturally or produced during processing that chemically or physically embeds all the microstructural elements in foods (Aguilera, 2019; Parada &

Aguilera, 2007). The post-ingestion and intragastric de- and restructuring of these foods significantly modulate gastric emptying and the release of nutrients for absorption in the intestine (Guo et al., 2020). Previous studies have shown that the mechanical and biochemical disintegration of liquid and semi-solid foods occurs faster than that of solid foods (Lamothe et al., 2017). However, the digestion kinetics of these foods are also influenced by their composition, their structural arrangements and the type of processing involved in their manufacture. Ye et al. (2016) investigated the gastric digestion of processed and raw whole milk using an in vitro dynamic digestion model [the human gastric simulator (HGS)]. They found that the milks formed clots of different structures (coagula) within the stomach. These differences in clot structure influenced the rate of delivery of nutrients (protein and fat), which was reflected in the composition of the gastric digesta. Similarly, Fang, Rioux, Labrie, and Turgeon (2016) studied five commercial cheese samples with diverse initial hardness, cohesiveness and chewiness, and found that these properties affected the rate of disintegration of proteins during gastrointestinal digestion.

The modification of the proteins in milk by acid and rennet coagulation when producing dairy gels, such as yoghurt and cheese, can alter the digestion kinetics and nutrient release in the gastrointestinal cavity. An in vivo study carried out with six multi-cannulated mini-pigs investigated the effect of the type of gel structure, using yoghurt and cheese-like gels, on protein metabolism (Barbé et al., 2014). The concentration of amino acids generated from the hydrolysis of an acid gel (AG) in the duodenal effluents and blood plasma was much higher than that of a rennet gel (RG). This variation in plasma content was linked to the different digestion behaviours of both gels during the gastric phase. The structure of the AG rapidly disintegrated in the gastric fluids, showing limited molecular arrangement of the protein network. In contrast, the RG formed a compact aggregate in the stomach that delayed the gastric emptying. Le Feunteun and Mariette (2008) reported that this micro-densification of the

rennet protein network was associated with acidification. This was further endorsed by Floury et al. (2018) while visually observing in situ the microstructural changes in both gels during gastric digestion using time-lapse synchrotron deep UV microscopy. However, these studies did not report the effect of the gel protein matrix on the lipolysis of embedded oil droplets and the further bioaccessibility of lipophilic bioactive compounds.

Among the few studies reported on the digestibility of fortified food matrices, only one recently published article discusses the digestion dynamics of a stirred yoghurt matrix fortified with the flavonoid rutin and how interactions between the food matrix and rutin affected the release and bioaccessibility of the flavonoid during digestion (Acevedo-Fani et al., 2021). The results revealed that fortification of the yoghurt with a casein–rutin co-precipitate enhanced the protection and solubility of the rutin during gastrointestinal digestion, compared with the co-digestion of an unfortified yoghurt with a rutin vegetable capsule. An earlier study by our research group studied the behaviour of milk fat globules during the gastric digestion of heated and unheated whole milk using an HGS (Ye et al., 2016). They found that most of the fat globules were trapped within the clots as they formed and that their release into the intestine was linked with the rate at which the respective clot disintegrated. Similarly, the digestion kinetics of protein gels in the stomach can play a key role in defining the availability of oil for lipolysis and the bioaccessibility of fortified lipophilic bioactive compounds.

Therefore, the objective of this study was to investigate the impact of two gelled dairy protein matrices, i.e. an AG and an RG loaded with CNE, on the bioaccessibility of curcumin during in vitro gastrointestinal digestion. These gels were designed to have the same composition and rheological properties and differed only in their mode of coagulation. An HGS was employed as a tool in this study, to examine the impact of physicochemical changes in the

gel structures during the gastric phase on the subsequent lipolysis and the bioaccessibility of curcumin in the small intestine.

4.3 Materials and methods

4.3.1 Chemicals and ingredients

Curcumin (purity ≥ 95%) was purchased from Xi'an Lukee Bio-Tech Co. Ltd, Xi'an, China. Sodium caseinate and low-heat skim milk powder were purchased from Fonterra Co-operative Group, Auckland, New Zealand. According to the specification, the protein and fat contents of the skim milk powder were 32.9% and 0.9% respectively. Soybean oil (Essenté) was purchased from Davis Trading Company, Palmerston North, New Zealand, and was used without further purification. Pepsin from porcine gastric mucosa (EC 3.4.23.1; product no. P7125), pancreatin (EC 232.468.9; P7545) from porcine pancreas (8×USP specifications) and bile bovine (EC 232.369.0; B3883) were purchased from Sigma-Aldrich (St. Louis, MO, USA). All other solutions were prepared from analytical-grade chemicals and Milli-Q water (water purified by treatment with a Milli-Q apparatus; Millipore Corp., Bedford, MA, USA).

4.3.2 Preparation and characterization of curcumin-loaded nanoemulsion

The Curcumin-loaded oil-in-water nanoemulsion was prepared by first dissolving 0.03% curcumin in lipid fraction for 2 h under continuous stirring at 60 °C. Meanwhile, the aqueous phase was prepared by reconstituting 1% sodium caseinate with Milli-Q water, while stirring at room temperature for 2 h. The coarse emulsion was prepared by blending the appropriate amount of both oil and aqueous phases using a high-speed shear mixer (Ultra turrax) for 2 min at room temperature, to obtain 20% oil in the final emulsion. Followed by passing through double-stage high-pressure homogenizer (APV 2000, Albertslund, Denmark) for 4 cycles at 350/50 bar pressure, to obtain fine nanoemulsion. The mean particle size (D3,2), zeta potential and encapsulation efficiency of CNE was 0.187 ± 0.011 µm, – 58.83 ± 3.32 mV and 94.31% ±

0.77 respectively (Annexure 2). The prepared stock nanoemulsion was stored at 4°C until further use.

4.3.3 Dairy gels

The curcumin loaded nanoemulsion were mixed with low-heated skim milk for 2 h at room temperature so that the final oil and protein content would be equal to 5% and 4%, respectively. This reconstituted milk was further coagulated with acid and rennet to produce acid and rennet gel. AG was prepared by adding 1.6% w/w GDL to skim milk, mixing the sample for 2 min, and keeping the gels at 30°C for 6 h. Then the gels were immediately stored at 4°C. For the rennet coagulation, the pH of the reconstituted milk was adjusted to 6.5 by 1 M HCl. The temperature of the sample was raised to 32°C and 36 µL of rennet per 100 mL (equivalent to the final activity of 3.8 international milk-clotting unit (IMCU)) was pipetted into the sample. The samples were gently stirred for 2 min and shifted to a water bath maintained at 32°C for 6 h and likewise, these samples were also stored at 4°C for further analysis. The final pH of AG and RG was 4.4 and 6.5, respectively.

4.3.4 Rheological measurement of dairy gels

The processing conditions were optimized so that both gels had the same elastic modulus (G′), viscous modulus (G″) and loss tangent (tan δ). These properties of the dairy gels were monitored using a rheometer (AR-G2; TA Instruments, New Castle, DE, USA) with a cup-and-bob geometry and the method modified from S. Li, Ye, and Singh (2020). Briefly, a low-amplitude oscillation test was performed by setting the oscillation frequency to 0.1 Hz with a strain of 1% in time sweep mode and the gap at 5.92 mm. After treatment with glucono- δ-lactone and rennet, 20 mL of each reconstituted milk was pipetted into the rheometer, which was operated at the required set temperature, i.e. 30 °C for the AG and 32 °C for the RG. Changes in G′ and G″ were recorded for the first 6 h during the gelation process, followed by

the next 6 h at 4 °C (mimicking the storage conditions) within the same geometry. Both gels displayed similar final values, i.e. G′ ~ 262 Pa, G″ ~ 53 Pa and tan δ ~ 0.20 (Annexure 3). Ultimately, we were able to produce both gels with similar viscoelastic properties to investigate the impact of structure on the release of the bioactive compound through in vitro gastrointestinal digestion.

4.3.5 In vitro gastric digestion

The dynamic gastric model (HGS) designed by Fanbin Kong and Singh (2010) was used to perform the in vitro gastric digestion of the dairy gels. Simulated salivary fluid (SSF) and simulated gastric fluid (SGF) were prepared according to the INFOGEST standardized nature protocol (Brodkorb et al., 2019) with slight modifications. Briefly, a serving size of 200 g of both iso-caloric food systems was firstly diluted with pre-warmed SSF (pH 7), followed by the addition of CaCl2 to achieve a concentration of 1.5 mM in the final mixture. Samples were mixed and incubated for 2 min at 37 °C. To simulate the mastication process in the mouth, both the AG and the RG were stirred three times clockwise and anticlockwise each for 20 s, with a silicone spatula.

For the gastric phase, the fasting state of the stomach was mimicked by adding 28 mL of pre-warmed 1x concentrated SGF solution (pH 1.5) and pepsin to the oral bolus solution (Mudie et al., 2014; Steingoetter et al., 2006). This mixture was then introduced into the latex stomach of the gastric chamber (HGS) and maintained at 37 °C by a heater and a thermostat. The SGF (1.25x concentrated) and the pepsin solution were added using two separate pumps at rates of 2.0 mL/min and 0.5 mL/min respectively (X. Wang, Lin, Ye, Han, & Singh, 2019). To simulate the actual peristaltic contractions in the gastric chamber, the roller frequency was adjusted to 3 times per minute. A 60 mL feeding syringe was used to mimic the mixing during the back pressure applied by the duodenum. This syringe was filled with air and air was pumped

inside twice from the bottom before each gastric emptying, which allowed the mixing of the internal fluids and pushed the compact protein matrix (clot) that formed as a result of the digestion away. In this experiment, the digesta were emptied from the bottom of the chamber every 20 min at a rate of 2.5 mL/min and were filtered through a sieve with a pore size of 1 mm. The gastric digestion was carried out for 240 min and the emptying of 50 mL of gastric digesta from the bottom of the chamber was performed every 20 min at a rate of 2.5 mL/min. Samples were collected at different time intervals (20, 60, 120, 180 and 240 min) and were adjusted to pH 7 with 1 M NaOH and/or 1 M HCl (to stop the activity of pepsin). Each digesta sample was divided into two halves; the portions were stored at –25 °C and 4 °C for physicochemical characterization and intestinal digestion respectively.

4.3.6 pH measurement of gastric digesta

The pHs of the AG and the RG were recorded before and after mixing with SSF and fasting SGF. The initial pH refers to the pH of the fresh samples before adding SSF and the pH of the emptied digesta was recorded every 20 min, with the assumption that this corresponded to the pH within the HGS.

4.3.7 Total solids in digesta and clot

To determine the total solids contents of the digesta collected at different times and the clot obtained at the end of the digestion, samples were collected and dried at 105 °C overnight in a hot air oven. The dried mass of each sample was weighed and the total solids percentage was calculated as:

$$\text{Total solids content (\%)} = \frac{Dry\ weight\ of\ sample}{Initial\ weight\ of\ sample} \times 100$$

4.3.8 Measurement of oil content

The emptied digesta samples collected at different times were analysed using the AACC 30-10 Mojonnier ether extraction method, as previously described by X. Wang et al. (2019). Briefly, this extraction process occurs in two steps. Firstly, sample preparation involves weighing 10 mL of digested sample in a dry Mojonnier tube, with the addition of ammonium hydroxide solution and 2–3 drops of phenolphthalein, which are added to disperse the casein and sharpen the ether–aqueous interface respectively. Secondly, the extraction procedure involves the addition of ethanol, diethyl ether and petroleum ether, which extract the oil from the sample. These solvents were evaporated in a pre-weighed flask and the fat content was analysed gravimetrically.

4.3.9 Protein profile of gastric clot and emptied digesta

The time-dependent hydrolyses of the proteins in undigested and digested samples of the AG and the RG were analysed according to their molecular weight and separated using sodium dodecyl sulphate-polyacrylamide gel electrophoresis (SDS-PAGE) as described by Ye et al. (2016). Fresh samples and digesta from each time point were diluted fivefold with Milli-Q water and then mixed with sample buffer at a ratio of 1:1; 7 μL of each mixture was loaded on to the glycine gel. The electrophoresis analysis was conducted at 120 V for approximately 90 min. After staining and destaining, these gels were scanned using the Molecular Imager Gel Doc XR system (Bio-Rad Laboratories, Hercules, CA, USA). For solid samples, i.e. the gastric clot/curd, sample preparation and loading were performed according to the protocol described by X. Wang, Ye, Lin, Han, and Singh (2018). Briefly, 4.5 mg of freeze-dried sample was mixed with sample buffer and 10 μL was loaded in the well.

4.3.10 Microstructure of curds and gastric digesta

The arrangements of nanometre-sized lipid droplets entrapped within the acid or rennet protein matrix were examined using a confocal laser scanning microscope (Leica SP5 DM6000B; Leica Microsystems, Heidelberg, Germany). Fluorescent dyes, i.e. Nile Red (0.1% w/v in acetone) to stain the oil droplets and Fast Green (1.0% w/v in water) to stain the milk proteins, were firstly mixed with the samples to ensure a uniform dye concentration; this was followed by gel formation with acid and enzyme. A plastic ring was fixed on the flat surface of the glass slide using petroleum jelly; then a 300 µL sample was pipetted into the centre of the ring and covered with a glass coverslip. The sample was incubated in the chamber under the same conditions as described in Section 4.2.3. In addition, structural deformation during the digestion process at different times was examined using confocal microscopy. The solid curd samples and the liquid digesta, after 10 and 5 min of staining, were placed on the concave surface of confocal microscope slides (Sail; Sailing Medical-Lab Industries Co. Ltd, Suzhou, China) and were observed using oil immersion lenses.

4.3.11 In vitro intestinal digestion

The gastric digesta emptied at 20, 120 and 240 min were further subjected to in vitro static intestinal digestion according to the procedure described by Brodkorb et al. (2019). Briefly, 20 mL of simulated intestinal fluid [pH 7 and containing 10 mM bile and pancreatin (trypsin activity 100 U/mL)] was mixed with a gastric digestion sample in a digestion flask to achieve a final ratio of 1:1. The digestion was carried out for 2 h at 37 °C and the pH of the mixture was continuously monitored and adjusted back to 7 using 0.1 M and 1 M NaOH. The release of free fatty acids (FFAs) during the lipid digestion was measured using a pH-stat method and was calculated from the amount of NaOH needed to neutralize the FFAs using the following equation:

$$\frac{\mu mol_{fatty\ acid}}{mL_{gastric\ digesta}} = \frac{V_{NaOH}(t) - C_{NaOH} \times 1000}{V_{gastric\ digesta}}$$

Here V_{NaOH} (t) is the volume of NaOH used at digestion time t, μmol, C_{NaOH} is the concentration of the NaOH solution used to titrate the acid released in 2 h, i.e. 0.05 M, and $V_{gastric\ digesta}$ is the volume of the gastric digesta, i.e. 20 mL.

4.3.12 Particle and droplet size of gastrointestinal digesta

The mean particle sizes (D4,3) of the gastrointestinal digesta were immediately characterized using a static light scattering device (Mastersizer 2000; Malvern Instruments Ltd, Malvern, Worcestershire, UK). A mixture of 2% SDS and 50 mM EDTA was mixed with the gastrointestinal digesta at a ratio of 1:2 for 1 h to dissociate the casein micelles and measure the oil droplet size (D3,2). The mean particle diameter was calculated as the average of triplicate measurements on individual samples.

4.3.13 Curcumin encapsulation efficiency and bioaccessibility

The percentages of curcumin encapsulated in a nanoemulsion oil droplet, in the mixed micelle fraction and in the total intestinal digesta fraction were calculated according to the protocol defined by B. Zheng et al. (2018), with slight modifications. Briefly, 100 μL of nanoemulsion was diluted 50-fold with chloroform and was centrifuged using a Heraeus Multifuge X3R centrifuge (Thermo Scientific) at 3800 g and 20 °C for 15 min. The upper aqueous phase was sucked out of the tube and the bottom phase was measured at 419 nm using a UV spectrophotometer. The curcumin concentration in the separated chloroform layer was determined using a standard calibration curve; the curcumin concentration on the x-axis was plotted against the maximum absorbance (λmax) on the y-axis (data not shown). Linearity was studied using a regression equation, i.e. ($y = 0.1556x + 0.0065$; $R^2 = 0.9922$). The curcumin encapsulated inside the oil droplet was quantified using the following formula:

Encapsulation efficiency (%) = $\frac{C_{Nano}}{C_{Actual}} \times 100$

Here, C_{Nano} is the measured concentration of curcumin in the emulsion and C_{Actual} is the actual concentration of curcumin used in the formulation.

For both dairy gels, the intestinal digesta obtained at different times were divided into two fractions. One portion was centrifuged (38200 g and 20 °C for 30 min) with a T-865 rotor (Sorvall WX Ultra 100; Thermo Scientific, Asheville, NC, USA) to remove non-dissolved solids and to isolate the mixed micelle fraction containing solubilized curcumin. The mixed micelle fraction and the total digesta fraction were dispersed in chloroform, vortexed and centrifuged for 60 min at 3800 g to separate hydrophobic curcumin. The curcumin concentration was quantified using the standard curve (Annexure 1). The bioaccessibility of curcumin was calculated using the following equation:

Bioaccessibility (%) = $\frac{C_{micelle}}{C_{digesta}} \times 100$

Here, $C_{micelle}$ is the measured concentration of curcumin in the micelle phase and $C_{digesta}$ is the actual concentration of curcumin in the intestinal digesta.

4.2.14 Statistical analysis

T-tests and two-way analysis of variance tests were carried out using Minitab software (Minitab version 16; Minitab, Inc., State College, PA, USA) to determine the significance of the differences. Significance was established at $P < 0.05$. All tests were replicated twice with at least duplicates per sample.

4.4 Results and discussion

4.4.1 Change in the pH during gastric digestion

The pH profiles of the AG and the RG in the HGS with an increasing time of digestion are shown in Fig. 4.1. The pH of both gels decreased linearly during gastric digestion. At 0

min, after mixing the oral processed samples with SGF in the gastric chamber, the pH values of the AG and the RG were 4.30 ± 0.05 and 6.09 ± 0.01 respectively. The changes in the pH profiles observed during digestion of the dairy gels were affected by the initial pH of both gels; the final pH values of the gels were 2.07 ± 0.07 and 2.58 ± 0.15 for the AG and the RG respectively. The initial difference in the pH of the gels would have influenced the activity of pepsin and the consequent breakdown of the gels during digestion. For the AG, the pepsin activity during digestion would be expected to be relatively high because the initial pH of the gel was close to the optimal pH at which pepsin has its highest activity (pH ~ 2). This process would have been enhanced further with the gradual addition of SGF and the lowering of the pH.

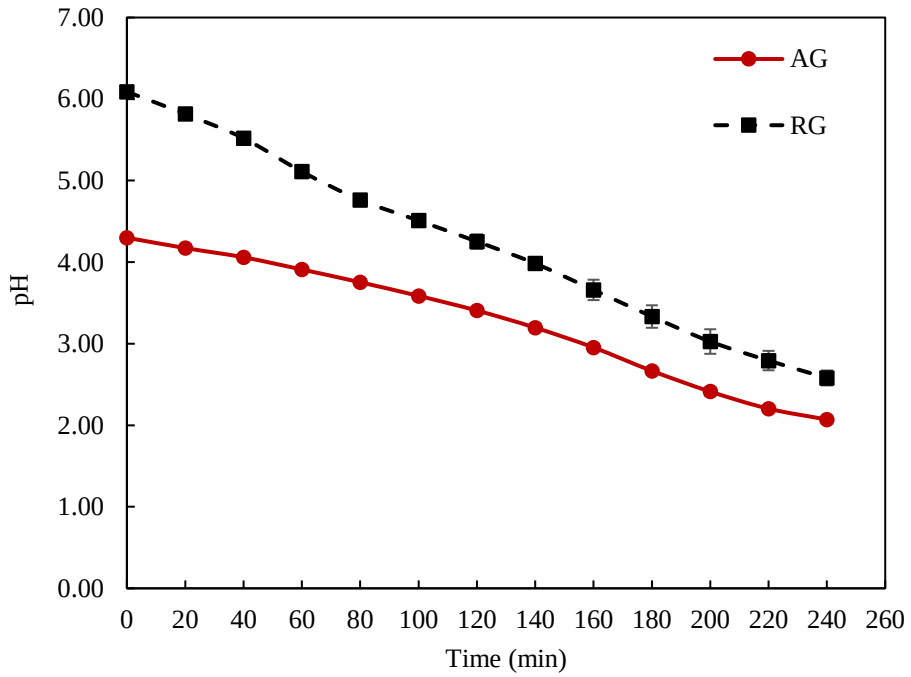

Fig. 4. 1 Changes in the pH of AG (acid gel) and RG (rennet gel) submitted to gastric digestion using a human gastric simulator.

4.4.2 Disintegration of gels during gastric digestion

The visual changes in the AG and the RG that occurred during digestion are shown in Fig. 4.2A. Because of the oral processing step and the mechanical action of the HGS, both gels were broken down into small pieces of curd-like particles. During gastric digestion, the AG curd particles disintegrated more rapidly than the RG curd particles. At 20 min, the curds formed by both gels appeared to be similar, i.e. watery, glossy and soft. However, thereafter, the volume of the AG curd rapidly became smaller and only very few curd particles (> 1 mm) were observed at 180 min. No AG curd particles remained in the gastric chamber at 240 min. This may have been due to the weakening of internal bonds of the casein micelles (because of the dissolution of micellar calcium phosphate) during AG formation, which facilitated the penetration of SGF and pepsin, resulting in a rapid hydrolysis (Floury et al., 2018). In contrast, the RG curd particles started to restructure into a dense protein network under the influence of the gastric fluids and transformed into numerous compact structured clots within the first hour of digestion. This initial shrinking of the RG protein network may have been a result of the microsyneresis that occurred because of the gradual addition of SGF (Le Feunteun & Mariette, 2008). There was little reduction in the apparent number of clots with an increase in the digestion time, as large amounts of curd particles were seen in the gastric chamber at 240 min. Barbé et al. (2014) conducted a similar study, in double-jacketed beakers, on the in vitro digestion of acid and rennet gels produced from skim milk. They observed a similar clotting phenomenon in the RG and attributed a lower level of residual casein in the RG gastric digesta to the retention of highly condensed particles in the stomach.

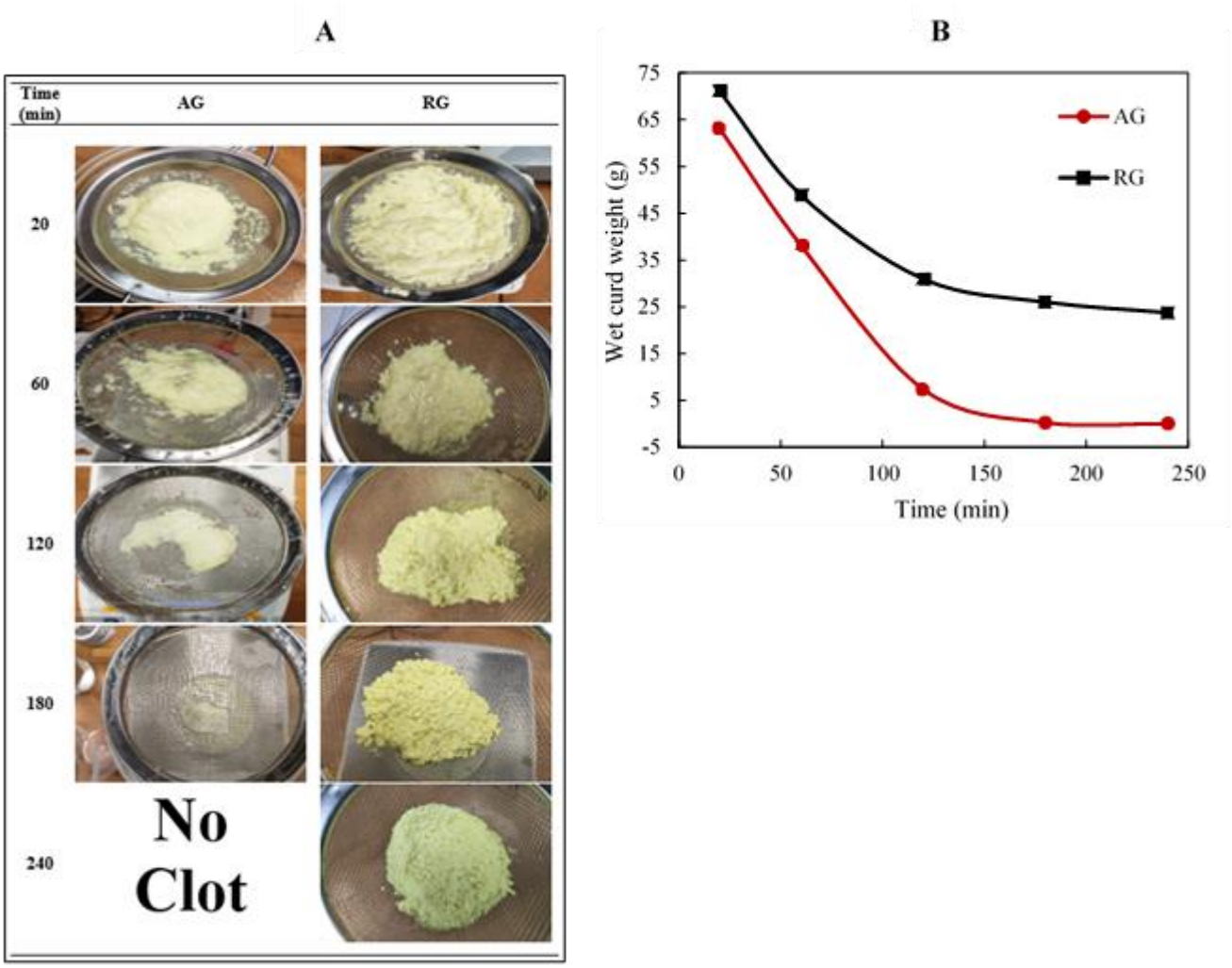

Fig. 4. 2 Images (A) and changes in wet weight (B) of curds formed by AG (acid gel) and RG (rennet gel) within the gastric chamber at selected time points.

To record the changes in the weight of the curd inside the HGS, the digestion process was stopped at different time points. The curd recovered was filtered through a sieve (1 mm) before weighing to remove excess gastric fluid. The weight of the AG curd retained within the HGS was about 62 g at 20 min and was significantly ($P < 0.05$) reduced to 0.17 g at 180 min, whereas the weights of the RG curd were 69 g and 23 g after 20 and 240 min of gastric digestion respectively (Fig. 4.2B). These results confirm previous studies that showed that the AG matrix had faster digestion kinetics than the RG matrix (Barbé et al., 2014; Floury et al., 2018).

The confocal micrographs showed different initial structures for the AG and the RG (Fig. 4.3, row M): the AG had a tighter protein network than the RG. In the AG, the casein particles showed higher interconnectivity, forming clusters and strands with small pores. However, the RG appeared to be more like a space-filling gel, in which the casein micelles clustered, showing a system-spanning network with a fractal-like appearance. The confocal image of the RG was similar to the micrograph of a rennet-induced skim milk gel reported by Lucey (2008).

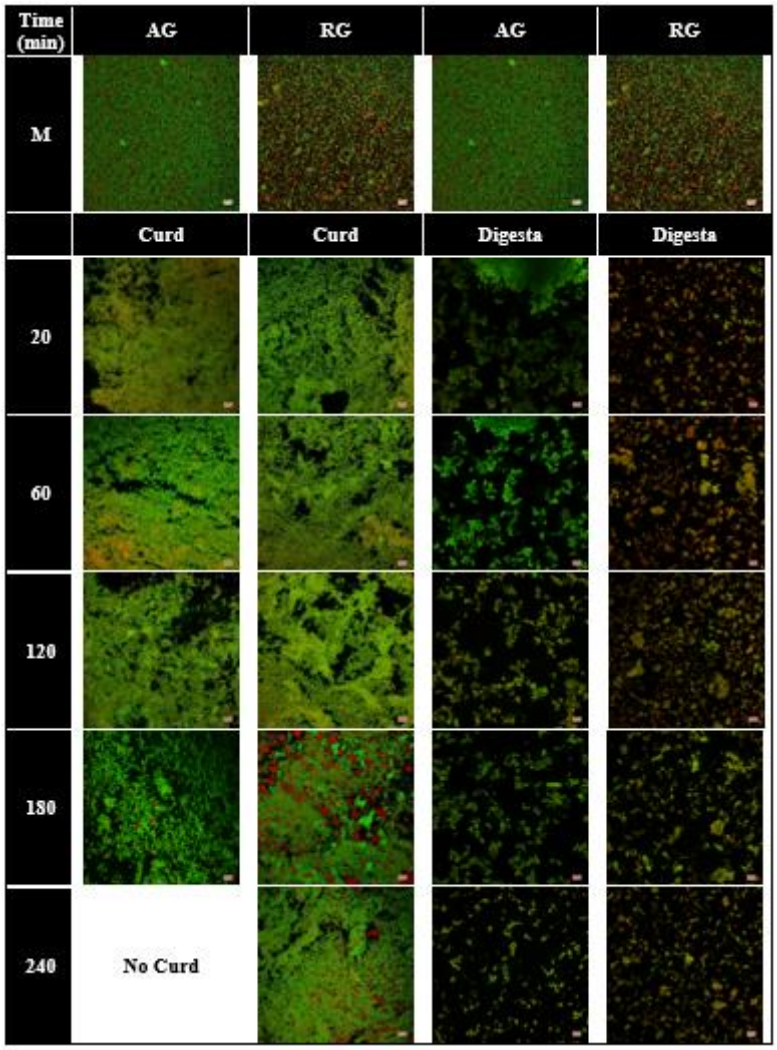

Fig. 4. 3 Confocal microscopy images of curcumin-nanoemulsion-loaded AG (acid gel) and RG (rennet gel) (row M) and their curds and digesta samples during gastric digestion at selected time points. Red colour represents the oil droplets and green shows the protein. The scale bar of all images is 10 μm.

Emulsified oil droplets in both gels were evenly distributed throughout the protein matrix, minimally influencing the structure of the curds (Figs. 4.3 AG curd and RG curd). The even distribution of the oil droplets can probably be explained by the absorption of sodium caseinate at the interface of the nanoemulsion droplets, which would facilitate these oil droplets becoming an integral part of the gel matrix (Sandoval-Castilla, Lobato-Calleros, Aguirre-Mandujano, & Vernon-Carter, 2004).

In the early stages of digestion of the AG (20 min), an open network of proteins entrapping homogeneously distributed emulsion droplets was observed in the curd recovered from the stomach. With an increase in the digestion time, this protein network became more open, with a large number of dark spaces, and the curd particles were much smaller after 180 min (Fig. 4.3, AG curd). At 240 min, all the curd particles were probably smaller than 1 mm, so that they were able to exist freely in the HGS chamber.

The microstructure of the RG curd at 20 min of digestion appeared to be more open than that of the AG curd (Fig. 4.3, RG curd). However, the protein network of the RG curd became denser with an increase in the digestion time, and the curd appeared to be a very close and fine-knitted mesh of protein with numerous uneven dark interspersed pores at long digestion times (240 min). The size of the oil droplets increased, indicating the possibility of coalescence during digestion. As well as coalescing, most of the oil droplets remained embedded within the protein network. These results are in agreement with our previous results; during the digestion of whole milk, most of the fat globules were retained in the gastric curd (Ye et al., 2016).

The protein composition of the curd retained in the HGS at different digestion times was determined using SDS-PAGE under reducing conditions (Figs. 4.4, A-C and B-C). The protein compositions of the gels before digestion were very similar, expect for the presence of one

prominent band at 15 kDa in the RG sample (lane M); this band represented para-κ-casein, produced by the action of rennet on κ-casein (Q. Li & Zhao, 2019).

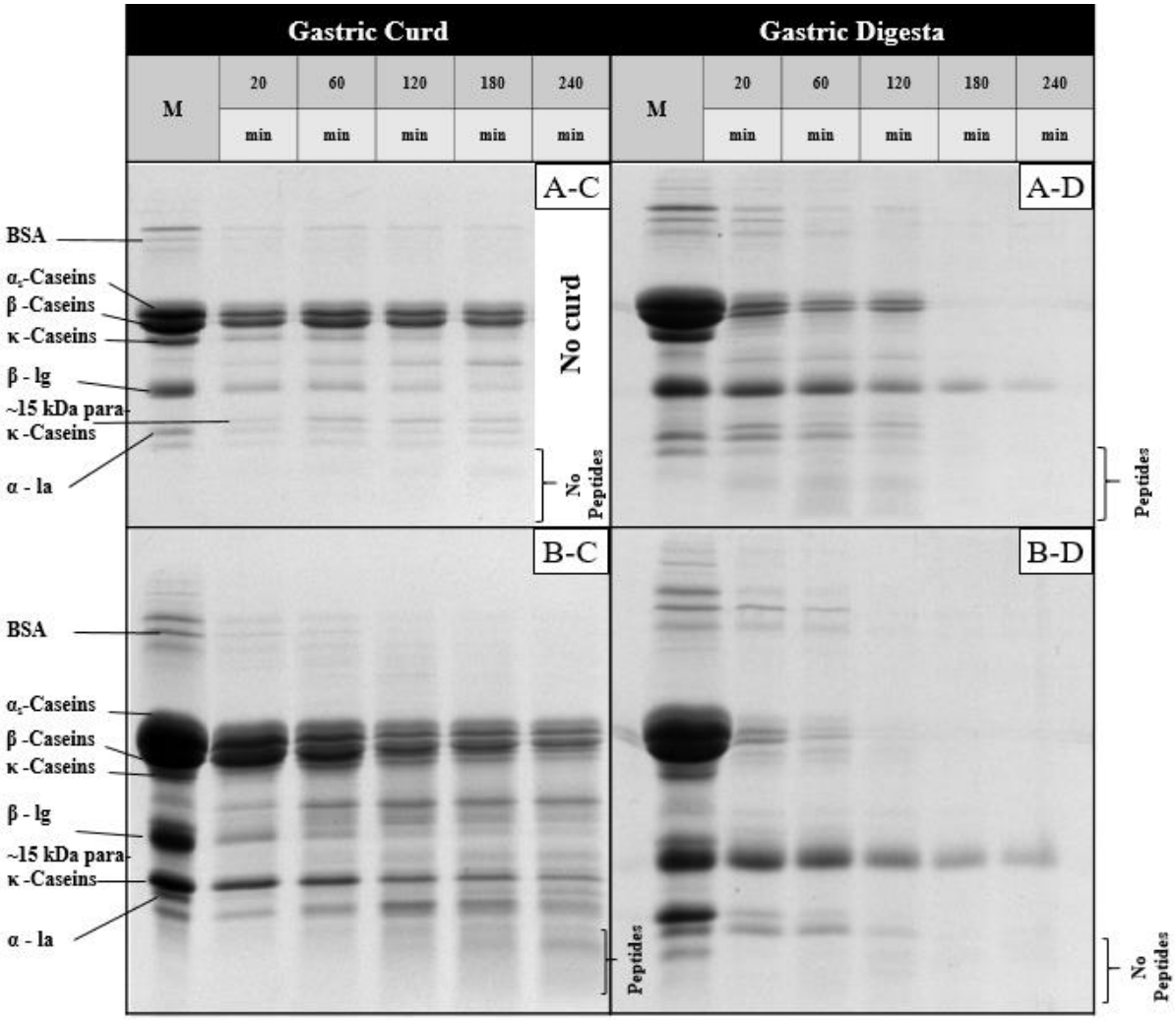

Fig. 4. 4 SDS-PAGE patterns under reducing conditions of gastric curd (C) and digesta (D) samples obtained at different time points of gastric digestion of AG (acid gel) (A) and RG (rennet gel) (B). M represents the native samples before digestion.

In the AG curds from the gastric digestion, the casein profile showed no significant changes in the intensities of the bands throughout the digestion; however, in the RG curds, the intensities of the casein bands appeared to decrease with an increase in the digestion time. The κ-casein band was still observed clearly in the curd of the AG at all digestion times, although there was a slight decrease in its intensity with an increase in the digestion time. At the same

time, a para-κ-casein band, which increased in intensity with time, was also observed (Fig. 4.4A-C). However, for the RG, the κ-casein band was not observed in the curd, and the para-κ-casein band decreased in intensity with increasing digestion time (Fig. 4.4B-C). In contrast, the whey protein bands were very faint in all curd samples during digestion (Figs. 4.4, A-C and B-C), indicating that they were not involved in the formation of the curd.

Interestingly, the patterns of many of the newly formed peptide bands appeared to be different for the gastric curd samples of the gels. The intensity and the number of peptide bands at each digestion time were considerably higher in the RG curd than in the AG curd (Fig. 4.4B-C). This may have indicated faster emptying of the peptides produced from the AG curd, whereas the restructuring of the RG curd during gastric digestion may have reduced the flux of protein and peptides into the digesta (see Section 4.3.3).

These differences in digestion behaviour between the gels can be related to the initial differences in coagulation. The coagulation of milk by rennet generally destabilizes the casein micelles by cleaving the C-terminal part (residues 106–169) of κ-casein, resulting in the less hydrophilic peptide (para κ-casein) on the surface of the micelles. These rennet-altered micelles have reduced steric stabilization and electrostatic repulsion and aggregate in the presence of calcium ions. In contrast, the pH changes (up to the isoelectric point of casein, i.e. pH 4.6) during the acid coagulation of milk result in a complete loss of colloidal calcium phosphate, shrinking of the κ-casein "hairs" and neutralization of the electrical charges of the casein, thus altering the internal structure of the casein micelle (Lucey, 2008). Apparently, a slight decrease in the concentration of colloidal calcium phosphate is associated with the casein micelles during pre-acidification of the milk prior to rennet gelation. However, this does not affect the structural features of the micelles (Choi, Horne, & Lucey, 2007).

4.4.3 Changes in the gastric digesta

The disintegration of the dairy gels during digestion led to different compositions of the digesta emptied from the HGS at different times. The changes in particle size of the emptied digesta during digestion were found to be significantly different for both gel structures (Fig. 4.5A). The size of the emptied AG particles in the gastric digesta gradually decreased from ~ 23 to ~ 2 µm over the digestion period. In contrast, the D4,3 value of the RG particles increased dramatically from ~ 29 to ~ 152 µm after 120 min of gastric digestion. Thereafter, the particle size decreased to ~ 51 µm at 240 min.

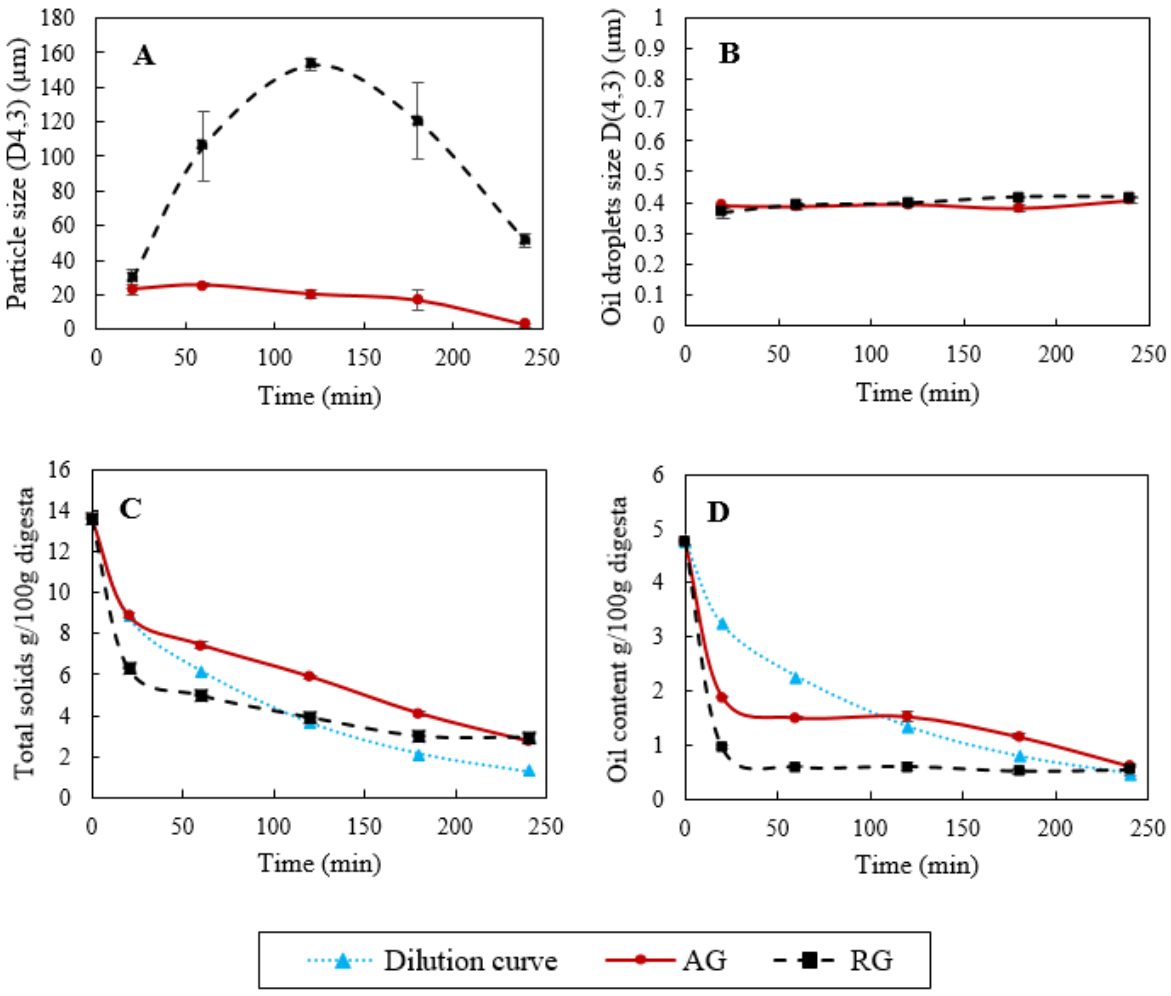

Fig. 4. 5 Changes in particle size ($D_{4,3}$) (A), oil droplet size ($D_{4,3}$) (B), total solids (C) and oil content (D) of gastric digesta during gastric digestion of AG (acid gel) and RG (rennet gel) in a human gastric simulator. Error bars indicate the standard error.

The droplet sizes of the emulsions embedded within the curd particles were found to be less affected during the gastric digestion (Fig. 4.5B). No change in the oil droplet size was observed in either the AG or the RG during digestion.

The total solids contents of the emptied digesta of the AG and the RG as a function of the digestion time are presented in Fig. 4.5C. This represents the number of small gel particles (< 1 mm) that passed through to the small intestine at different time points following the mechanical and enzymatic disintegration of the gels in the HGS. The total solids content of the emptied digesta of the AG during the first 60 min was significantly ($P < 0.05$) higher than that of the RG, indicating faster gastric emptying of the AG, which was due to faster disintegration of the gel, as discussed in Section 4.3.2. With further digestion, this difference was reduced and, at the end of the digestion, the total solids contents of the digesta of the AG and the RG became almost similar, i.e. 2.72 and 2.96 g respectively.

The oil contents of the emptied digesta of both gels also showed a significant difference ($P < 0.05$) (Fig. 4.5D); in the initial stages of digestion, the oil content was lower than the hypothetical calculated oil value (i.e. the dilution curve), based on dilution of the digesta because of the gradual addition of SGF. This indicates that the oil droplets were entrapped or embedded within the curd particles that were retained inside the HGS. The oil content of the AG digesta remained comparatively higher than that of the RG digesta at all digestion times except at 240 min. This is consistent with the slower disintegration of the RG gels than the AG gels, as discussed in Section 4.3.2.

The confocal microscopy images of the AG emptied digesta showed a continuous disintegration of interconnected protein networks in the gastric environment (Fig. 4.3, AG digesta). During the first 60 min of AG digestion, small fragments of gel particles with embedded oil droplets could be seen to be gradually disintegrating and the curd particles

appeared to be almost dissolved at 240 min (Fig. 4.3, AG digesta). Despite the reduction in the size of the curd fragments, the emulsified oil droplets appeared to remain uniformly distributed within the fragments. A similar disintegration behaviour was reported by Wooster et al. (2014) using static in vitro gastric digestion of a yoghurt emulsion stabilized by a mixture of monoglyceride and sodium caseinate.

Similarly, the emptied digesta of the RG at 20 min appeared to contain dense curd particles containing embedded oil droplets. These curd particles appeared to become larger and denser until 120 min, but then gradually became smaller and fewer particles were observed by the end of the gastric digestion (Fig. 4.3, RG digesta).

SDS-PAGE was used to analyse the protein composition of the digesta samples. At the beginning of the digestion of the AG (lane 20), the bands representing αs1-casein and β-casein were very prominent in the gastric digesta but their intensity decreased with an increase in the digestion time (Fig. 4.4A-D). For the RG, these bands were comparatively very faint and disappeared just after 60 min of digestion (Fig. 4B-D). These results agreed with our previous results, which showed faster gastric emptying of the total solids in the gastric digesta of the AG than the RG (Fig. 4.5C). Similarly, compared to RG digesta, the appearance of new peptide bands in AG digesta within 20 min of digestion (Figs. 4.4, A-D and B-D), indicates higher activity of pepsin. This might be due to the initial lower pH of AG closer to the pepsin optimum pH (~ 2) that may have influenced the faster cleaving of milk protein into peptides.

In contrast to the caseins, the intensity of the whey protein (β-lactoglobulin and α-lactoalbumin) bands in the emptied gastric digesta of both gels gradually faded, showing a similar decreasing trend with an increase in the digestion time (Figs. 4.4, A-D and B-D). The decrease in the intensities of the β-lactoglobulin and α-lactoalbumin bands was attributed to the dilution by SGF during the digestion (Ye et al., 2019).

These outcomes show that the different disintegration behaviours of the dairy gels within the dynamic gastric digestion model (the HGS) affected the size, composition and structure of the digesta delivered to the small intestine. The restructuring of the RG within the gastric chamber slowed the emptying of protein and oil droplets with solubilized curcumin in the digesta, in comparison with the AG, which underwent minimal structural changes with faster breakdown during the gastric phase.

4.4.4 Intestinal digestion

4.4.4.1 Changes in particle size

Gastric digesta samples emptied at selected time points for both dairy gel systems were further subjected to intestinal digestion. The pH of the emptied digesta was adjusted to 7 to stop the enzymatic activity of the pepsin. Fig. 4.6 shows the particle size distributions of gastric digesta samples at 20, 120 and 240 min during intestinal digestion. The trend of particle breakdown was found to be similar for both gels. At the beginning of intestinal digestion, large particles were broken down rapidly, resulting in shifting of the peaks at the higher end towards smaller sizes (0.1–1 μm). However, as the digestion proceeded, the area of the peaks representing small particles and large particles (~ 10–1000 μm) gradually increased and decreased respectively. A similar behaviour was observed by Salvia-Trujillo et al. (2017) while studying the gastrointestinal behaviour of carotenoid-enriched oil-in-water emulsions with various droplets sizes. They described the particles with smaller size, showing a peak at around 0.2 μm, as being mixed micelles, whereas the large particles, with a peak at around 10 μm, corresponded to undigested products. This increase in the conversion of oil droplets into mixed micelles during intestinal digestion has been linked with improved bioaccessibility of lipophilic bioactive compounds. Mixed micelles are likely to penetrate through the semipermeable mucus layer to reach the surface of epithelium cells, thus making the solubilized bioactive compound available for absorption (Rein, Renouf, Cruz-Hernandez, et al., 2013; B. Zheng et al., 2018).

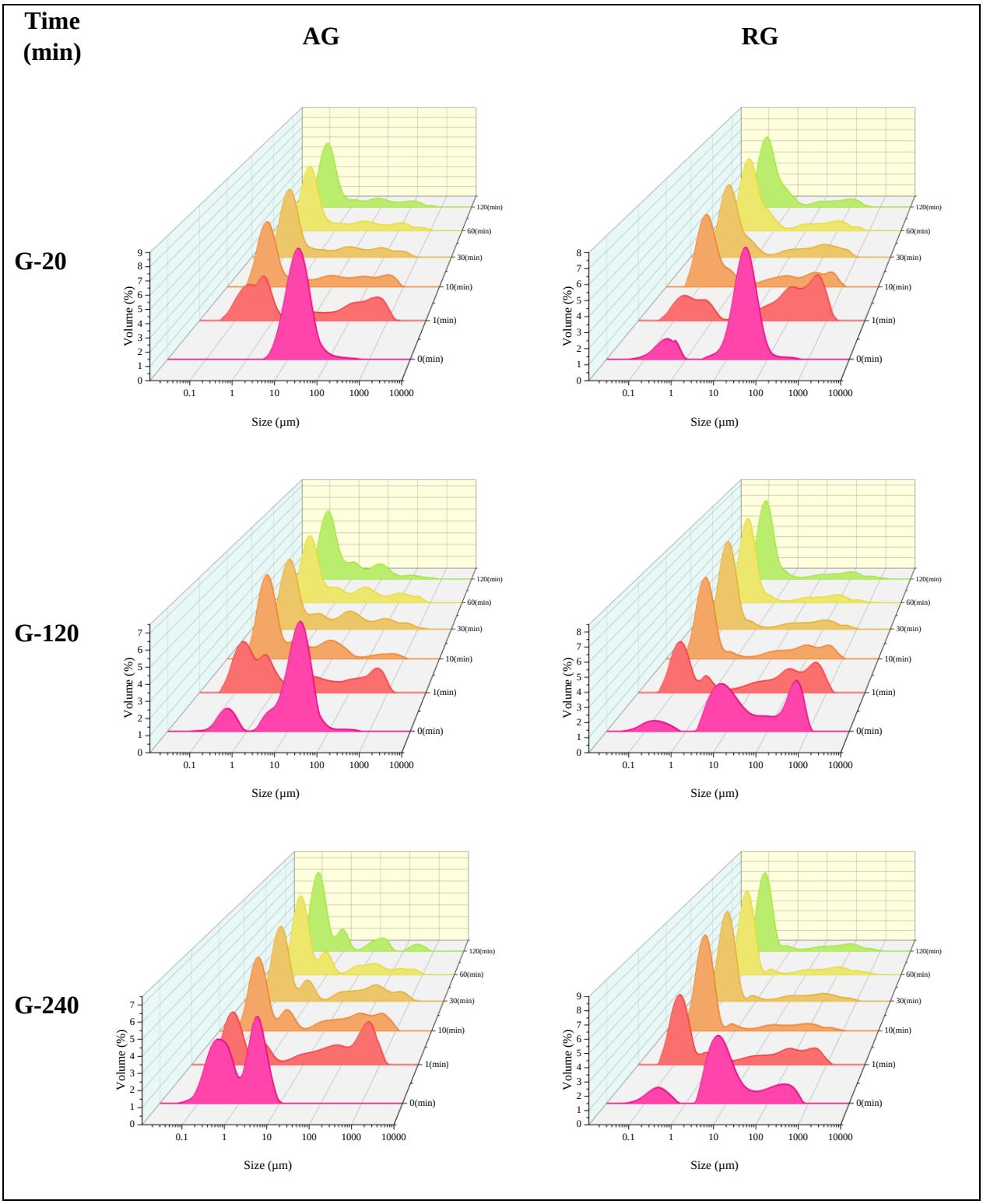

Fig. 4. 6 Particle size distributions of emptied gastric digesta (20, 120 and 240 min) before (0 min) and during the intestinal digestion of AG (acid gel) and RG (rennet gel) at different times (1, 10, 30, 60 and 120 min).

4.4.4.2 FFA release and curcumin bioaccessibility

The lipid digestion profiles of selected emptied gastric digesta of the AG and the RG were monitored during the small intestinal phase by determining the amount of FFA release (µmol) per millilitre of digesta sample (Fig. 4.7 A,B). The rate of lipolysis mediated by pancreatic lipase increased rapidly for both gels during the first 10 min of intestinal digestion and plateaued thereafter. This decrease in the lipolysis rate with the progression of intestinal digestion can be linked with the decreasing ratio of enzyme to oil (Guo et al., 2016) and/or aggregation of the digestion products formed as a result of lipolysis at the interface of the oil droplets (Giang et al., 2016). The release of FFAs from the AG digesta was markedly higher in the first 20 min of digestion (~ 63 µmol FFA/mL) than that from the RG digesta (~ 45 µmol FFA/mL) (Fig. 4.7B). Similarly, the amounts of FFA release in the gastric digesta samples emptied at 120 and 240 min respectively for AG and RG were 47 and 37 µmol FFA/mL and 25 and 27 µmol FFA/mL. The extent of FFA release from all the digesta samples of both gels was found to depend mainly on the oil content emptied in the gastric digesta at different times (Fig. 4.5D). This is in line with the previous study, in which the intestinal lipid digestion was influenced by the amount of oil emptied in the gastric digesta of different milk-protein-emulsified emulsions (X. Wang et al., 2019). Similarly, the gastric digesta particle and oil droplet size distributions of both gels may have influenced the variation in the lipid digestion during the intestinal phase. The large surface area of nanometre-sized oil droplets in the AG (smaller size, Fig. 4.5A) may have facilitated greater adsorption of lipase to the oil droplet surface, resulting in rapid hydrolysis of triglycerides into FFAs, even with a constant enzyme concentration (Salvia-Trujillo et al., 2017).

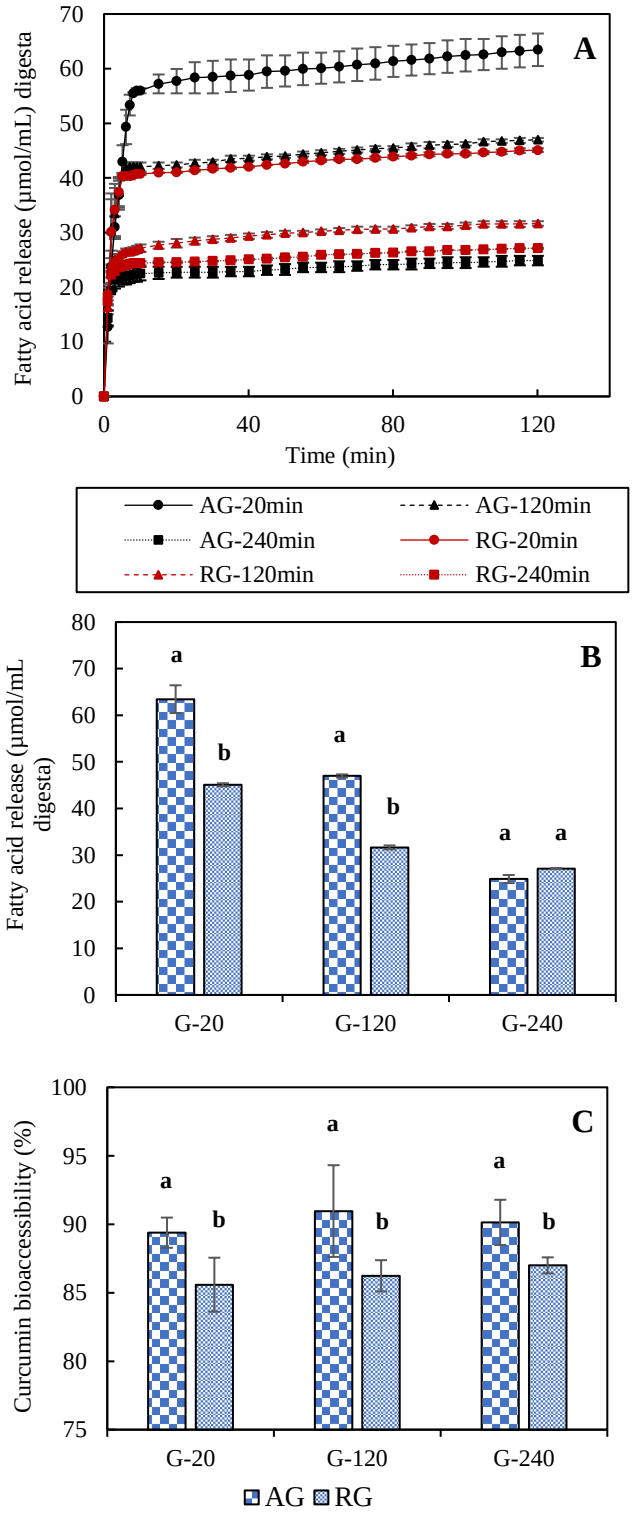

Fig. 4. 7 Effect of gel structure (AG, acid gel; RG, rennet gel) on free fatty acid release curve as a function of time (A), final concentration of released free fatty acid (B) and bioaccessibility of curcumin (C).

The bioaccessibility of curcumin ranged from around 85 to 91% and was dependent on the gel type (Fig. 4.7C). The bioaccessibility was relatively ($P < 0.05$) higher for the AG digesta samples (~ 90%) than for the RG digesta samples (~ 85%). The differences in curcumin bioaccessibility can probably be attributed to compositional and microstructural differences among the gastric digesta of both gels. Compared with the RG digesta, greater emptying of oil droplets in the AG digesta, with a more open structure of curd fragments, may have influenced the penetration of intestinal fluids, thus promoting the release of physically entrapped CNE. Previous studies have shown that these nanoemulsions enhance the incorporation of curcumin into the micelle phase because of their small size. These small oil droplets with larger surface area facilitate a faster lipolysis, and are subsequently transformed into mixed micelles with the aid of bile salts, facilitating solubilization of lipophilic curcumin, thus contributing to higher bioaccessibility (Öztürk, 2017).

In contrast to these compositional differences, the bioaccessible fraction of curcumin in the digesta samples with respect to their different emptying time points did not show any significant difference (Fig 4.7C). This suggests that different microstructure of both gel's fragments in gastric digestas may have influenced the transfer of curcumin toward the micellar phase during intestinal digestion. Similarly, the higher bioaccessibility of curcumin in the intestinal digesta samples of AG than that of RG at all digestion times indicates that the gel structure properties affected the release of curcumin in gastrointestinal fluids. This trend was basically similar to that observed in the FFA release from the AG and the RG (Fig. 4.7B). However, to confirm this association between the release of curcumin and the lipolysis of the oil droplets, as indicated by the release of FFAs, a correlation analysis was conducted (Fig. 4.8). The correlation coefficient for AG ($r = 0.9998$) and RG ($r = 0.9890$) indicated that the concentration of curcumin recovered from the intestinal digesta of both gels was positively correlated with the quantity of FFAs released. This finding is in accordance with Rao, Decker,

Xiao, and McClements (2013) and Mutsokoti et al. (2017); they observed a linear relation between FFA release and carotenoid bioaccessibility. Therefore, with a greater lipolysis, more curcumin could be released from the oil droplets and more FFAs could be incorporated into the mixed micelles, thus enhancing the solubility of curcumin in the mixed micelle phase.

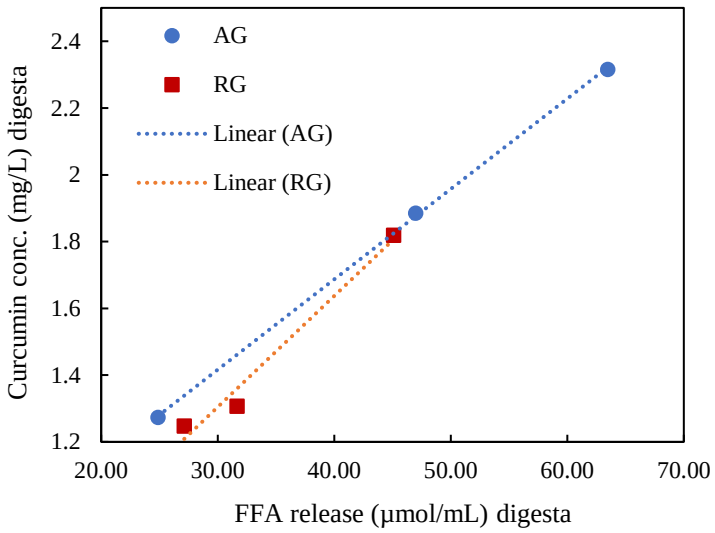

Fig. 4. 8 Correlation analysis of mean values (n = 2 independent *in vitro* digestions) obtained from free fatty acid (FFA) release and curcumin concentration in intestinal digesta samples.

4.5 Conclusions

The present study explored the influence of two complete dairy gel matrices (i.e. containing oil and protein) on the lipid digestion and bioaccessibility of a fortified CNE during gastrointestinal digestion. As both gels had the same composition and rheological properties, their different disintegration behaviours during dynamic gastric digestion directly influenced the emptying of oil droplets and the associated lipophilic curcumin from the stomach. The AG underwent faster disintegration and digestion in the gastric phase compared with the RG, which formed small gravel-stone-shaped clots and slowed the release of oil droplets and protein in the digesta, which resulted in greater digestion of lipid in the nanoemulsion and higher bioaccessibility of curcumin in the AG than in the RG. Further, gastric digesta samples emptied

at selected time points also had a significant impact on the release of FFAs and the concentration of curcumin during intestinal digestion. These findings highlight how the release of health-promoting bioactive compounds from functional foods can be manipulated by the complex dynamic processing behaviour within the gastrointestinal tract. This can further help in designing different therapeutic foods for specified populations.

.

Statement of contribution (DCR 16 forms)

MASSEY UNIVERSITY
TE KUNENGA KI PŪREHUROA
UNIVERSITY OF NEW ZEALAND

GRADUATE RESEARCH SCHOOL

STATEMENT OF CONTRIBUTION
DOCTORATE WITH PUBLICATIONS/MANUSCRIPTS

We, the student and the student's main supervisor, certify that all co-authors have consented to their work being included in the thesis and they have accepted the student's contribution as indicated below in the Statement of Originality.

Student name:	Haroon Jamshaid Qazi
Name and title of main supervisor:	Aiqian Ye / Professor
In which chapter is the manuscript/published work?	Chapter 5

Describe the contribution that the student and members of the supervisory team have made to the manuscript/published work:[1]

Haroon Jamshaid Qazi: Conceptualization, Methodology, Validation, Investigation, Formal analysis, Data curation, Writing – original draft, Visualization.
Aiqian Ye: Conceptualization, Methodology, Resources, Writing – review & editing, Project administration, Supervision, Funding acquisition.
Alejandra Acevedo-Fani: Writing – review & editing, Supervision.
Harjinder Singh: Conceptualization, Methodology, Writing – review & editing, Supervision.

Please select one of the following three options:

- ○ The manuscript/published work is published or in press
  Please provide the full reference of the research output:
- ◉ The manuscript is currently under review for publication
  Please provide the name of the journal:
  Food and Function
- ○ It is intended that the manuscript will be published, but it has not yet been submitted to a journal

Student's signature:	Haroon Jamshaid Qazi — Digitally signed by Haroon Jamshaid Qazi, DN: cn=Haroon Jamshaid Qazi, c=NZ, ou=Riddet Institute, email=h.j.qazi@massey.ac.nz, Date: 2023.06.20 11:13:08 +12'00'	Main supervisor's signature:	Aiqian Ye — Digitally signed by Aiqian Ye, DN: cn=Aiqian Ye, c=NZ, o=Massey University, ou=SF&AT, email=a.m.ye@massey.ac.nz, Date: 2023.06.20 12:13:05 +12'00'

This form should be placed at the beginning of each relevant thesis chapter.

[1] Refer to the Massey University Publishing and Authorship guidelines (OneMassey for staff, Stream for students) and/ or Contributor Roles Taxonomy (CRediT) guidelines for guidance.

Chapter 5: Impact of differently structured starch gels on gastrointestinal fate of curcumin-containing nanoemulsion

5.1 Abstract

In this study, we focused on the in vitro gastrointestinal digestion of curcumin-nanoemulsion-loaded corn starch gels formed using starches with different amylose contents, i.e. waxy (WCS), normal (NCS) and high amylose (HACS) corn starches and their impact on the release and bioaccessibility of curcumin. Curcumin nanoemulsion loading significantly increased the storage modulus of the WCS and NCS gels by interspersing in the gelatinized continuous phase, whereas it decreased in the HACS gel due to the formation of a weak network structure as a result of the incomplete gelatinized amylose granules. During the gastric digestion, the disintegration and emptying of the WCS+CNE gel from the stomach was the slowest compared to the other two gels. The changes in the stomach, influenced the emptying of total solids (HACS+CNE > NCS+CNE > WCS+CNE) into the gastric digestas, which further affected the rate of starch and lipid digestion during the intestinal phase. The HACS+CNE and NCS+CNE gels showed a higher and faster release of curcumin compared to WCS+CNE gel that showed a slower and sustained release during the intestinal digestion. This study demonstrated that the oral–gastric digestion of these starch gels was more dependent on the gel structures rather than on the molecular properties of starches. The dynamic gastric environment resulted in the formation of distinct gel structures, which significantly influenced the composition and microstructure of the emptied digesta, further affecting starch hydrolysis and curcumin bioaccessibility in the small intestine

.5.2 Introduction

Functional foods are highly valued because they provide significant physiological benefits and help to reduce disease recurrence in addition to providing basic nutrition. Dairy, bakery, confectionery, beverages and baby foods are some of the most popular food industry segments in which functional food products have been introduced (Khan et al., 2013; Menrad, 2003). Starch-based foods, such as bakery products, pasta, tortillas and cheese analogues, are widely consumed worldwide. The starch matrices in these products not only give the products their physicochemical and functional characteristics but also provide the human body with energy via hydrolysis into glucose units (J. Singh et al., 2013). The specific gelation and matrix formation properties of starches offer the potential to deliver various health-promoting bioactive compounds (Charalampopoulos, Wang, Pandiella, & Webb, 2002; Grossmann & McClements, 2021; Ötles & Cagindi, 2006).

The digestibility of pure starch-based foods during gastrointestinal digestion is markedly influenced both by the composition of the starch (i.e. amylose content, amylose chain length and amylose to amylopectin ratio) and by the texture and viscosity of the post-processing food matrix (Magallanes-Cruz et al., 2017; Pletsch & Hamaker, 2018; J. Singh et al., 2013). A recent study by M. Zheng et al. (2021) investigated the influence of different corn starch gel structures with different amylose contents on their disintegration behaviour during gastrointestinal digestion; during the oral–gastric digestion, starch hydrolysis in the gels was more dependent on the gel structure than on the molecular properties of the starch whereas, during the intestinal phase, the composition of the starch played a significant role. However, in the presence of other food components, such as proteins and lipids, their interaction with the starch during processing and digestion can alter the release of glucose (Y. Lu et al., 2019; J. Singh et al., 2010).

The fortification of food systems with lipophilic compounds such as curcumin is challenging because of their low chemical stability, poor absorption and poor water solubility (Francesco Donsì, 2018; D.J. McClements, Decker, & Weiss, 2007). Therefore, numerous studies have shown that emulsion based delivery systems can not only modify the dispersible status of curcumin in the food matrix but also improve its bioavailability during digestion (Araiza-Calahorra et al., 2018; Qazi et al., 2015; Sabet et al., 2021).

In the past few years, researchers have shown that the incorporation of emulsions into various food matrices affects their rheological and digestion profiles (Mun, Kim, Shin, & McClements, 2015; Qazi et al., 2021). Specific to starch-based oil-in-water emulsion gels designed by Dun, Liang, Li, Li, and Geng (2021), the addition of the emulsion significantly inhibited gelatinization and retrogradation, resulting in a delay in the digestion of three types of rice starch with different amylose contents. Similarly, the bioaccessibility of β-carotene was improved when it was delivered in an emulsion-filled hydrogel compared with in a conventional emulsion or a hydrogel (Mun, Kim, & McClements, 2015). To the best of our knowledge, all the published studies have demonstrated the changes in starch-based emulsion gels under static in vitro gastrointestinal conditions. Recent use of dynamic digestion units such as the human gastric simulator (HGS) has shown that the dynamic gastric phase has a significant influence on the physicochemical characteristics of the emptied digesta. In our previous study, emulsion gels based on acid or rennet gelation of milk showed different disintegration behaviours during the dynamic gastric phase (Qazi et al., 2021). However, unlike the protein structures, that are very sensitive to hydrolysis by pepsin in the stomach, the starches do not hydrolyze in the stomach. But, the distribution and volume percentage of the oil droplets in the emulsion, as well as their interaction with starches of different composition can affect the characteristics of the starch gels initially during gelation and further during gastrointestinal digestion.

Therefore, the aim of the present study was to understand the gelation and in vitro digestion properties of the curcumin nanoemulsion (CNE) loaded starch gels loaded that were formulated using waxy (WCS), normal (NCS) and high amylose (HACS) corn starch. Using the HGS, microstructural and compositional changes in the stomach and in the emptied digesta were investigated at selected timepoints. Their influence on the changes in particle size, lipid hydrolysis and curcumin bioaccessibility during the static intestinal phase were evaluated. These findings will be relevant to the development of starch-based functional food products supplemented with lipophilic bioactive components that may benefit human health.

5.3 Materials and methods

5.3.1 Chemicals and ingredients

Corn starches WCS (Avongel 3401x) and NCS (AVON) were obtained from New Zealand Starch (Auckland, New Zealand) and HACS (Hylon VII) was purchased from Ingredion (Auckland, New Zealand). The amylose content of WCS, NCS and HACS was ~ 0%, ~ 25% and ~ 70% respectively. Curcumin with a purity of 95% was obtained from Xi'an Lukee Bio-Tech Co. Ltd (Xi'an, China). Soybean oil (Essenté) was from Davis Trading Company (Palmerston North, New Zealand). Salivary α-amylase (3000 U/mL) was supplied by Megazyme International Ireland Ltd. (Bray, Ireland). Pepsin from porcine gastric mucosa (EC 232.629.3; P7000), pancreatin (EC 232.468.9; P7545) from porcine pancreas (8 x USP specifications) and bile bovine (EC 232.369.0; B3883) from porcine pancreas (8 x USP specifications) were acquired from Sigma-Aldrich (St. Louis, MO, USA). All additional chemicals and reagents were purchased from Sigma-Aldrich (Auckland, New Zealand) or Thermo Fisher Scientific (Auckland, New Zealand). All solutions were made with Milli-Q water (Millipore Corp., Bedford, MA, USA).

5.3.2 Preparation of starch gels loaded with CNE

Oil-in-water nanoemulsions (20% oil) loaded with curcumin were prepared following the method of Qazi et al. (2021). Briefly, 1% w/w of the emulsifier (sodium caseinate) in water at 25 ºC and 0.03% w/w curcumin in soybean oil at 60 ºC were stirred for 2 h, respectively. The oil and water phases were mixed and homogenized (APV 2000, Albertslund, Denmark) at 350/50 bar pressure to obtain nanoemulsion with an average particle size of ~ 187 nm. The prepared nanoemulsions were stored at 4 °C before being used in the preparation of starch gels.

Before being transferred to 30 mL plastic containers (33.50 mm in diameter and 16 mm in height), the three varieties of corn starch were dispersed in water for 2 h under continuous stirring. In each container, CNE was mixed with starch aqueous dispersion to achieve final starch and lipid contents in the suspension of 25% and 5%, respectively. The samples were placed in a water bath maintained at 95 °C, gently agitated for 2 min and then left to gel for another 28 min. After heating, the starch gels were cooled to room temperature and then transferred to a cold room at 4 ºC overnight before further analysis.

5.3.3 Pasting properties of starch gels loaded with CNE

A controlled-stress rheometer (MCR302, Anton Paar Physica, Graz, Austria) equipped with a starch cell (ST24-2D/2V/2V-30-SN18215) was used to measure the pasting properties of the starch gels loaded with CNE. The rheological measurements were made according to the protocol described by Dun et al. (2021) with slight modifications Briefly, 20 mL of a freshly made starch dispersions with CNE was poured into the rheometer cup and mixed for 1 min at 25 °C by rotating at a shear rate of 960 rev/s.Then, using the flow temperature ramp test, the temperature was increased to 95 °C at a rate of 2 °C/min for 20 min with a velocity of 160 rev/s. Finally, the rheometer was switched to small strain oscillation mode inside the linear

viscoelastic region (1% strain and 1 Hz frequency) and the temperature was reduced to 25 °C at a rate of 6 °C/min and then held for 30 min to track changes in the storage modulus.

5.3.4 Scanning electron microscopy

The microstructures of the starch gels loaded with CNE were examined by scanning electron microscopy. A small piece of sample from each gel was placed in primary fixative, i.e. modified Karnovsky's fixative (3% gluteraldehyde and 2% formaldehyde in 0.1 M phosphate buffer, pH 7.2), and allowed to fix overnight at room temperature. For each sample, three washes in phosphate buffer (0.1 M, pH 7.2) followed by dehydration in a graded ethanol series (25%, 50%, 75%, 95%, 100%) were performed for 15 min. Finally, the samples were washed for 1 h using 100% ethanol. Liquid CO_2 as the critical point fluid and 100% ethanol as the intermediary were used to critical point dry the sample using a Polaron E3000 series II critical point drying apparatus. Samples were mounted on to aluminium stubs using double-sided tape and sputter coated with approximately 100 nm of gold (Baltec SCD 050 sputter coater) before being observed in a FEI Quanta 200 environmental scanning electron microscope at an accelerating voltage of 20 kV. The images were captured at a magnification of 3000x.

5.3.5 In vitro digestion

An HGS was used for the gastric digestion of the starch gels loaded with CNE (Fanbin Kong & Singh, 2010). The gastric digestion followed the procedure reported previously by Qazi et al. (2021), integrating INFOGEST group specifications for starch-based food systems (Brodkorb et al., 2019; Mulet-Cabero, Egger, et al., 2020). The electrolyte compositions of all three simulated fluids, i.e. salivary (SSF), gastric (SGF) and intestinal (SIF), and the enzyme activity used in the protocol were does reported in Brodkorb et al. (2019).

The gels formed a day earlier were removed from cold storage and acclimatized to room temperature. A mechanical grinder (Breville, Model BFP100) was used to prepare simulated boluses of WCS+CNE, NCS+CNE and HACS+CNE (Fig. 5.1). All the gels were ground for 5 s. Then, 60 mL of SSF containing 75 U α -amylase/mL was mixed with 200 g of ground gel in a 1:1 ratio with the solids content of the sample (Mulet-Cabero, Egger, et al., 2020) for 2 min at 37 ºC. To emulate the fasting state of the human stomach, 28 mL of SGF (1x concentration, including pepsin) was added to the bolus mixture at the beginning of the gastric phase. During digestion, the HGS maintained the flow rates of SGF (1.25x concentration) and pepsin at 2.0 and 0.5 mL/min respectively, ensuring the correct composition of the final SGF in the gastric chamber (Fig. 5.1). The rollers in the HGS contracted three times per minute to mimic the stomach's natural peristaltic movement. To imitate the effects of gastric sieving, after every 20 min, the digesta sample (50 mL) was filtered through a 1-mm pore mesh, which prevented the emptying of bigger particles. The pH of the gastric digesta was promptly monitored at every 20-min interval and the digesta samples at selected timepoints were transferred to the cold room at 4 °C for physicochemical analysis and intestinal digestion.

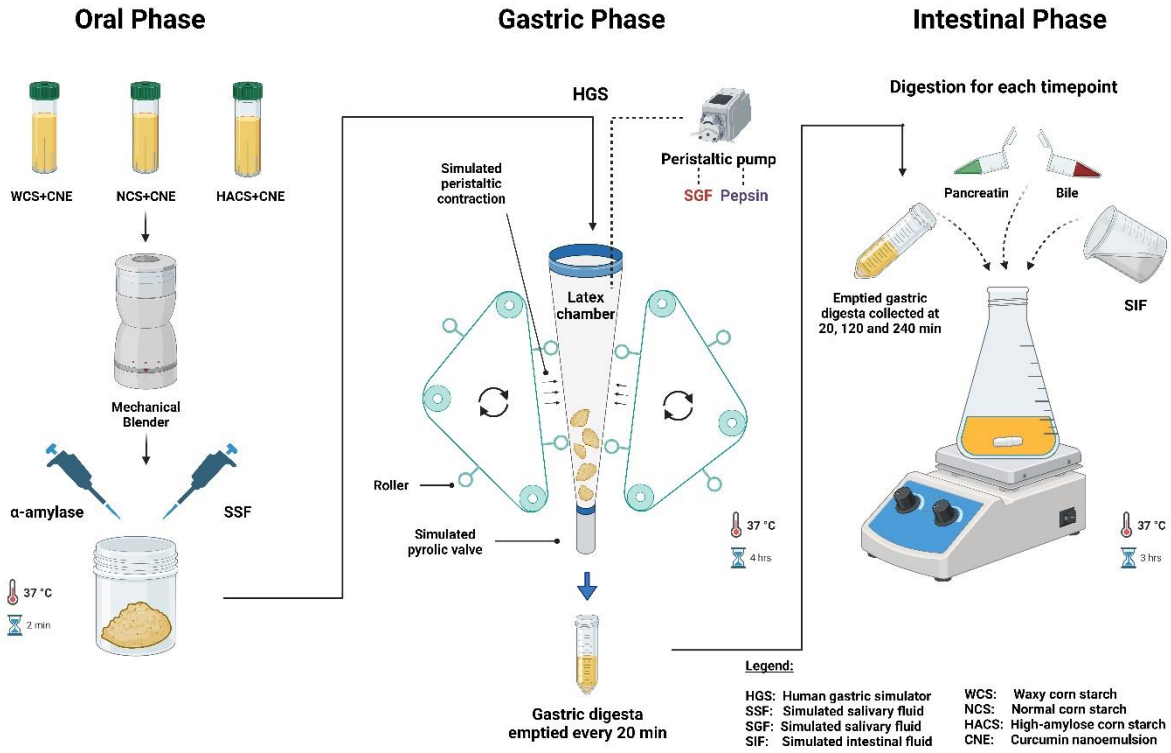

Fig. 5. 1 Graphical and schematic representation of the in vitro digestion of starch gels with curcumin nanoemulsion.

During the gastric digestion time of 240 min (Ye et al. 2016), the process was stopped at 20, 120 and 240 min to examine physical changes in the gel structures within the gastric compartment. These fractions were called the emptied digesta. To separate the starch gel fragments from the aqueous phase, the chyme of the HGS was collected and passed through a 1-mm sieve. When it was practicable, each sample's wet weight was determined in duplicate.

5.3.6 Changes in total solids and lipid content in the emptied digesta

The total solid content of the empty digesta samples obtained at different digestion times from different starch gel samples were determined by drying the samples in an hot air oven for overnight at 105 °C and the lipid content was quantified using the Mojonnier ether extraction method described in our previous study Qazi et al. (2021).

5.3.7 Changes in microstructures of gastric contents

A confocal laser scanning microscope (Leica SP5 DM6000B; Leica Microsystems, Heidelberg, Germany) was used to investigate the microstructures of the different starch gels, i.e. WCS+CNE, NCS+CNE and HACS+CNE, and the arrangement of the entrapped nanoemulsion before and after digestion. A solution of 0.1% (w/v) Fluorescein 5(6)-isothiocyanate in ethanol was used to stain starch (argon laser with excitation at a wavelength of 488 nm) and 0.1% (w/v) Nile Red in acetone was used to stain oil droplets (DPSS laser with excitation at a wavelength of 561 nm). To see the distribution of nanoemulsion within the different starch gels, the gels were produced in plastic rings fixed on the glass slides, according to the procedure described in Qazi et al. (2021). In addition, the microstructural changes in the gel structure within the gastric chamber and in the emptied digesta during the digestion process were examined at different times. The stained samples were placed on double concave microscope slides and visualized under a 63× oil immersion lens.

5.3.8 Particle and oil droplet sizes of gastrointestinal digesta

The mean particle sizes ($D_{4,3}$) of the gastrointestinal digesta collected at selected timepoints were determined using a Mastersizer 2000 (Malvern Instruments Ltd, Malvern, Worcestershire, UK). An emptied digesta sample at a selected timepoint was immediately added to an automated small volume sample dispersion unit (Hydro2000S). For the calculations in the system, the refractive index of the dispersed phase was 1.456 and that of the continuous phase was 1.33. The average particle sizes of the emptied digesta were measured in triplicate.

5.3.9 Free fatty acid (FFA) release during intestinal digestion

The gastric digesta emptied at 20, 120 and 240 min were further submitted to in vitro intestinal digestion (Fig. 5.1). The INFOGEST in vitro digestion protocol was used to imitate in vitro intestinal digestion under static conditions (Brodkorb et al., 2019). To reach a final

ratio of 1:1, 20 mL of SIF containing 10 mM bile and pancreatin (trypsin activity 100 U/mL) was mixed with a gastric digestion sample in a digestion flask. The intestinal digestion was carried out at 37 °C for 3 h, and the pH of the mixture was constantly checked and corrected to 7 using 0.1 M and 1 M NaOH.

The release of FFAs during lipid digestion was detected using a pH-stat technique and calculated using the following equation:

$$\frac{\mu\text{mol}_{fatty\ acid}}{mL_{gastric\ digesta}} = \frac{V_{NaOH}(t) - C_{NaOH} \times 1000}{V_{gastric\ digesta}}$$

where $V_{NaOH}(t)$ is the volume of NaOH used at digestion time *t*, µmol, C_{NaOH} is the concentration of the NaOH solution used to titrate the acid released in 2 h, i.e. 0.05 M, and $V_{gastric\ digesta}$ is the volume of the gastric digesta, i.e. 20 mL.

5.3.10 Starch hydrolysis of intestinal digesta

Following gastric digestion, the hydrolysis of all three starch systems during the digestion of intestine was quantified using the method described by (Do, Singh, Oey, & Singh, 2019). Initially, the total starch content at the selected timepoints of gastric digestion was determined using the Megazyme total starch kit. Further, the Megazyme D-glucose assay kit (GOPOD-FORMAT, K-GLUC, Megazyme International Ireland Ltd.) was used to measure the glucose content of gastric digesta samples at 0 min and at 2, 20, 40, 60, 90, 120, 150 and 180 min of intestinal digestion. To stop the enzymatic activity, 3 mL of absolute ethanol was combined with 0.5 mL of duplicated aliquots of digesta samples. The resulting mixtures were vortexed and centrifuged for 30 min at 3800 x *g*. In addition, the soluble dextrins in 0.1 mL of ethanolic supernatant were completely digested to glucose for 10 min at pH 5.2 and 37 °C using 0.5 mL of acetate buffer containing 0.1 mL of amyloglucosidase and 3.75 mg of invertase per 10 mL of acetate buffer. The samples were recentrifuged and 0.1 mL of the supernatants were mixed

with 3 mL of GOPOD reagent; they were incubated at 50 °C for 20 min and the absorbances were measured at 510 nm using a UV spectrophotometer. The percentage of starch hydrolysis was calculated using the following equation:

$$\%\ Starch\ Hydrolysis\ = 0.9\ \times \frac{G_p}{S_i}$$

Where G_p is the glucose produced and S_i is the initial amount of starch.

5.3.11 Curcumin bioaccessibility

The fraction of curcumin that was released from the emulsion gel in the gastrointestinal tract after lipid digestion and that became available for intestinal absorption was defined as the curcumin bioaccessibility. At the end of the small intestinal phase, each sample was separated into two sub-samples. One sub-sample was centrifuged at 38,000 x *g* for 30 min using a T-865 rotor (Sorvall WX Ultra 100; Thermo Scientific, Asheville, NC, USA) to separate the clear middle layer (i.e. the mixed micelle; $C_{Micelle}$). To extract the curcumin from the raw digesta ($C_{RawDigesta}$), the second sub-sample of intestinal digesta mixture was used. For both, 2 mL of each sub-sample were mixed with 10 mL of HPLC-grade ethanol in different tubes and vortexed for 30 s. The sample was then centrifuged (13,000 x *g*, 10 min) to exclude any traces of excess biopolymers or bile salt debris and the supernatant layer was filtered through a 0.22 µm filter before high performance liquid chromatography (HPLC). An HPLC method for the quantification of curcumin was employed as described earlier by (Sabet et al., 2021) with slight modification. Curcumin was quantified using a 1200 HPLC system (Agilent Technologies, Santa Clara, CA, USA) controlled by EziChrom software (Agilent Technologies) and equipped with an autosampler and a Synergi Hydro-RP 4 µm analytical column (150 mm x 4.6 mm, 4 µm, Phenomenex, Torrance, CA, USA). Curcumin was detected at 425 nm (25 °C) using a mobile phase containing 5% acetic acid and acetonitrile (25:75). The relationship between curcumin and the detected concentration in ethanol was linear between 0.1 and 10 µg

curcumin/mL (r^2 = 0.999) and the standard curve was produced accordingly. The following equation was used to calculate the curcumin bioaccessibility:

$$\text{Bioaccessibility (\%)} = 100 \times \frac{C_{Micelle}}{C_{RawDigesta}}$$

Where $C_{Micelle}$ and $C_{Raw\ Digesta}$ are the concentrations of curcumin in the micelle fraction and the raw digesta respectively after intestinal digestion.

5.3.12 Statistical analysis

Data plotting and statistical analysis (one-way analysis of variance and Tukey's multiple comparison test) were performed using Minitab software (Minitab version 16; Minitab, Inc., State College, PA, USA). Differences were considered to be statistically significant at a level of $p < 0.05$. All of the gels' digestion experiments were run at least twice, with each sample being examined in triplicate. Data were shown as the mean ± standard deviation.

5.4 Results and discussion

5.4.1 Characterization of gels

Figs. 5.2(A) and 1(B) show the pasting properties of the various corn starches loaded with CNE. The pasting onset temperatures of the WCS+CNE and NCS+CNE gels were within the range 65–67 ºC whereas that of the HACS+CNE gel was above 80 ºC [Fig. 5.2(A)]. The higher gelation temperature exhibited by HACS has been linked to β-type crystalline amylopectin and the double helix orientation of amylose, both of which inhibit swelling by maintaining the integrity of the starch granules; thus a higher temperature and greater energy input are required for the granules to become disordered (Huang et al., 2015; Richardson, Jeffcoat, & Shi, 2000). Compared with the WCS+CNE gel, the NCS+CNE and HACS+CNE gels were firm because amylose contributed to the gel strength and firmness (Kibar, Gönenç, & Us, 2010). The NCS+CNE gel reached its peak viscosity in a relatively short time, with the

WCS+CNE and HACS+CNE gels taking longer. The NCS+CNE gel had the highest pasting viscosity and the HACS+CNE gel had the lowest [Fig. 5.2(A)]. Moreover, the peak viscosities of the WCS+CNE and NCS+CNE gels were significantly higher than those of the gels without CNE (Annexure 4). This was attributed to the emulsion droplets acting as active fillers in these gels, which interspersed into the continuous phase of the system and thus elevated the effective concentrations of the continuous phase and increased the viscosity of the system (Dun et al., 2021; Q. Wang et al., 2023). In contrast, the HACS gels showed no significant change in peak viscosity, indicating that the incomplete gelation because of the higher amylose content did not allow the emulsion droplets to interact within the continuous phase which can be also observed in the HACS+CNE scanning electron microscopy image (Fig. 5.3C).

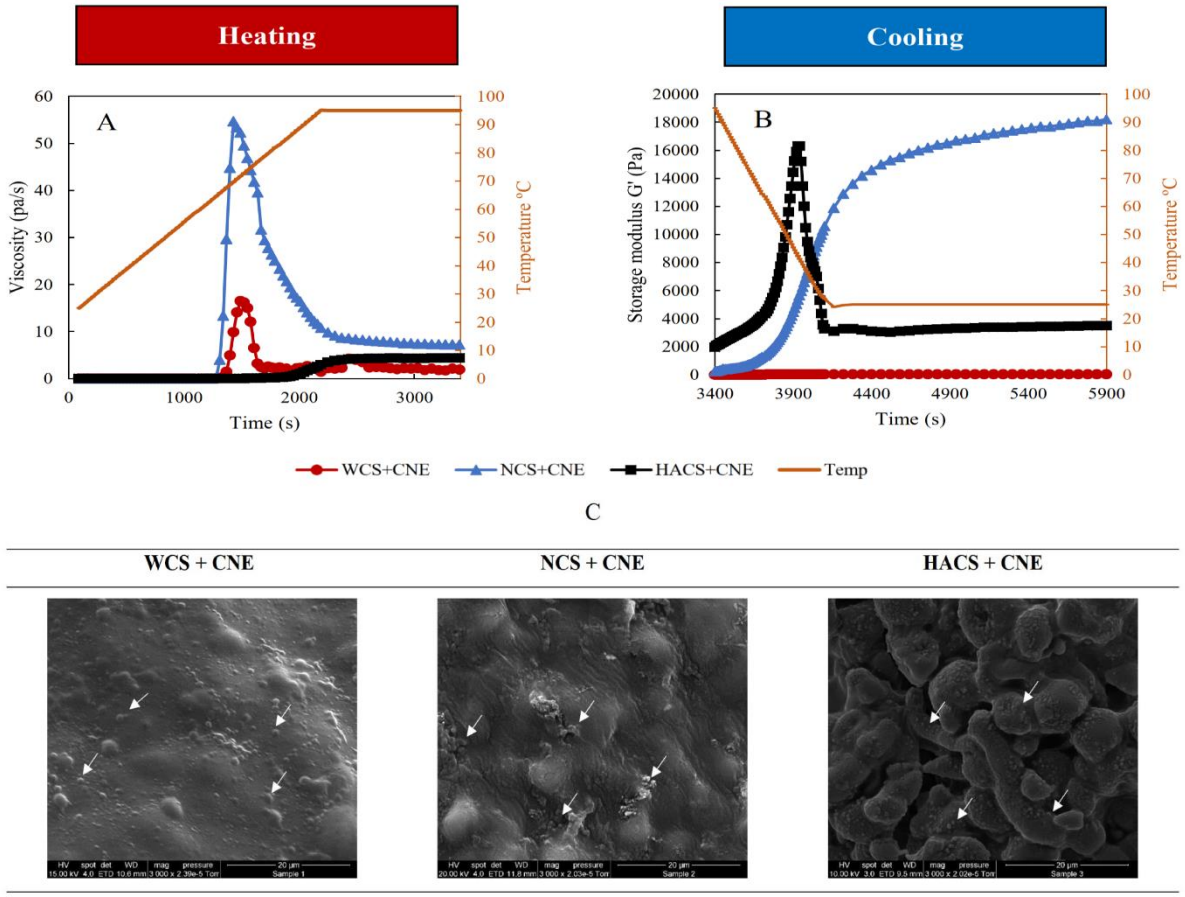

Fig. 5. 2 (A, B) Pasting profiles of different corn starch solutions with curcumin nanoemulsion (CNE). (A) Development of viscosity (Pa.s) during heating (25–95ºC) and (B) change in storage modulus (G') during cooling (95–25 ºC) of the starch gels. (C) Microstructures of starch gels loaded with CNE using scanning electron microscopy at 3000x magnification. White arrows indicate CNE in the gel matrix. WCS, waxy corn starch; NCS, normal corn starch; HACS, high amylose corn starch.

The G' values of the starch gels loaded with CNE were determined during the cooling stage and the holding stage [Fig. 5.2(B)]. They increased rapidly as the temperature dropped below 60 ºC. The final G' values of the WCS+CNE and NCS+CNE gels were approximately 1.5 and 2 times higher than those of the gels without CNE [Fig. 5.2(B) and Annexure 4 Fig. 4.1(B)], indicating that caseinate-stabilized emulsion droplets played a significant role in strengthening the gel matrix by acting as an active filler. Similar results were observed by Torres, Tena, Murray, and Sarkar (2017), who demonstrated that an octenyl-succinic-

anhydride-stabilized emulsion acted as an “active filler” in gels prepared with native wheat starch, which further raised the storage modulus of the gels. In contrast, for the HACS+CNE gel at 50 ºC, the G’ decreased from 16,000 Pa to less than 4000 Pa by the end of the cooling stage [Fig. 5.2(B)] whereas it kept on increasing for the HACS gel without CNE [Annexure 4]. The formation of a weak network structure, in addition to the high amylose content, may have been produced by the CNE, which may have disrupted the long-range interactions of amylose within the gel, resulting in lower structure cohesiveness and early exudation of water because of amylose retrogradation (Weber, Clerici, Collares-Queiroz, & Chang, 2009; Zhao, Li, Wang, & Wang, 2022).

This suggestion was confirmed by microscopic examination of the surface of the starch gels loaded with CNE [Fig. 5.2(C)]. All the gels containing CNE had a nodular appearance [Fig. 5.2(C), white arrows], which was absent in the gels without CNE [Annexure 4]. The WCS+CNE gel had the continuous and homogeneous microstructure of a gel-like network with solubilized amylopectin, whereas the microstructure of the NCS+CNE gel confirmed the non-uniform surface, showing the involvement of amylose granules filled into the almost intact amylopectin network. In the NCS+CNE gel, the amylose granules and the CNE played the same role as the gravel stones and sand particles in a cement mixture (i.e. a gelatinized amylopectin network), providing strength to the structure. However, in contrast, the microstructure of the HACS+CNE gel differed significantly. The CNE can be seen to be embedded in the solubilized amylopectin layer surrounding only the surface of the swollen amylose granules, which may have prevented both (i.e. the CNE and the amylose crystalline structure) from contributing to the gel strength (Fig. 5.3). Moreover, the dark space between the granules confirmed the porous nature of the gel and the fact that it was not completely intact, which could have played a role in the exudation of water that was observed during cold storage.

5.4.2 Oral–gastric phase

5.4.2.1 Physical changes in gel structure during oral–gastric digestion

The changes in gel structure before and after oral–gastric digestion were observed visually after the gels had been passed through a 1-mm sieve to separate the liquid fraction [Fig. 5.3(A)]. All three starch gels demonstrated significantly distinct features in the appearance when mimicking the mastication step with a mechanical grinder. Even after being ground, the WCS+CNE gel retained its slimy and sticky appearance (Annexure 5 Fig. 5.1). However, the NCS+CNE gel disintegrated into smaller fragments and the HACS+CNE gel transformed into a coarse paste [Fig. 5.3(A) Initial]. Further, to visualize the structural changes in the appearance during the dynamic gastric phase, the digestion was stopped at selected timepoints, i.e. 20, 120 and 240 min, and the gels were separated from the liquid fraction (Fig. 5.3; G20, G120 and G240). The WCS+CNE gel appeared to be slimy at all three timepoints, but its adhesiveness appeared to be slightly reduced as the digestion progressed. In contrast, the structures of the NCS+CNE and HACS+CNE gels changed significantly during the gastric digestion. At 20 min, NCS gel fragments transformed into a mushy paste, whereas the HACS+CNE gel appeared to be a lumpy paste. Both gel structures became dry in appearance as the digestion progressed, with the NCS+CNE gel appearing to be grainy and the HACS+CNE gel appearing to be lumpy at 120 and 240 min. The acid hydrolysis, enzymatic digestion and mechanical contraction used in the HGS were probably responsible for these changes during the gastric digestion (M. Zheng et al., 2021).

The recorded mean weights of the gel structures retained within the HGS revealed that the WCS+CNE gel disintegrated much more slowly than the other three gels; the weight of the WCS+CNE gel decreased from 146 to 97 g whereas the weights of NCS+CNE and HACS+CNE reduced from 103 to 45 g and 68 to 13 g respectively by the end of the digestion time These differences in the gel disintegration behaviours in the HGS can be attributed to the

different initial rheological properties of the gel structures, which were influenced by the ratio of amylopectin to amylose.

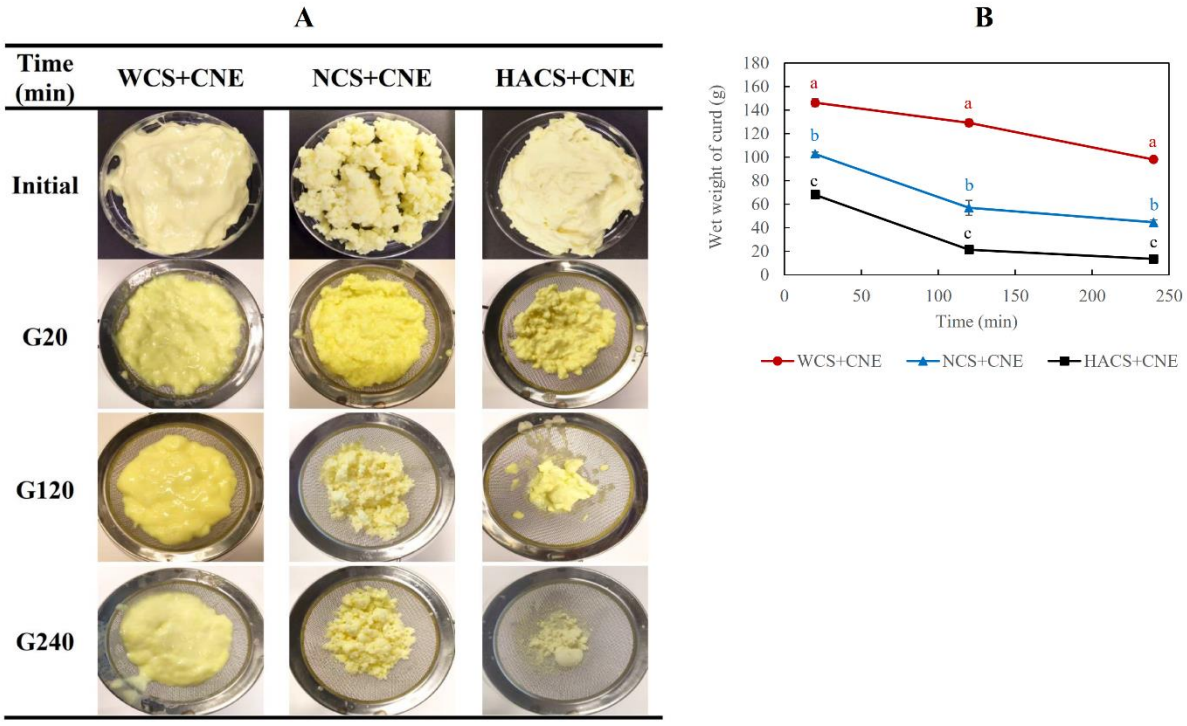

Fig. 5. 3. (A) Visual appearance of the starch gel structures after grinding and before mixing with the SSF (Initial) and within the gastric chamber during the digestion of 200 g of starch gel, i.e. waxy corn starch (WCS), normal corn starch (NCS) and high amylose corn starch (HACS) loaded with curcumin nanoemulsion (CNE). (B) Changes in the wet weight of the starch gels at 20 (G20), 120 (G120) and 240 (G240) min of gastric digestion.

5.4.2.2 Microstructures of gastric chyme and emptied digesta

The confocal micrographs showed different initial structures for the WCS+CNE, NCS+CNE and HACS+CNE gels (Fig. 5.4, row 0): the WCS+CNE gel had a completely gelatinized starch matrix in which encapsulated oil droplets were randomly entrapped. In contrast, the NCS+CNE gel structure was very compact with swollen starch granules, whereas the HACS+CNE gel had more irregular oval-shaped and slightly gelatinized starch granules, which is consistent with previous reports (X. Chen et al., 2017; M. Zheng et al., 2021) and also corresponds with the earlier scanning electron microscopy images [Fig. 5.2(C)]. Furthermore,

the WCS+CNE gel revealed more dark spaces within the gel, which could explain its loose gel network and lower gel strength (Fig. 5.4).

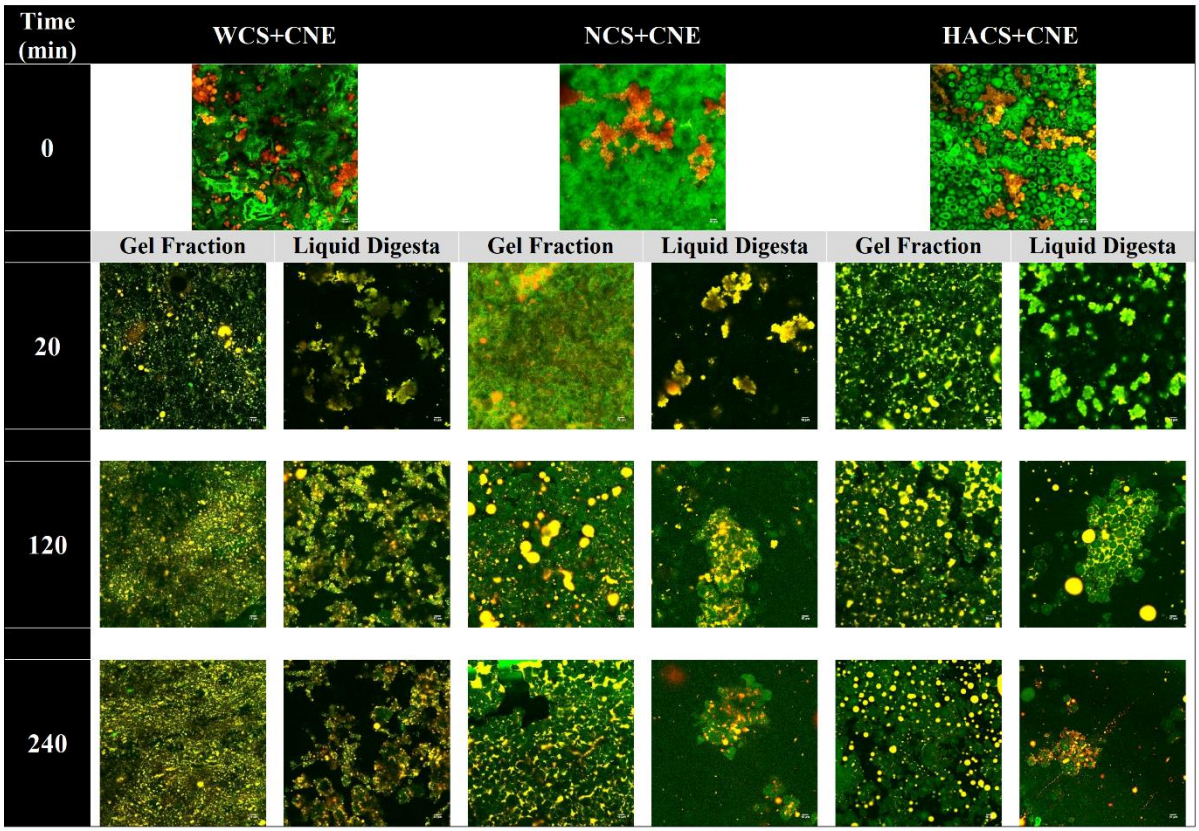

Fig. 5. 4 Confocal laser scanning microscopy images of gel fractions and gastric digesta during the digestion of various starch gels in a human gastric simulator. WCS, waxy corn starch; NCS, normal corn starch; HACS, high amylose corn starch; CNE, curcumin nanoemulsion.

After 20 min of gastric digestion, the WCS+CNE gel fraction had a fine-knitted interconnected gel network entrapping the oil droplets evenly (Fig. 5.4 Gel Fraction). With the progression of the gastric digestion, the gel matrix became more compact with fewer pores. In contrast, the comparatively compact gel structures at 20 min of the NCS+CNE and HACS+CNE gel fractions began to open up with more interspaces as the digestion progressed. Additionally, the oil droplets observed in the micrographs of the NCS+CNE and HACS+CNE gels at 120 and 240 min of digestion appeared to undergo higher degree of coalescence compared with those in the WCS+CNE gel (Fig. 5.4, rows 120 and 240). The greater extent of

coalescence can be attributed to the larger gel interspaces which may have allowed the enzymes to reach deeper into the gel structure and to hydrolyse the casein layer surrounding the oil droplets.

The extent of gel disintegration within the gastric chamber affected the microstructure of the emptying gel fragments and the composition of the emptied gastric digesta (Fig. 5.4 Liquid Digesta). At 20 min, the digesta samples of all gels contained numerous small-sized gel fragments with distinct shapes. The HACS+CNE gel micrograph at 20 min revealed that a comparatively higher content of solid particles was emptied in the digesta, which is consistent with the faster HACS+CNE gel disintegration in the stomach (Fig. 5.4, row 20). Although the solids contents of the NCS+CNE and HACS+CNE gels decreased over time, the size and the compactness of the gel fragments increased, which is consistent with the changes observed visually [Fig. 5.3(A)]. Furthermore, there were more coalesced oil droplets emptying within the gel fragments. In contrast, the WCS+CNE gel fragments were more evenly dispersed with uniformly distributed emulsified oil droplets.

5.4.2.3 Physicochemical changes in the emptied liquid digesta

Fig. 5.5 shows the changes with respect to pH, particle size, solids content and lipid content in the gastric digesta emptied from the HGS at various digestion times. The pH values of the gel samples after mixing with the SSF and the fasting SGF were reduced from 6.63, 6.01 and 5.88 to 3.43, 3.58 and 3.96 for the WCS+CNE, NCS+CNE and HACS+CNE gels respectively [Fig. 5.5(A)]. The significantly low pH values observed after mixing with the fasting SGF demonstrate that none of the three starch matrices had high buffering capacity, as previously observed in various milk-based matrices (Qazi et al., 2021, 2022). Furthermore, with the gradual addition of SGF over time, the pH of the emptied digesta samples decreased gradually and had decreased to 1.70 at 240 min. During the first hour of digestion, the

HACS+CNE gel had a comparatively slower decrease in pH, which was followed by the NCS+CNE and WCS+CNE gels. These initial differences in the pH could have been related to the total content of gel fragments observed in the emptied gastric digesta. However, there were no significant differences among the WCS+CNE, NCS+CNE and HACS+CNE gels during the subsequent digestion from 60 to 240 min.

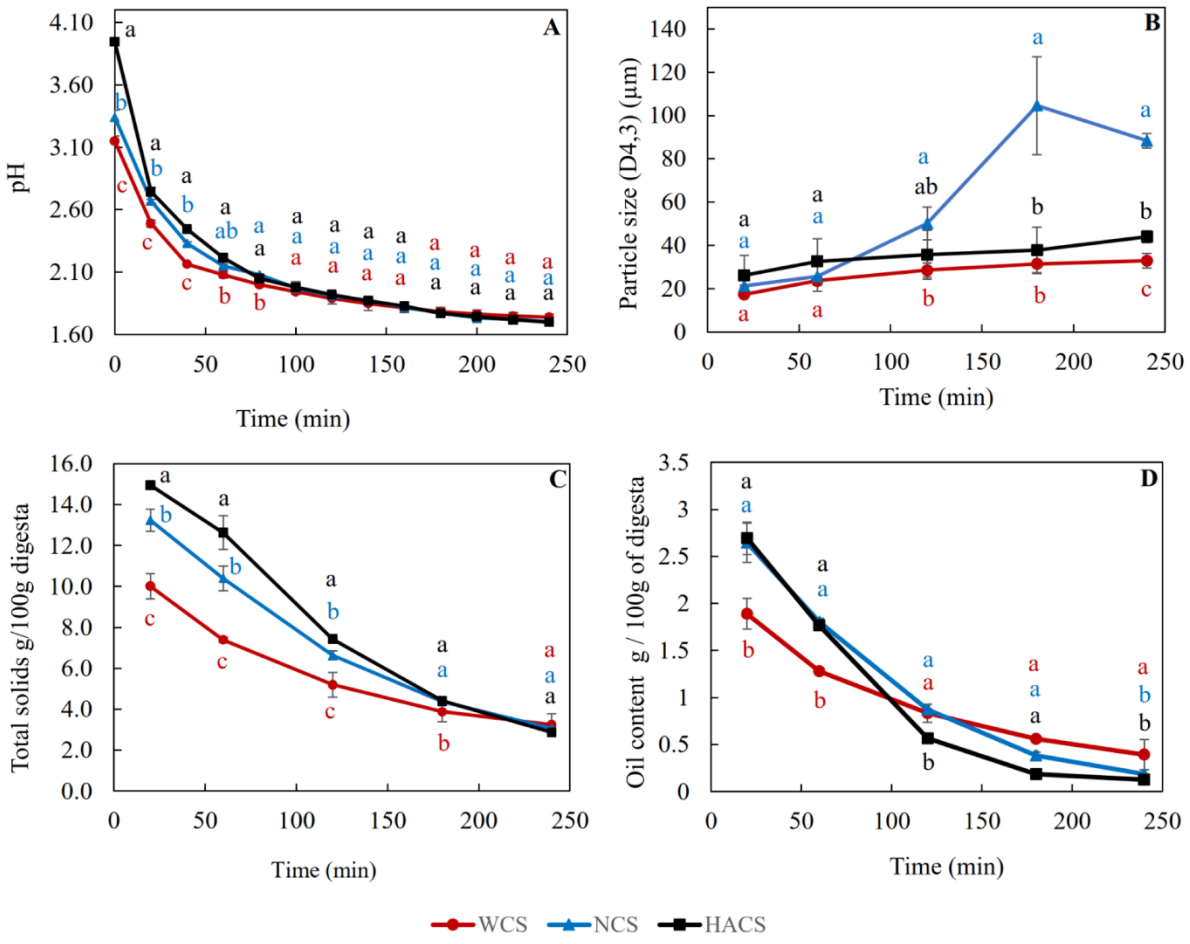

Fig. 5. 5 Changes in the emptied gastric digesta because of the dynamic in vitro gastric digestion of the various starch gels: (A) pH; (B) particle size ($D_{4,3}$); (C) total solids content; (D) lipid content. Error bars display the standard deviations. WCS, waxy corn starch; NCS, normal corn starch; HACS, high amylose corn starch; CNE, curcumin nanoemulsion.

The average particle sizes of the gel fragments emptied from the gastric chamber for the WCS+CNE and HACS+CNE gels showed no significant change throughout the digestion [Fig. 5.5(B)]. However, for the NCS+CNE gel, the particle size of the gel fragments increased significantly from 50 to 105 μm and slightly decreased to 88 μm at 120, 180 and 240 min respectively. This shifting of the particle size to a larger size distribution has been observed by M. Zheng et al. (2021) and Schwanz Goebel, Kaur, Colussi, Elias, and Singh (2019) and has been attributed to swelling in the gel structures, which may have been influenced by the low pH of the gastric fluid.

During the first 120 min of gastric digestion, the HACS+CNE gel showed significantly ($p < 0.05$) faster total solids emptying than the WCS+CNE and NCS+CNE gels [Fig. 5.5(C)]. These findings are consistent with the photographs and the wet weights of the gastric gel fractions [Figs. 5.3(A) and (B)]. In contrast, the other two gels remained in the stomach for a longer period of time, but this difference became less pronounced as the digestion progressed, and the total solids contents of the WCS+CNE, NCS+CNE and HACS+CNE digesta were almost identical at the end of the digestion process.

The lipid content of the emptied digesta gradually decreased as the digestion progressed [Fig. 5.5(D)]. The order of lipid content in the digesta at the end of 240 min of digestion was WCS+CNE > NCS+CNE > HACS+CNE, which is consistent with the changes occurring within the HGS, as discussed earlier. During the initial 60 min of digestion, the NCS+CNE gel had a significantly higher release of lipid content [Fig. 5.5(D)] which can be explained by differences in the structural and swelling patterns of the starch gels within the gastric chamber, which are influenced primarily by variations in amylose/amylopectin content and by the dynamic environment provided inside the HGS. The WCS+CNE gel demonstrated a lower

release of lipid content, which is consistent with the earlier observation that the majority of the WCS+CNE gel fraction remained within the gastric compartment.

5.4.3 Intestinal phase

5.4.3.1 Particle size

The changes in particle size of the gastric digesta from the different starch gels that were emptied at 20, 120 and 240 min were monitored after digestion in the SIF at 0, 1, 10, 30, 60 and 120 min (Fig. 5.6). The WCS+CNE gel, with an initial particle size distribution between 1 and 100 μm at 0 min, shifted to a particle size distribution with multiple peaks in the range between 0.1 and 1000 μm at longer digestion times. The volume of particles with a size between 0.1 and 1 μm increased steadily over time. However, the absence of these particles in this size range and the formation of a narrower peak between 1 and 100 μm with no further significant change during the intestinal digestion of the NCS+CNE and HACS+CNE gels indicated that they were less susceptible to enzymatic hydrolysis.

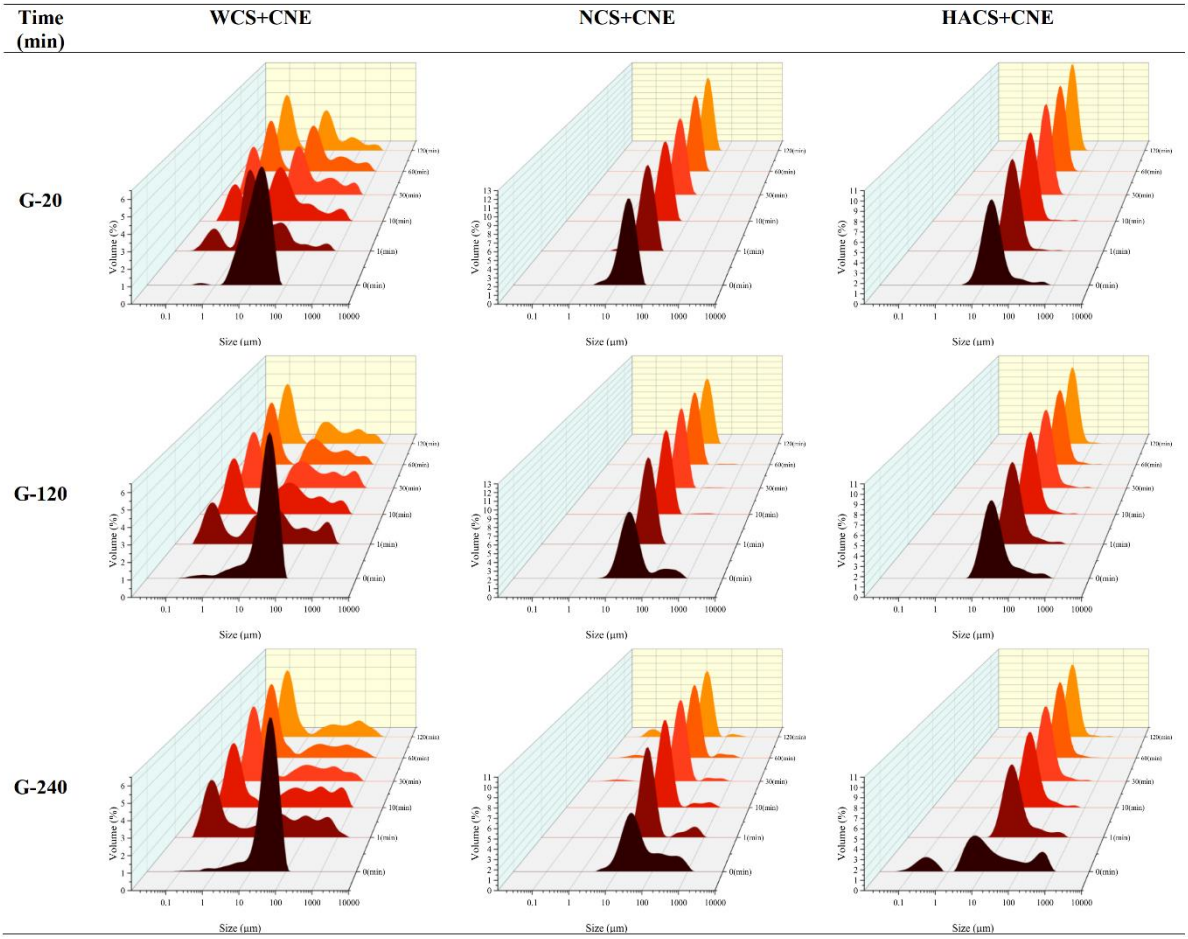

Fig. 5. 6 Particle size distribution changes in the emptied gastric digesta [20 (G20), 120 (G120) and 240 (G240) min) before (0 min) and throughout the intestinal digestion at different timepoints (1, 10, 30, 60 and 120 min). WCS, waxy corn starch; NCS, normal corn starch; HACS, high amylose corn starch; CNE, curcumin nanoemulsion.

5.4.3.2 Starch hydrolysis

The starch is primarily digested by the enzymes into glucose through a number of steps, and this process is influenced by the enzyme activity and the characteristics of the starch. The functional control of the glycaemic index is directly correlated with the rate of starch digestion. In order to identify the nutritionally significant starch fractions, the glucose released from the starch during a certain duration of starch hydrolysis was examined. As expected, before the intestinal phase was initiated, the rate of starch hydrolysis and glucose release was low in the corresponding gastric digesta samples for all three starch gels (Fig. 5.7), which was due to the

inactivation of salivary amylase at low pH in the gastric chamber (Freitas, Le Feunteun, Panouillé, & Souchon, 2018; Mulet-Cabero, Egger, et al., 2020). After adjusting the pH to 7 and the addition of SIF containing pancreatic α-amylase, rapid hydrolysis was observed within the first 2 min, which then plateaued after about 10 min (Fig. 5.7). Meanwhile, the WCS+CNE gel displayed the lowest glucose release from G20 sample; this was probably due to differences in gel breakdown in the oral phase and the stomach chamber [Fig. 5.3(A, B)]. Even though the HACS+CNE digesta fraction released more glucose from the G20 sample during the intestinal digestion, its rate of starch hydrolysis was the slowest [Fig. 5.7(B)]. This might be due to the weak gel formed (Fig. 5.2B) and faster gel fragments emptying rate of HACS+CNE gel into the digesta, which resulted in a larger proportion of amylopectin accessible for hydrolysis by pancreatic amylase compared to the other two gels digesta samples at the same timepoint. (Dun et al., 2021; J. Singh et al., 2010; M. Zheng et al., 2021). Furthermore, for G120 and G240, the amount of glucose released from the digesta samples reduced, which corresponded to the changes in the total solids content [Fig. 5.5(C)]. This resulted in significantly increase in percentage of starch hydrolysis possibly because of changes in the enzyme–substrate interaction. Additionally, the higher starch hydrolysis and glucose release in the G240 sample of the WCS+CNE gel could also be attributed to its higher amylopectin content, which is more rapidly hydrolysed by amylase despite the delayed gastric disintegration and gastric emptying of gel fragments (Lin et al., 2018). Although the quantity of amylose and the degree of starch swelling played a role, the rheological properties of the gels impacted their structure and its breakdown patterns in the gastric phase. These patterns in turn impacted on the amount of starch that was transported to the small intestine for digestion.

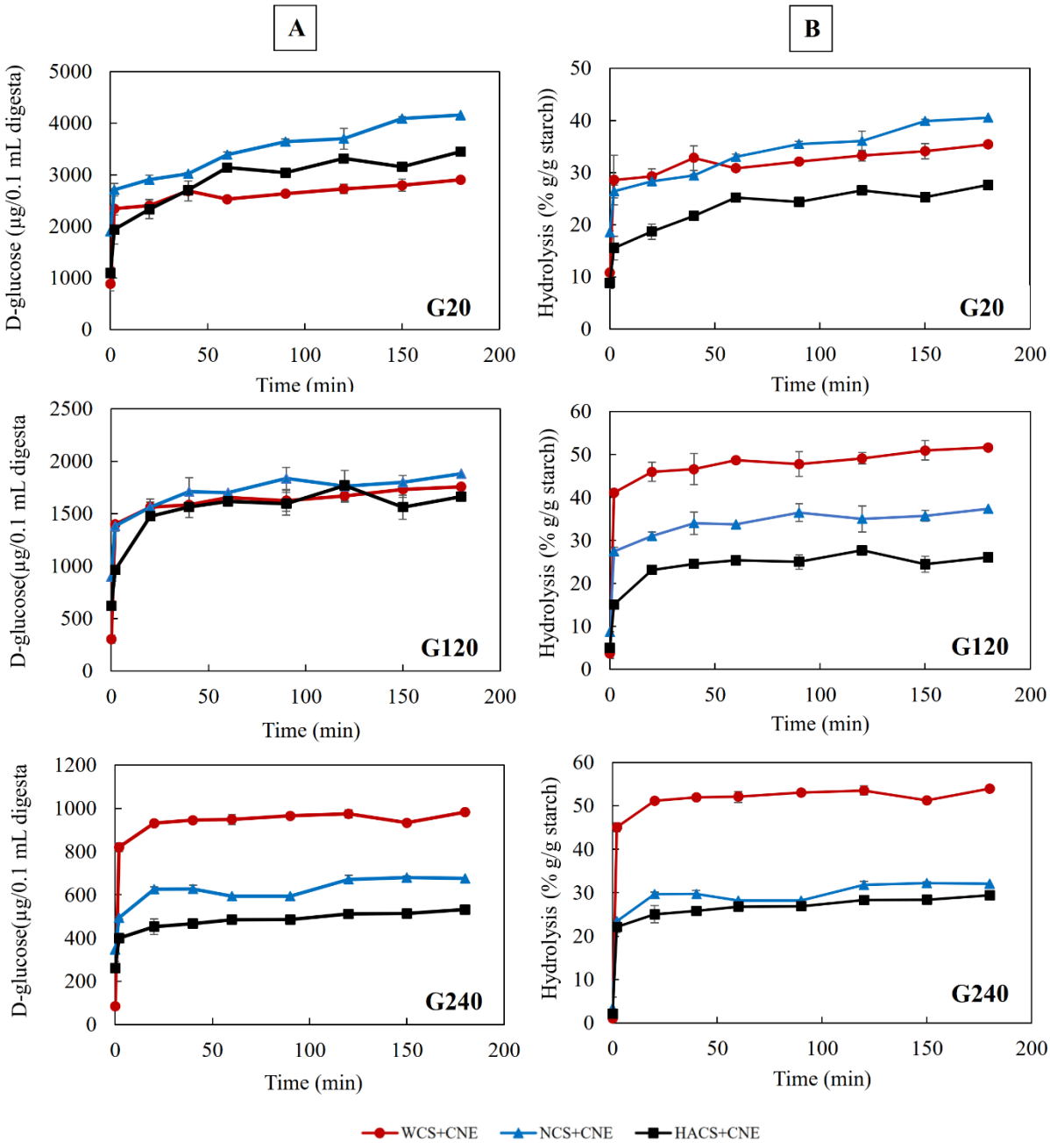

Fig. 5. 7 (A) D-glucose release behaviour and (B) starch hydrolysis of gastric digesta emptied at 20 min (G20), 120 min (G120) and 240 min (G240) during in vitro intestinal digestion of differently structured corn starch gels containing curcumin nanoemulsion (CNE). WCS, waxy corn starch; NCS, normal corn starch; HACS, high amylose corn starch.

5.4.3.3 FFA release and bioaccessibility of curcumin

A pH-stat was used to determine the FFA release curves and the total amount of FFAs released. As illustrated in Fig. 5.8(A), there was a higher release of FFAs in the samples

emptied at 20 min of the gastric phase, which was followed by those emptied at 120 and 240 min for all three starch systems. This matched the compositional differences in the digesta samples, caused by changes in the gels under dynamic gastric conditions. Similar results were reported in the gastrointestinal digestion of milk protein beverages (Niu et al., 2020; Qazi et al., 2022) and milk gels (Qazi et al., 2021) with nanoemulsions containing various active ingredients. However, the pattern for all starch-based gel systems changed when the quantity of FFAs released was estimated per gram of lipid as a function of time [Fig. 5.8(B)]. The gastric digesta emptied at 240 min had the highest rate of lipolysis, followed by the gastric digesta emptied at 120 min and, finally, the gastric digesta emptied at 20 min. Guo et al. (2016) reported similar behaviour when they investigated FFA release during the intestinal digestion of whey protein emulsion gels. They attributed these results to the changes in the gel structure or the colloidal structure of gel fragments during intestinal digestion, which may have influenced the lipolysis of the oil droplets embedded within the starch matrix. Moreover, previous studies have also highlighted that the starch hydrogel matrix plays a role in keeping the emulsion droplets well dispersed in the gastrointestinal tract, which increases the specific surface area of lipids exposed to pancreatic lipase (Mun & McClements, 2017).

Finally, the bioaccessibility of curcumin incorporated within the various corn starch gels was examined and the results are shown in Fig. 5.8(C). More than 80% of the curcumin was bioaccessible in the gastric digesta samples that were discharged at 20 and 120 min. These bioaccessibility values are comparable with those found in our previous study on the digestion of dairy gels (Qazi et al., 2021). This finding indicated that curcumin may have been more thoroughly incorporated into the mixed micelles in the small intestine because of the small size and large surface area of the nanoemulsion (Araiza-Calahorra et al., 2018; Francesco Donsì, 2018). All three starch gel matrices had no significant effect on the proportion of bioaccessible curcumin fraction in the digesta emptied at 20 and 120 min. However, at 240 min, the digesta

fractions of the NCS+CNE and HACS+CNE gels had significantly (p < 0.05) lower bioaccessible fractions of curcumin than that of the WCS+CNE gel. This could have been because of the greater aggregation of the lipid droplets seen in the digesta fraction of these starch matrices during the gastric phase (Fig. 5.4 Liquid Digesta), which may have slowed the formation of the mixed micelles, and thus affected the curcumin bioaccessibility (Salvia-Trujillo et al., 2013).

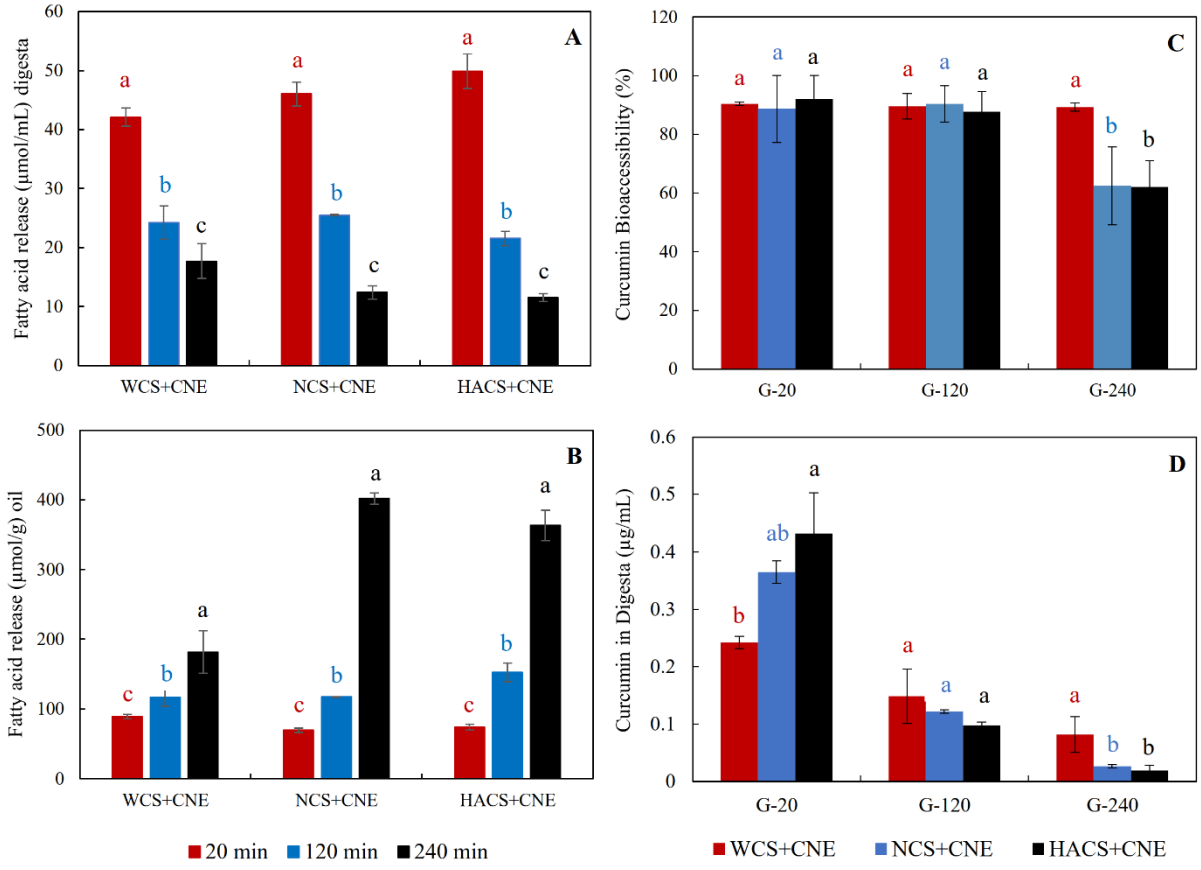

Fig. 5. 8 Free fatty acid (FFA) release behaviour per millilitre of gastric digesta (A) and per gram of oil (B), the bioaccessibility of curcumin (C) and the curcumin mass (D) in emptied gastric digesta fractions at 20 min (G20), 120 min (G120) and 240 min (G240) during the in vitro intestinal digestion of differently structured corn starch gels. WCS, waxy corn starch; NCS, normal corn starch; HACS, high amylose corn starch; CNE, curcumin nanoemulsion.

When the quantities of curcumin in these digesta fractions were examined [Fig. 5.8(D)], the gastric digesta emptied at 20 min had released most of the curcumin, followed by the digesta

emptied at 120 and 240 min. This corresponds to the concentration of oil droplets in the gastric digesta as well as the amount of FFAs released. This was consistent with previous findings in which the dynamic breakdown of recombined milk systems (Qazi et al., 2022) and dairy gels (Qazi et al., 2021) formed with acid and rennet coagulation in the stomach impacted the nature of the emptied digesta, this in turn affected the release of curcumin in the small intestine.

5.5 Conclusions

Using a dynamic digestion protocol, the effects of different CNE-loaded corn starch matrices, with different amylose contents, on the digestion and the bioaccessibility of curcumin were determined. These differences not only altered the rheological and textural features of the loaded gels but also affected their digestive profiles. Under dynamic gastric conditions in the HGS, the HACS+CNE gel disintegrated and emptied much more rapidly than the highly adhesive WCS+CNE gel, which showed very little disintegration inside the gastric chamber even after a long digestion time, whereas the NCS+CNE gel fell somewhere in the middle. These changes in the HGS impacted the compositional and microstructural profile of the emptied digesta, which significantly altered the rate of starch hydrolysis, the release of FFAs and the bioaccessible fraction of curcumin during intestinal digestion. Despite having a higher amylose content, the HACS+CNE gel had essentially identical concentrations of glucose release to the WCS+CNE and NCS+CNE gels, demonstrating the importance of a physical state of the material in the dynamic gastric stage. In previous research, this stage had almost been neglected when accounting for the glycaemic responses of various starches and the rate of delivery and bioaccessibility of loaded bioactive compounds.

.

Chapter 6. Overall discussion, Conclusions and Future Recommendation

6.1 Overall Discussion and Conclusions

Curcumin is a lipophilic pigment with, a very low solubility in water, and therefore it is essential to dissolve this compound in oil in the appropriate amount during the formation of the nanoemulsion. Based on the curcumin solubility (0.39 mg/g) in soybean oil, nanoemulsions were made by homogenizing the oil phase containing curcumin with the water phase containing sodium caseinate in a high-pressure homogenizer. The homogenisation condition and the formulation used were adequate to create nano-sized emulsion with mean particle size ($D_{3,2}$) and zeta potential of 0.187 ± 0.011 μm and – 58.83 ± 3.32 mV respectively. The decision to use nanoemulsion was made because prior research has shown that they significantly increase curcumin's oral bioavailability by at least nine times when compared to curcumin taken with absorption enhancers. Additionally, the nanoemulsion formulation demonstrated excellent stability over 60 days of storage. The nanoemulsion's small droplets reduced creaming velocity and enhanced Brownian diffusion, thus exhibiting greater kinetic stability. Additionally, it has been noted that sodium caseinate is very effective emulsifying agent, which prevents emulsion droplets from flocculation.

Following the aim of this study, the curcumin nanoemulsion were firstly incorporated into recombined milk system (Chapter 3). These milk systems were prepared using different skim milk powders (i.e. low heat, medium heat and high heat) that have undergone different degree of preheat treatment during processing. This preheating step denatures the whey proteins, i.e. β-lactoglobulin (β-LG) and α-lactalbumin (α-LA), forming aggregates that further associate with the casein micelles, and specifically with κ-casein. These modified casein micelle/denatured whey protein complexes largely determine the functionalities and applications of SMPs. These different recombined milk samples had a comparable visible

appearance and had 5% oil and 4% protein, but they behaved very differently in the gastric phase. All the recombined milk systems formed a curd when they were digested in the dynamic gastric chamber (HGS). Both the extent of preheat treatment of skim milk prior to powder manufacturing and the curcumin nanoemulsion supplementation modified the structure and consistency of the gastric curds. Under dynamic gastric conditions, the recombined milk made from high heat SMP formed a soft curd that resulted in faster outflow of the curd fragments along with entrapped CNEs, compared with recombined milk made from low heat and medium heat milk powders. The curds formed by these two recombined milk systems retained the maximum proportion of total solids, while allowing a small fraction to pass through to the liquid digesta. This difference became less pronounced as the digestion progressed and, at the end of the process, the total solids contents of the all the digesta samples were almost identical.

These changes in the curd structure significantly affected the pattern of release of protein, lipid and curcumin content. The gastric digesta emptied at 20 min showed a higher content of curcumin, followed by the gastric digesta emptied at 120 and 240 min. This was in accordance with the concentration of oil droplets in the gastric digesta and the amount of free fatty acid release. It is worth noting, that the percentage of curcumin from the high heated recombined milk digesta samples decreased linearly, whereas the other two digesta samples decreased logarithmically. This logarithmic tendency observed in low and medium heated recombined milk systems suggested that structural changes in the curd had a larger effect on the curcumin fraction's release in the digesta.

Extending this work the same milk formulation with added CNE was structurally modified by acid or rennet with an aim to investigate the impact of gel matrices, on the bioaccessibility of curcumin during *in-vitro* gastrointestinal digestion (Chapter 4). The gels were designed to have similar composition and physical properties. However, the production

of both gels with the same viscoelastic properties was more challenging because of the different modes of coagulation. Recombined milk made from high heat SMP produced a high G' for acid gels, but rennet gel had very low G'. In contrast, recombined milk produced from low heat SMP has high G' for rennet gel and low G' for acid gel. Low-heat skim milk was ultimately chosen to make a firm acid and rennet gel with a similar enough G' value to imitate the actual food products.

Unlike the milk systems (Chapter 3), the disintegration pattern of the gels in the gastric chamber was completely different. During gastric digestion, acid gel curd particles showed much faster disintegration compared to rennet gel curd particles. The weight of acid gel curd rapidly reduced and only very few curd particles (> 1 mm) were observed at 180 min and no acid gel curd particles remained in the gastric chamber at 240 min. The faster disintegration of the acid gel was linked to the weakening of casein micelles internal bond (due to dissolution of micellar calcium phosphate) during gel formation, which facilitated the penetration of SGF and pepsin, resulting in a rapid hydrolysis. In Contrast, rennet gel curd particles under the influence of stomach secretions reorganized into dense protein particles and changed into a variety of compact structured clots that remained in the HGS even after 4 hrs of digestion.

The disintegration of milk gels during digestion led to the differing compositions of the digesta delivered to the small intestine from the HGS at different times. The changes in particle sizes, total solid, oil content and microstructures of emptied digesta during digestion were found to be significantly different for both gel structures. The restructuring of rennet gel within the gastric environment, slowed the emptying of protein and oil droplets along with curcumin in the digesta compared to acid gel that underwent minimal structural changes with faster breakdown during the gastric phase. The extent of free fatty acid released from all the digesta samples of both gels was found to be dependent mainly upon the pattern of oil content of the

gastric digesta emptied at different times. The bioaccessibility of curcumin from the acid gel digesta samples was higher ($P < 0.05$) than that from the rennet gel digesta samples. The variations in curcumin bioaccessibility from both gels could be ascribed to compositional and microstructural differences in the gastric digesta of both gels. Additionally, the correlation analysis confirmed the linear relation between free fatty acid release and curcumin bio-accessibility. Therefore, with greater lipolysis, more curcumin would be released from oil droplets and more FFAs could be incorporated into the mixed micelles, thus enhancing the solubility of curcumin in the mixed micelles phase.

In the case of starch-based gels, the structure and viscosity of the post-processing food matrix as well as the starch chemical composition (such as its amylose concentration, amylose chain length, and amylose to amylopectin ratio) had a significant impact on how easily they can be digested. Therefore, a study was undertaken on the gelation and in vitro digestion properties of the CNE loaded starch gels, formulated using waxy (WCS), normal (NCS) or high amylose (HACS) corn starch (Chapter 5). CNE was combined with starch aqueous dispersion to produce final starch and lipid concentrations in the solution of 25% and 5%, respectively. The samples were put in a 95°C water bath, lightly agitated for 2 minutes, and then allowed to gel for another 28 minutes. The rheological study showed that compared with the WCS+CNE gel, the NCS+CNE and HACS+CNE gels were firm because amylose contributed to the gel strength and firmness. Additionally, the peak pasting viscosities of the WCS+CNE and NCS+CNE gels were significantly higher than those of the gels without CNE. This was ascribed to the fact that the emulsion droplets acted as active fillers in these gels and interspersed into the continuous phase of the system, raising the effective concentrations of the continuous phase and raising the viscosity of the system. Similarly, the CNE in HACS+CNE gels resulted in the formation of a weak network structure due to high amylose content and CNE interactions, which may have disrupted the long-range interactions of amylose within the

gel, resulting in lower gel cohesiveness and early exudation of water because of amylose retrogradation.

During in vitro digestion, when the mastication phase was simulated with a motorized grinder, all three starch gels showed noticeably unique characteristics. The WCS+CNE gel's viscous, sticky appearance persisted even after grinding. The HACS+CNE gel, on the other hand, changed into a grainy slurry while the NCS+CNE gel broke up into smaller pieces. Further, during the gastric phase, the WCS+CNE gel structure appeared slimy at all three timepoints, but its adhesiveness appeared to be slightly reduced as the digestion progressed. In contrast, the structures of the NCS+CNE transformed into a mushy paste and HACS+CNE gel appeared to be a lumpy paste and they became dry in appearance with the progression of digestion. The recorded mean weights of the gel particles retained within the HGS revealed that the WCS+CNE gel disintegrated much more slowly than the other three gels. These variations in the HGS's gel disintegration behaviors were ascribed to the various initial textures of the gel structures, which were affected by the amylopectin to amylose ratio. This disintegration pattern in the gastric chamber resulted in different total solids and lipid content in the emptied digesta. Since the bulk of the WCS+CNE gel component stayed inside the gastric compartment, the WCS+CNE gel showed a reduced release of total solid and lipid content.

The modifications occurring within the gel had a substantial impact on the starch breakdown and the release of glucose during intestinal digestion. Due to the variation in composition, starch hydrolysis proceeded in the following order: WCS+CNE > NCS + CNE > HACS+CNE. It was interesting to see that, during intestinal digestion, the HACS+CNE digesta portion emptied at 20 min released more glucose than the WCS+CNE gel, which showed the lowest glucose release. These differences resulted from the various patterns of the gel

disintegration in the mouth and the stomach. These compositional differences in the digesta samples, which were caused by changes in the gels' structures and the colloidal structures of gel fragments, also affected the release of free fatty acids and the bioaccessible portion of curcumin.

Overall, starch and dairy-based food systems differ in their composition, properties, and applications. Starch molecules can associate and form a gel structure when heated in the presence of water. Whereas proteins in milk, such as casein, can form gels under certain conditions. Both starch and dairy-based ingredients are used to achieve gel-like textures in food products, they differ in their composition, gelling mechanisms, textures, and applications. The choice between them depends on the desired characteristics of the final product and the specific requirements of the formulation. Similarly, the in vitro digestion of starch-based foods primarily involves the breakdown of complex carbohydrates into simple sugars, while the digestion of dairy-based gels focuses on the breakdown of proteins into peptides and amino acids. The rate of digestion, types of enzymes involved, and the resulting digestion products differ between these two types of gels during in vitro digestion.

The impact of starch-based and dairy-based food systems on the release of fortified bioactive compounds is complex and multifaceted. It depends on factors such as the nature of the bioactive compounds, the composition of the food matrix, and the dynamics of digestion. The encapsulation, digestion kinetics, and interactions within the food system all contribute to the overall bioavailability and release of fortified compounds in these matrices.

In this study, we explored that the key factors associated to the release and bioaccessibility of fortified curcumin from the food matrix were the initial food composition and structures as well as their subsequent behaviour of breakdown in the gastric environment. The dynamic HGS settings produced considerable changes in the curd/gel fragments as well as

the pattern of emptying. Higher lipid emptying of digesta samples was positively correlated with higher curcumin release in those samples. Thus, by manipulating food structures, we can ultimately regulate or control the release of specific nutrients by modifying how foods break down and process in the body. This can further help in designing different functional foods for specific population.

6.2 Recommendation for future work

Future studies have been suggested to fill the significant gaps that emerged during this PhD project:

6.2.1 Real food matrix effect

The current study focused on the influence of initial structures of model food systems and their in vitro disintegration in the gastrointestinal tract. This research involved starch/lipid and protein/lipid based food systems, and the results showed how these food components interact and affect digestion patterns. However, the inclusion of other food components, such as the combination of protein, lipids, and polysaccharides in a single meal composition, may lead to far more complicated chemical interactions and structural organisation at the macro-, meso-, and microscopic level. As a result, real fortified food matrices (i.e. noodles, curries, cereals) that are part of our common diet might be a future study path to examine. Furthermore, dietary supplements marketed for specific populations, such as sports supplements and infant formulae, have significantly different formulations and include a variety of bioactive compounds. It would be fascinating to investigate how these formulations affect the rate of delivery of the loaded bioactive chemicals.

6.2.2 Food matrix effect on other bioactive compounds and delivery systems

This PhD thesis have demonstrated how various food matrices affect curcumin's bioaccessibility when it is added to food as a nanoemulsion. Many delivery systems (such as

liposomes, solid lipid particles), each of which will have a distinct effect on the release of the bioactive substances (i.e. lipophilic and hydrophilic) have been studied. However, how these delivery systems interact with the different food matrices is not known. Thus, future research should examine how various bioactive substances, encapsulating materials, and delivery mechanisms affect the structure and characteristics of foods both during preparation and during digestion.

6.2.3 Using new dynamic gastric and intestinal models

In this thesis, gastric digestion research showed that in vitro dynamic models (HGS) with pertinent physiological conditions for the stomach (such as enzyme concentrations, pH, and physical contractions) play a key role in more accurately simulating the conditions of gastric digestion. However, a newly designed human gastric model with a J-shaped stomach, which is more similar in form to the human stomach, can potentially have an effect on the kinetics of food matrix breakdown. This can be used in future research because it can affect the makeup and microstructure of emptied digesta, and thus the bioaccessibility and bioavailability of enriched bioactive substances and nutrients. Moreover, there results obtained in this study can be validated across different dynamic gastrointestinal model available internationally.

6.2.4 Caco-2 cell work

Bioaccessibility is generally assessed by in vitro methodologies that only estimate the amount of compounds available for intestinal absorption. The bioactive substances interacting with other dietary components during digestion may not be entirely released, and the released bioactive substances may thus ineffectively absorbed. To determine the bioavailability, there are three crucial aspects: solubilization, permeability, and metabolism. This study only investigated the influence of initial food structure and structures generated in the gastrointestinal system on curcumin bioaccessibility (i.e. curcumin fraction solubilized in the micelle phase). Thus, the permeability/absorption of the bioaccessible curcumin fraction can

be assessed through the commonly used cell models i.e. human intestinal epithelial cell line (Caco-2) in the future. This will help us to understand if the improved stomach stability of the emulsions with complex surfaces has any effect on Caco-2 cells survival and benefit in terms of cellular curcumin absorption. Moreover, the effect of different delivery systems on cell toxicity can also be assessed.

6.2.5 Use of non-invasive technologies

With the recent development of non-invasive technologies, such as real-time MRI, spatiotemporal mapping, high-resolution manometry, and computational modelling, it is now possible to use these techniques to offer relevant information on how food structures change during digestion and to correlate this knowledge with in vitro research.

One of the key factors that affects how well food disintegrates and nutrients are released during stomach digestion is the mobility of gastric juice inside food matrices. However, the process by which the gastric juice's acid and moisture diffusion effect food degradation is still far from being fully understood. Utilising the magnetic resonance imaging (MRI) method, it is possible to see the spatial and temporal distribution of gastric juice and the swell of food during stomach digestion. Because it depends on the distinctive absorption and emission of energy from corresponding protons in the digested sample, MRI provides several benefits over optical imaging for characterising the gastric juice diffusion process.

Similar to MRI, hyperspectral imaging (HSI) is a labelling-free analytical technique utilised in the field of food science research. This method is becoming more important for revealing the spatiotemporal distribution of chemical content inside food matrix and for giving quantifiable data to assess the gastric juice diffusion phenomena during digestion.

On the other hand, recently the computational solid mechanics and fluid dynamics are being used to develop models that could predict food mixing and fragmentation. These

computer models are still in their early phases, but they appear to be adaptable to a range of food structures with various rheological characteristics. Therefore, it is likely that these methods might be applied in the future to forecast the fragment sizes of bolus and chyme in the upper GI tract.

6.2.6 Animal and human trials

The in vitro digestion models have limitations and are unable to accurately represent all the physiological conditions that exist in the human body in its natural state. In the body of an animal or a person, food processing is a much more complex process that is regulated by neural and hormonal responses. The in vivo studies should therefore be used to verify the in vitro digestion findings.

In animal or human studies, the quantity of the bioactive compounds or its metabolites in the blood system after consumption of the meal can also be used to assess the oral delivery of bioactive substances. Although human studies are the gold standard, cannulated piglets can be used as an excellent model of human digestion, absorption, and metabolism. The outcomes of in vivo studies can be used to compare with those of in vitro studies.

Annexures

Annexure 1: Standard curve of curcumin in chloroform using UV spectrophotometer at 425 nm wavelength.

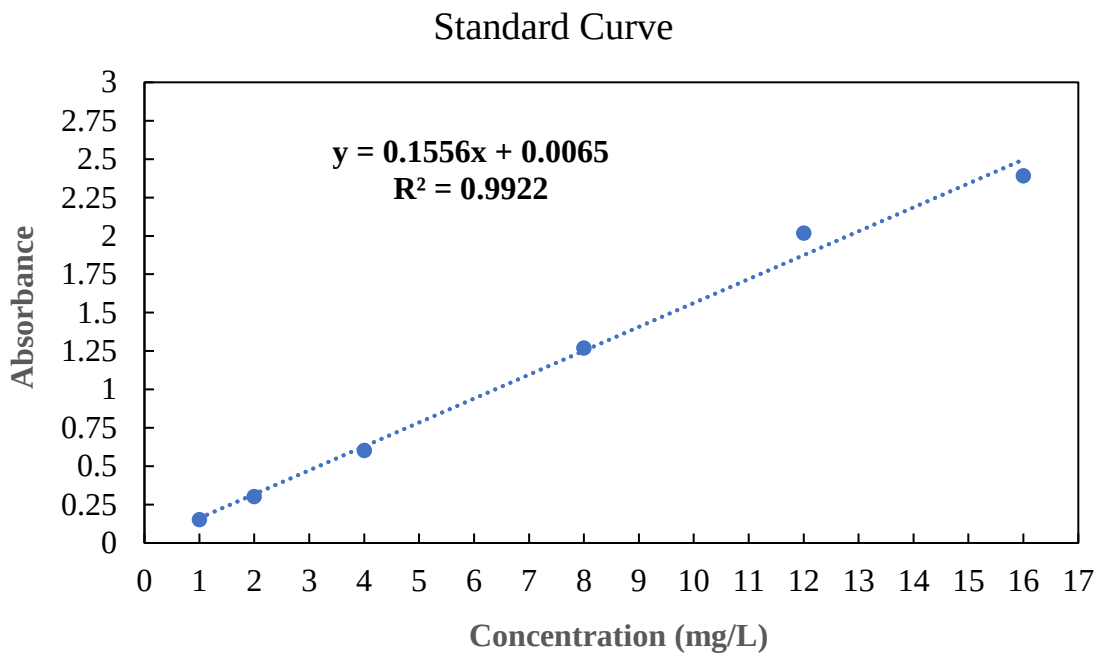

Fig. A1. 1 Standard curve of curcumin.

Annexure 2: Physiochemical properties of curcumin loaded nanoemulsions

In this study, curcumin-loaded nanoemulsions were obtained by homogenizing the oil phase containing curcumin, with the aqueous phase containing sodium caseinate in a high-pressure homogenizer. The homogenisation treatment and the formulation used was adequate to create nano-sized emulsion having mean particle size ($D_{3,2}$) and zeta potential of 187 ± 11 nm and – 58.83 ± 3.32 mV respectively. In addition, the stability of these nanoemulsions was determined after 30 and 60 days of storage at 4°C (Table A2.1). Result showed the mean particle size of nanoemulsions only increased slightly, about 20 nm during the 60 days of

storage. In other words, curcumin-loaded nanoemulsions exhibited a good stability during storage. Solans, Izquierdo, Nolla, Azemar, and Garcia-Celma (2005), ascribed the higher kinetic stability of nanoemulsions to small emulsion droplets which reduce the creaming velocity and enhance Brownian diffusion. Moreover, sodium caseinate have been described to be very efficient in stabilizing oil droplets, which prevent them from aggregation (Kumar et al., 2016).

Table A2. 1 Surface area mean particle size ($D_{3,2}$) and volume weighted mean diameter ($D_{4,3}$) distribution of curcumin loaded nanoemulsions at 0, 30 and 60 days of storage.

	Day 0		Day 30		Day 60	
	D(3,2)	D(4,3)	D(3,2)	D(4,3)	D(3,2)	D(4,3)
Average Particle size (nm) ± S.D	187 ± 11	334 ± 19	189 ± 04	345 ± 11	207 ± 06	350 ± 13

Annexure 3: Rheological properties of curcumin loaded nanoemulsions

To evaluate the effect of different microstructures formed during the acid and enzyme coagulation on the release behaviour of curcumin in the gastrointestinal tract, the milk studied in the early section was processed to produce acid and rennet gels. The oil and protein ratio in both studied gels were kept iso-caloric to avoid the impact of compositional variations on the disintegration during the digestion. However, the production of both gels with the same viscoelastic properties was more challenging because of the different mode of coagulation. Firstly, an attempt was made to make the gels using heated skim milk powder that produced a high G' for acid gels, but RG was comparatively very weak. According to Lucey (2008), heating milk results in the formation of stiffer AG with reduced syneresis because of association of denatured whey proteins with casein micelle. However, the whey protein in RG

forms a coating on the casein surface, thus preventing the κ-casein hydrolysis induced by rennet (Dalgleish & Corredig, 2012). In the same way, these trends are opposite if these gels are prepared with raw milk (Lucey, 2008). Therefore, low-heat skim milk finally selected to prepare a firm rennet gel with higher storage modulus. After obtaining the constant G' value for RG, viscoelastic properties of AG were optimized to get a G' value close to that of RG. Moreover, the concentration of rennet and acid added were also kept close enough to mimic the real food products.

Fig. A3.1 shows the storage modulus of both gels optimized using dynamic oscillation measurements within rheometer. On addition of GDL in milk, the pH of the AG continuously decreased from 6.67 to 4.58 during the first 6 h. Following the incubation, the decreasing trend of pH was comparatively slower (4.58 - 4.45) during next 6h storage at 4°C. Though, the pH value of RG remained constant i.e. 6.5. The initial lag phase between addition of acid or enzyme and onset of gelation in the acid-induced gel was higher (92 min), compared to that of the RG (17 min). After 360 min of incubation the G' of AG and RG were 107.60 ± 11.75 Pa and 235.6 ± 14.06 Pa respectively. However, the G' value of the AG almost doubled (~264 Pa) after 6 h of cold storage at 4°C, while the RG showed a slight increase to ~258 Pa. This increase in G' during cold storage has also been observed by (Anema, Lee, Lowe, & Klostermeyer, 2004; Bikker, Anema, Li, & Hill, 2000; Serra, Trujillo, Guamis, & Ferragut, 2009) and was explained as rearrangement along with particle fusion within the gels, making them more rigid compared to the freshly prepared ones. Ultimately, we were able to produce both gels with similar elastic modulus to investigate the impact of structure on the release of the bioactive compound through in-vitro gastric digestions.

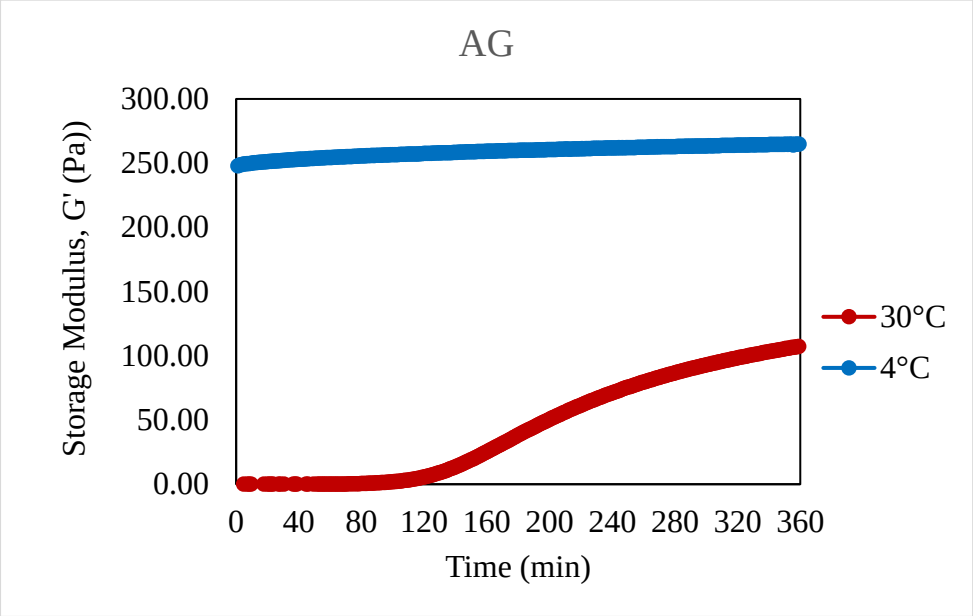

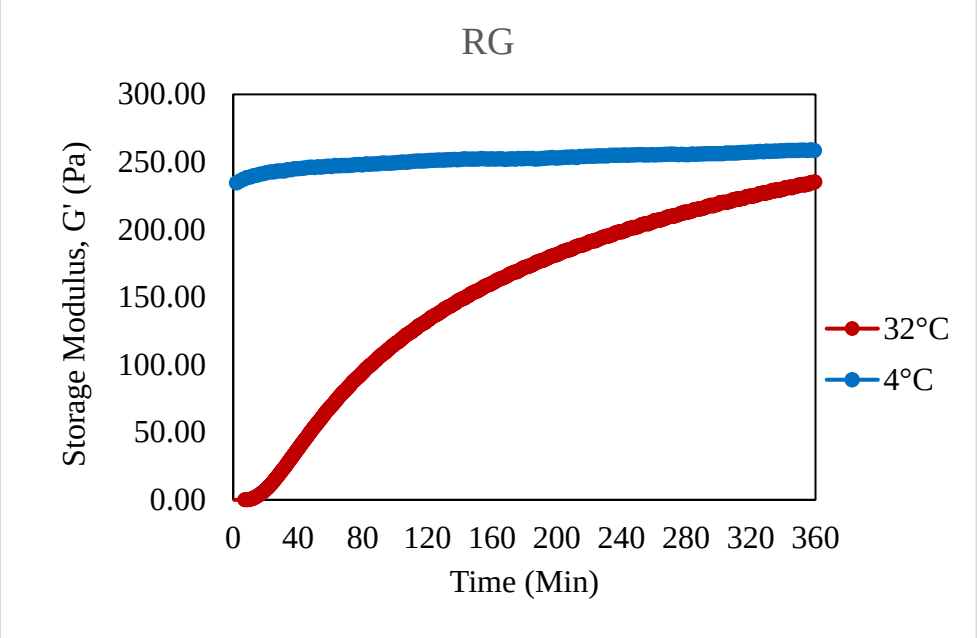

Fig.A3. 1 Low amplitude dynamic oscillation measurement over the first 6 h of gelation period of AG at 30 °C and RG at 32 °C, respectively (red line); and next 6 h under cold storage at 4 °C (blue line). Duplicate gave similar profiles.

Annexure 4: Rheological properties and microstructures of starch gels without CNE

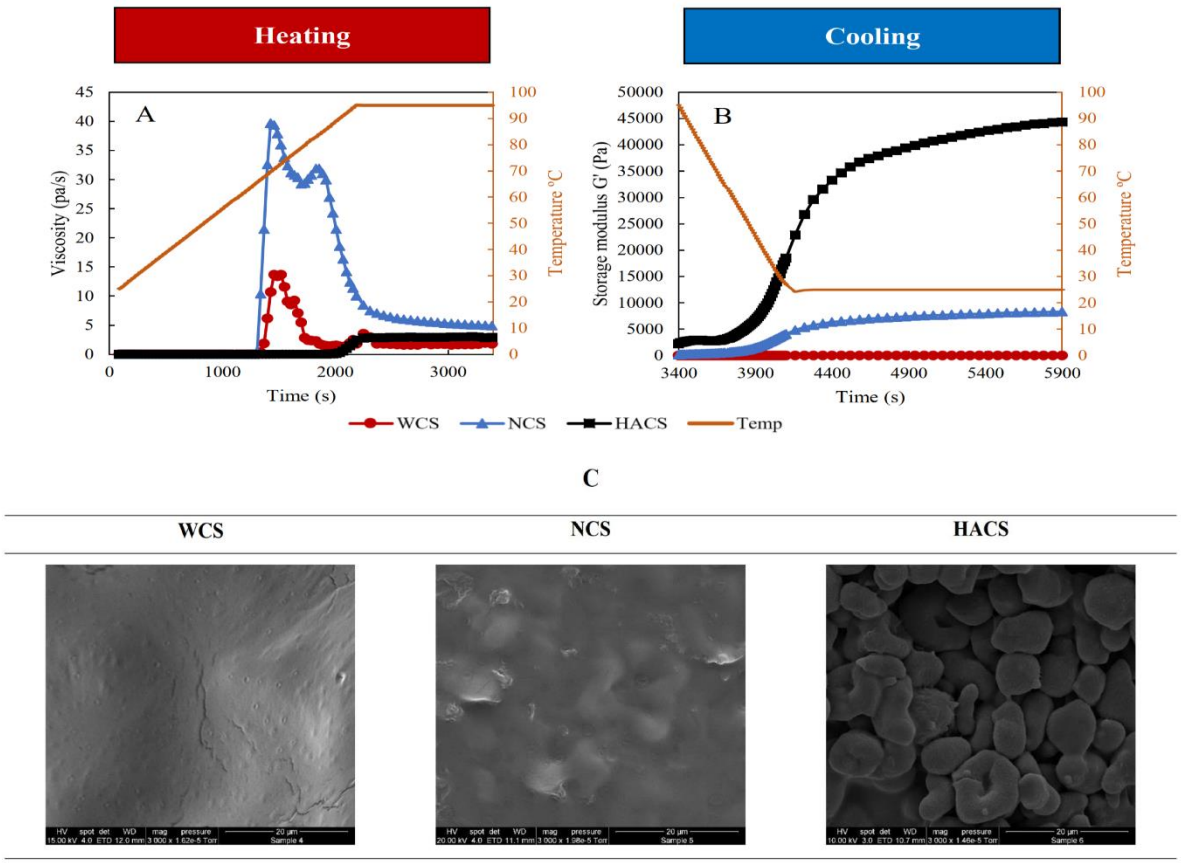

Fig.A4. 1(A, B) Pasting profiles of different corn starch solutions without curcumin nanoemulsion (CNE). (A) Development of viscosity (Pa.s) during heating (25–95 ºC) and (B) change in storage modulus (G') during cooling (95–25 ºC) of the starch gels. (C) Microstructures of starch gels without CNE using scanning electron microscopy at 3000x magnification. WCS, waxy corn starch; NCS, normal corn starch; HACS, high amylose corn starch.

Annexure 5: Structure of starch gels after grinding to mimic the oral phase.

WCS+CNE	
NCS+CNE	
HACS+CNE	

Fig.A5. 1 Visual appearance of the starch gel structures after grinding.

Bibliography

Acevedo-Fani, A., Dave, A., & Singh, H. (2020). Nature-assembled structures for delivery of bioactive compounds and their potential in functional foods. *Frontiers in chemistry*, *8*, 564021.

Acevedo-Fani, A., Ochoa-Grimaldo, A., Loveday, S. M., & Singh, H. (2021). Digestive dynamics of yoghurt structure impacting the release and bioaccessibility of the flavonoid rutin. *Food Hydrocolloids*, *111*, 106215. doi:https://doi.org/10.1016/j.foodhyd.2020.106215

Acevedo-Fani, A., & Singh, H. (2021). Biopolymer interactions during gastric digestion: Implications for nutrient delivery. *Food Hydrocolloids*, *116*, 106644. doi:https://doi.org/10.1016/j.foodhyd.2021.106644

Agarwal, S., Vivekanandan, S., David, T., Mitra, M., Palanivelu, J., & Chidambaram, R. (2019). Nanoemulsions: Industrial production and food-grade applications. In *Polymers for Agri-Food Applications* (pp. 159-182): Springer.

Aguilera, J. M. (2005). Why food microstructure? *Journal of Food Engineering*, *67*(1), 3-11. doi:https://doi.org/10.1016/j.jfoodeng.2004.05.050

Aguilera, J. M. (2018). The food matrix: implications in processing, nutrition and health. *Critical Reviews in Food Science and Nutrition*, 1-18. doi:10.1080/10408398.2018.1502743

Aguilera, J. M. (2019). The food matrix: Implications in processing, nutrition and health. *Critical Reviews in Food Science and Nutrition*, *59*(22), 3612-3629.

Ahmad, A., & Ahmed, Z. (2019). 3 - Fortification in beverages. In A. M. Grumezescu & A. M. Holban (Eds.), *Production and Management of Beverages* (pp. 85-122): Woodhead Publishing.

Akgün, D., Gültekin-Özgüven, M., Yücetepe, A., Altin, G., Gibis, M., Weiss, J., & Özçelik, B. (2020). Stirred-type yoghurt incorporated with sour cherry extract in chitosan-coated liposomes. *Food Hydrocolloids, 101*, 105532. doi:https://doi.org/10.1016/j.foodhyd.2019.105532

Almeida, H. H. S., Barros, L., Barreira, J. C. M., Calhelha, R. C., Heleno, S. A., Sayer, C., . . . Ferreira, I. C. F. R. (2018). Bioactive evaluation and application of different formulations of the natural colorant curcumin (E100) in a hydrophilic matrix (yogurt). *Food Chemistry, 261*, 224-232. doi:https://doi.org/10.1016/j.foodchem.2018.04.056

Alongi, M., & Anese, M. (2021). Re-thinking functional food development through a holistic approach. *Journal of Functional Foods, 81*, 104466.

Alsanei, W. A., Chen, J., & Ding, R. (2015). Food oral breaking and the determining role of tongue muscle strength. *Food Research International, 67*, 331-337. doi:https://doi.org/10.1016/j.foodres.2014.11.039

Altin, G., Gültekin-Özgüven, M., & Ozcelik, B. (2018). Liposomal dispersion and powder systems for delivery of cocoa hull waste phenolics via Ayran (drinking yoghurt): Comparative studies on in-vitro bioaccessibility and antioxidant capacity. *Food Hydrocolloids, 81*, 364-370. doi:https://doi.org/10.1016/j.foodhyd.2018.02.051

Amjadi, S., Ghorbani, M., Hamishehkar, H., & Roufegarinejad, L. (2018). Improvement in the stability of betanin by liposomal nanocarriers: Its application in gummy candy as a food model. *Food Chemistry, 256*, 156-162. doi:https://doi.org/10.1016/j.foodchem.2018.02.114

Anand, P., Kunnumakkara, A. B., Newman, R. A., & Aggarwal, B. B. (2007). Bioavailability of curcumin: problems and promises. *Molecular Pharmaceutics, 4*(6), 807-818. doi:10.1021/mp700113r

Anema, S. G., Lee, S. K., Lowe, E. K., & Klostermeyer, H. (2004). Rheological properties of acid gels prepared from heated ph-adjusted skim milk. *Journal of Agricultural and Food Chemistry, 52*(2), 337-343. doi:10.1021/jf034972c

Ansari, M. M., & Kumar, D. S. (2012). Fortification of food and beverages with phytonutrients. *Food and Public Health, 2*(6), 241-253.

Araiza-Calahorra, A., Akhtar, M., & Sarkar, A. (2018). Recent advances in emulsion-based delivery approaches for curcumin: From encapsulation to bioaccessibility. *Trends in Food Science & Technology, 71*, 155-169. doi:https://doi.org/10.1016/j.tifs.2017.11.009

Araiza-Calahorra, A., Glover, Z. J., Akhtar, M., & Sarkar, A. (2020). Conjugate microgel-stabilized Pickering emulsions: Role in delaying gastric digestion. *Food Hydrocolloids, 105*, 105794.

Augustin, M. A., & Sanguansri, L. (2015). Challenges and solutions to incorporation of nutraceuticals in foods. *Annual Review of Food Science and Technology, 6*(1), 463-477. doi:10.1146/annurev-food-022814-015507

Bagale, U., Kadi, A., Malinin, A., Potoroko, I., Sonawane, S., & Potdar, S. (2022). Ultrasound-assisted stable curcumin nanoemulsion and its application in bakery product. *International Journal of Food Science, 2022*, 4784794. doi:10.1155/2022/4784794

Bao, C., Jiang, P., Chai, J., Jiang, Y., Li, D., Bao, W., . . . Li, Y. (2019). The delivery of sensitive food bioactive ingredients: Absorption mechanisms, influencing factors, encapsulation techniques and evaluation models. *Food Research International, 120*, 130-140.

Barbé, F., Ménard, O., Gouar, Y. L., Buffière, C., Famelart, M.-H., Laroche, B., . . . Dupont, D. (2014). Acid and rennet gels exhibit strong differences in the kinetics of milk protein

digestion and amino acid bioavailability. *Food Chemistry, 143*, 1-8. doi:https://doi.org/10.1016/j.foodchem.2013.07.100

Betoret, E., Betoret, N., Vidal, D., & Fito, P. (2011). Functional foods development: Trends and technologies. *Trends in Food Science & Technology, 22*(9), 498-508. doi:https://doi.org/10.1016/j.tifs.2011.05.004

Bikker, J. F., Anema, S. G., Li, Y., & Hill, J. P. (2000). Rheological properties of acid gels prepared from heated milk fortified with whey protein mixtures containing the A, B and C variants of β-lactoglobulin. *International Dairy Journal, 10*(10), 723-732. doi:https://doi.org/10.1016/S0958-6946(00)00096-0

Bornhorst, G. M., & Singh, R. P. (2014). Gastric Digestion in vivo and in vitro: how the structural aspects of food influence the digestion process. *Annual Review of Food Science and Technology, 5*(1), 111-132. doi:10.1146/annurev-food-030713-092346

Boyd, B. J., Salim, M., Clulow, A. J., Ramirez, G., Pham, A. C., & Hawley, A. (2018). The impact of digestion is essential to the understanding of milk as a drug delivery system for poorly water soluble drugs. *Journal of Controlled Release, 292*, 13-17. doi:https://doi.org/10.1016/j.jconrel.2018.10.027

Brodkorb, A., Egger, L., Alminger, M., Alvito, P., Assunção, R., Ballance, S., . . . Recio, I. (2019). INFOGEST static in vitro simulation of gastrointestinal food digestion. *Nature Protocols, 14*(4), 991-1014. doi:10.1038/s41596-018-0119-1

Čakarević, J., Torbica, A., Belović, M., Tomić, J., Sedlar, T., & Popović, L. (2021). Pumpkin oil cake protein as a new carrier for encapsulation incorporated in food matrix: Effect of processing, storage and in vitro digestion on bioactivity. *International Journal of Food Science & Technology, 56*(7), 3400-3408.

Campbell, J., Berry, J., & Liang, Y. (2019). Anatomy and physiology of the small intestine. In *Shackelford's Surgery of the Alimentary Tract, 2 Volume Set* (pp. 817-841): Elsevier.

Capuano, E., Oliviero, T., Fogliano, V., & Pellegrini, N. (2018). Role of the food matrix and digestion on calculation of the actual energy content of food. *Nutrition Reviews, 76*(4), 274-289. doi:10.1093/nutrit/nux072

Carbonell-Capella, J. M., Buniowska, M., Barba, F. J., Esteve, M. J., & Frígola, A. (2014). Analytical methods for determining bioavailability and bioaccessibility of bioactive compounds from fruits and vegetables: A Review. *Comprehensive Reviews in Food Science and Food Safety, 13*(2), 155-171. doi:10.1111/1541-4337.12049

Chang, Y., McLandsborough, L., & McClements, D. J. (2012). Physical properties and antimicrobial efficacy of thyme oil nanoemulsions: influence of ripening inhibitors. *Journal of Agricultural and Food Chemistry,* 60(48), 12056-12063. doi:10.1021/jf304045a

Charalampopoulos, D., Wang, R., Pandiella, S., & Webb, C. (2002). Application of cereals and cereal components in functional foods: a review. *International journal of food microbiology, 79*(1-2), 131-141.

Chen, B., McClements, D. J., & Decker, E. A. (2013). Design of foods with bioactive lipids for improved health. *Annual Review of Food Science and Technology, 4*(1), 35-56. doi:10.1146/annurev-food-032112-135808

Chen, J. (2009). Food oral processing—A review. *Food Hydrocolloids, 23*(1), 1-25. doi:https://doi.org/10.1016/j.foodhyd.2007.11.013

Chen, X., Du, X., Chen, P., Guo, L., Xu, Y., & Zhou, X. (2017). Morphologies and gelatinization behaviours of high-amylose maize starches during heat treatment. *Carbohydrate Polymers, 157*, 637-642. doi:https://doi.org/10.1016/j.carbpol.2016.10.024

Choi, J., Horne, D., & Lucey, J. (2007). Effect of insoluble calcium concentration on rennet coagulation properties of milk. *Journal of Dairy Science, 90*(6), 2612-2623.

Cifelli, C. J. (2021). Looking beyond traditional nutrients: the role of bioactives and the food matrix on health. *Nutrition Reviews, 79*(Supplement_2), 1-3.

Comunian, T. A., Chaves, I. E., Thomazini, M., Moraes, I. C. F., Ferro-Furtado, R., de Castro, I. A., & Favaro-Trindade, C. S. (2017). Development of functional yogurt containing free and encapsulated echium oil, phytosterol and sinapic acid. *Food Chemistry, 237*, 948-956. doi:https://doi.org/10.1016/j.foodchem.2017.06.071

Dalgleish, D. G., & Corredig, M. (2012). The structure of the casein micelle of milk and its changes during processing. *Annual Review of Food Science and Technology, 3*(1), 449-467. doi:10.1146/annurev-food-022811-101214

de Campo, C., Queiroz Assis, R., Marques da Silva, M., Haas Costa, T. M., Paese, K., Stanisçuaski Guterres, S., . . . Hickmann Flôres, S. (2019). Incorporation of zeaxanthin nanoparticles in yogurt: Influence on physicochemical properties, carotenoid stability and sensory analysis. *Food Chemistry, 301*, 125230. doi:https://doi.org/10.1016/j.foodchem.2019.125230

de Lourdes Samaniego-Vaesken, M., Alonso-Aperte, E., & Varela-Moreiras, G. (2012). Vitamin food fortification today. *Food & nutrition research, 56*, 10.3402/fnr.v3456i3400.5459. doi:10.3402/fnr.v56i0.5459

Delfanian, M., & Sahari, M. A. (2020). Improving functionality, bioavailability, nutraceutical and sensory attributes of fortified foods using phenolics-loaded nanocarriers as natural ingredients. *Food Research International, 137*, 109555. doi:https://doi.org/10.1016/j.foodres.2020.109555

Devezeaux de Lavergne, M., van de Velde, F., van Boekel, M. A. J. S., & Stieger, M. (2015). Dynamic texture perception and oral processing of semi-solid food gels: Part 2: Impact of breakdown behaviour on bolus properties and dynamic texture perception. *Food Hydrocolloids, 49*, 61-72. doi:https://doi.org/10.1016/j.foodhyd.2015.02.037

Dima, C., Assadpour, E., Dima, S., & Jafari, S. M. (2020). Bioactive-loaded nanocarriers for functional foods: from designing to bioavailability. *Current Opinion in Food Science, 33*, 21-29. doi:https://doi.org/10.1016/j.cofs.2019.11.006

Do, D. T., Singh, J., Oey, I., & Singh, H. (2019). Modulating effect of cotyledon cell microstructure on in vitro digestion of starch in legumes. *Food Hydrocolloids, 96*, 112-122. doi:https://doi.org/10.1016/j.foodhyd.2019.04.063

Domínguez, R., Pateiro, M., Munekata, P. E., McClements, D. J., & Lorenzo, J. M. (2021). Encapsulation of bioactive phytochemicals in plant-based matrices and application as additives in meat and meat products. *Molecules, 26*(13), 3984.

Donhowe, E. G., Flores, F. P., Kerr, W. L., Wicker, L., & Kong, F. (2014). Characterization and invitro bioavailability of β-carotene: Effects of microencapsulation method and food matrix. *LWT - Food Science and Technology, 57*(1), 42-48. doi:10.1016/j.lwt.2013.12.037

Donsì, F. (2018). Chapter 11 - Applications of Nanoemulsions in Foods. In S. M. Jafari & D. J. McClements (Eds.), *Nanoemulsions* (pp. 349-377): Academic Press.

Donsì, F., Sessa, M., & Ferrari, G. (2013). Nanometric-size delivery systems for bioactive compounds for the nutraceutical and food industries. In *Bio-Nanotechnology*.

Đorđević, V., Balanč, B., Belščak-Cvitanović, A., Lević, S., Kalušević, A., Kostić, I., . . . Nedović, V. (2015). Trends in encapsulation technologies for delivery of food bioactive compounds. *Food Engineering Reviews, 7*(4), 452-490.

Douglas Jr, F. W., Greenberg, R., Farrell Jr, H. M., & Edmondson, L. F. (1981). Effects of ultra-high-temperature pasteurization on milk proteins. *Journal of Agricultural and Food Chemistry, 29*(1), 11-15.

Dun, H., Liang, H., Li, S., Li, B., & Geng, F. (2021). Influence of an O/W emulsion on the gelatinization, retrogradation and digestibility of rice starch with varying amylose

contents. *Food Hydrocolloids, 113*, 106547. doi:https://doi.org/10.1016/j.foodhyd.2020.106547

Dupont, D., Barbe, F., Le Feunteun, S., Ménard, O., Le Gouar, Y., Deglaire, A., . . . Laroche, B. (2015, 2015-11-10). *Structuring food for improving nutrient bioavailability: the case of dairy gels.* Paper presented at the 29. EFFoST International Conference, Athènes, Greece.

Egger, L., Ménard, O., Baumann, C., Duerr, D., Schlegel, P., Stoll, P., . . . Portmann, R. (2017). Digestion of milk proteins: Comparing static and dynamic in vitro digestion systems with in vivo data. *Food Research International*. doi:https://doi.org/10.1016/j.foodres.2017.12.049

Eggersdorfer, M., & Wyss, A. (2018). Carotenoids in human nutrition and health. *Archives of Biochemistry and Biophysics, 652*, 18-26. doi:https://doi.org/10.1016/j.abb.2018.06.001

El-Kholy, W. M., Soliman, T. N., & Darwish, A. M. G. (2019). Evaluation of date palm pollen (Phoenix dactylifera L.) encapsulation, impact on the nutritional and functional properties of fortified yoghurt. *PloS one, 14*(10), e0222789.

El Sohaimy, S. (2012). Functional foods and nutraceuticals-modern approach to food science. *World Applied Sciences Journal, 20*(5), 691-708.

Elzoghby, A. O., Abo El-Fotoh, W. S., & Elgindy, N. A. (2011). Casein-based formulations as promising controlled release drug delivery systems. *Journal of Controlled Release, 153*(3), 206-216. doi:https://doi.org/10.1016/j.jconrel.2011.02.010

Er, B., Sert, D., & Mercan, E. (2019). Production of skim milk powder by spray-drying from transglutaminase treated milk concentrates: Effects on physicochemical, powder flow, thermal and microstructural characteristics. *International Dairy Journal, 99*, 104544. doi:https://doi.org/10.1016/j.idairyj.2019.104544

Eržen, N., Kač, M., & Pravst, I. (2014). Perceived healthfulness of dairy products and their imitations. *Agro FOOD Ind Hi Tech, 25*, 24-27.

Esatbeyoglu, T., Ulbrich, K., Rehberg, C., Rohn, S., & Rimbach, G. (2015). Thermal stability, antioxidant, and anti-inflammatory activity of curcumin and its degradation product 4-vinyl guaiacol. *Food & Function, 6*(3), 887-893. doi:10.1039/C4FO00790E

Espín, J. C., García-Conesa, M. T., & Tomás-Barberán, F. A. (2007). Nutraceuticals: Facts and fiction. *Phytochemistry, 68*(22), 2986-3008. doi:https://doi.org/10.1016/j.phytochem.2007.09.014

Ezhilarasi, P., Indrani, D., Jena, B. S., & Anandharamakrishnan, C. (2013). Freeze drying technique for microencapsulation of Garcinia fruit extract and its effect on bread quality. *Journal of Food Engineering, 117*(4), 513-520.

Ezhilarasi, P. N., Indrani, D., Jena, B. S., & Anandharamakrishnan, C. (2014). Microencapsulation of Garcinia fruit extract by spray drying and its effect on bread quality. *Journal of the Science of Food and Agriculture, 94*(6), 1116-1123. doi:doi:10.1002/jsfa.6378

Fagan, C. C., O'Callaghan, D. J., Mateo, M. J., & Dejmek, P. (2017). Chapter 6 - The Syneresis of Rennet-Coagulated Curd. In P. L. H. McSweeney, P. F. Fox, P. D. Cotter, & D. W. Everett (Eds.), *Cheese (Fourth Edition)* (pp. 145-177). San Diego: Academic Press.

Fang, X., Rioux, L.-E., Labrie, S., & Turgeon, S. L. (2016). Commercial cheeses with different texture have different disintegration and protein/peptide release rates during simulated in vitro digestion. *International Dairy Journal, 56*, 169-178. doi:https://doi.org/10.1016/j.idairyj.2016.01.023

Fardet, A., Dupont, D., Rioux, L.-E., & Turgeon, S. L. (2018). Influence of food structure on dairy protein, lipid and calcium bioavailability: A narrative review of evidence. *Critical Reviews in Food Science and Nutrition*, 1-24. doi:10.1080/10408398.2018.1435503

Fathi, M., Martín, Á., & McClements, D. J. (2014). Nanoencapsulation of food ingredients using carbohydrate based delivery systems. *Trends in Food Science & Technology, 39*(1), 18-39.

Feher, J. J. (2017). *Quantitative human physiology: an introduction*: Academic press.

Flores, F. P., & Kong, F. (2017). In vitro release kinetics of microencapsulated materials and the effect of the food matrix. *Annual Review of Food Science and Technology, 8*(1), 237-259. doi:10.1146/annurev-food-030216-025720

Floury, J., Bianchi, T., Thévenot, J., Dupont, D., Jamme, F., Lutton, E., . . . Le Feunteun, S. (2018). Exploring the breakdown of dairy protein gels during in vitro gastric digestion using time-lapse synchrotron deep-UV fluorescence microscopy. *Food Chemistry, 239*, 898-910. doi:https://doi.org/10.1016/j.foodchem.2017.07.023

Francisco, C. R. L., Heleno, S. A., Fernandes, I. P. M., Barreira, J. C. M., Calhelha, R. C., Barros, L., . . . Barreiro, M. F. (2018). Functionalization of yogurts with Agaricus bisporus extracts encapsulated in spray-dried maltodextrin crosslinked with citric acid. *Food Chemistry, 245*, 845-853. doi:https://doi.org/10.1016/j.foodchem.2017.11.098

Freitas, D., Le Feunteun, S., Panouillé, M., & Souchon, I. (2018). The important role of salivary α-amylase in the gastric digestion of wheat bread starch. *Food & Function, 9*(1), 200-208.

Fructuoso, I., Romão, B., Han, H., Raposo, A., Ariza-Montes, A., Araya-Castillo, L., & Zandonadi, R. P. (2021). An overview on nutritional aspects of plant-based beverages used as substitutes for cow's milk. *Nutrients, 13*(8), 2650.

Galanakis, C. M. (2017). Chapter 1 - Introduction. In C. M. Galanakis (Ed.), *Nutraceutical and Functional Food Components* (pp. 1-14): Academic Press.

Giang, T. M., Gaucel, S., Brestaz, P., Anton, M., Meynier, A., Trelea, I. C., & Le Feunteun, S. (2016). Dynamic modeling of in vitro lipid digestion: Individual fatty acid release and

bioaccessibility kinetics. *Food Chemistry, 194*, 1180-1188. doi:https://doi.org/10.1016/j.foodchem.2015.08.125

Gomes, G. V. d. L., Sola, M. R., Rochetti, A. L., Fukumasu, H., Vicente, A., & Pinho, S. C. d. (2019). β-carotene and α-tocopherol coencapsulated in nanostructured lipid carriers of murumuru (Astrocaryum murumuru) butter produced by phase inversion temperature method: characterisation, dynamic in vitro digestion and cell viability study. *Journal of Microencapsulation, 36*(1), 43-52.

Gomez-Estaca, J., Balaguer, M. P., Gavara, R., & Hernandez-Munoz, P. (2012). Formation of zein nanoparticles by electrohydrodynamic atomization: Effect of the main processing variables and suitability for encapsulating the food coloring and active ingredient curcumin. *Food Hydrocolloids, 28*(1), 82-91. doi:https://doi.org/10.1016/j.foodhyd.2011.11.013

Gómez-Estaca, J., Gavara, R., & Hernández-Muñoz, P. (2015). Encapsulation of curcumin in electrosprayed gelatin microspheres enhances its bioaccessibility and widens its uses in food applications. *Innovative Food Science & Emerging Technologies, 29*, 302-307. doi:https://doi.org/10.1016/j.ifset.2015.03.004

Gonçalves, R. F. S., Vicente, A. A., & Pinheiro, A. C. (2023). Incorporation of curcumin-loaded lipid-based nano delivery systems into food: Release behavior in food simulants and a case study of application in a beverage. *Food Chemistry, 405*, 134740. doi:https://doi.org/10.1016/j.foodchem.2022.134740

Graebin, C. S., Ribeiro, F. V., Rogério, K. R., & Kümmerle, A. E. (2019). Multicomponent reactions for the synthesis of bioactive compounds: a review. *Current Organic Synthesis, 16*(6), 855-899.

Grossmann, L., & McClements, D. J. (2021). The science of plant-based foods: Approaches to create nutritious and sustainable plant-based cheese analogs. *Trends in Food Science & Technology, 118*, 207-229. doi:https://doi.org/10.1016/j.tifs.2021.10.004

Guo, Q., Ye, A., Bellissimo, N., Singh, H., & Rousseau, D. (2017). Modulating fat digestion through food structure design. *Progress in Lipid Research, 68*, 109-118. doi:https://doi.org/10.1016/j.plipres.2017.10.001

Guo, Q., Ye, A., Lad, M., Dalgleish, D., & Singh, H. (2016). Impact of colloidal structure of gastric digesta on in-vitro intestinal digestion of whey protein emulsion gels. *Food Hydrocolloids, 54*, 255-265. doi:https://doi.org/10.1016/j.foodhyd.2015.10.006

Guo, Q., Ye, A., Singh, H., & Rousseau, D. (2020). Destructuring and restructuring of foods during gastric digestion. *Comprehensive Reviews in Food Science and Food Safety, 19*(4), 1658-1679. doi:10.1111/1541-4337.12558

Havea, P. (2006). Protein interactions in milk protein concentrate powders. *International Dairy Journal, 16*(5), 415-422.

Hermund, D. B., Karadağ, A., Andersen, U., Jónsdóttir, R., Kristinsson, H. G., Alasalvar, C., & Jacobsen, C. (2016). Oxidative stability of granola bars enriched with multilayered fish oil emulsion in the presence of novel brown seaweed based antioxidants. *Journal of Agricultural and Food Chemistry, 64*(44), 8359-8368. doi:10.1021/acs.jafc.6b03454

Hidalgo, A., Brandolini, A., Čanadanović-Brunet, J., Ćetković, G., & Tumbas Šaponjac, V. (2018). Microencapsulates and extracts from red beetroot pomace modify antioxidant capacity, heat damage and colour of pseudocereals-enriched einkorn water biscuits. *Food Chemistry, 268*, 40-48. doi:https://doi.org/10.1016/j.foodchem.2018.06.062

Hodgkinson, A. J., Wallace, O. A. M., Boggs, I., Broadhurst, M., & Prosser, C. G. (2018). Gastric digestion of cow and goat milk: Impact of infant and young child in vitro

digestion conditions. *Food Chemistry, 245*, 275-281. doi:https://doi.org/10.1016/j.foodchem.2017.10.028

Horn, A. F., Green-Petersen, D., Nielsen, N. S., Andersen, U., Hyldig, G., Jensen, L. H. S., . . . Jacobsen, C. (2012). Addition of fish oil to cream cheese affects lipid oxidation, sensory stability and microstructure. *Agriculture, 2*(4), 359. Retrieved from http://www.mdpi.com/2077-0472/2/4/359

Huang, J., Shang, Z., Man, J., Liu, Q., Zhu, C., & Wei, C. (2015). Comparison of molecular structures and functional properties of high-amylose starches from rice transgenic line and commercial maize. *Food Hydrocolloids, 46*, 172-179. doi:https://doi.org/10.1016/j.foodhyd.2014.12.019

Huppertz, T., & Chia, L. W. (2021). Milk protein coagulation under gastric conditions: A review. *International Dairy Journal, 113*, 104882. doi:https://doi.org/10.1016/j.idairyj.2020.104882

Istenič, K., Cerc Korošec, R., & Poklar Ulrih, N. (2016). Encapsulation of (−)-epigallocatechin gallate into liposomes and into alginate or chitosan microparticles reinforced with liposomes. *Journal of the Science of Food and Agriculture, 96*(13), 4623-4632.

Jamwal, R. (2018). Bioavailable curcumin formulations: A review of pharmacokinetic studies in healthy volunteers. *Journal of Integrative Medicine, 16*(6), 367-374. doi:https://doi.org/10.1016/j.joim.2018.07.001

Jiang, T., Liao, W., & Charcosset, C. (2020). Recent advances in encapsulation of curcumin in nanoemulsions: A review of encapsulation technologies, bioaccessibility and applications. *Food Research International, 132*, 109035. doi:https://doi.org/10.1016/j.foodres.2020.109035

Joardder, M. U., Kumar, C., & Karim, M. (2017). Food structure: Its formation and relationships with other properties. *Critical Reviews in Food Science and Nutrition, 57*(6), 1190-1205.

Joung, H. J., Choi, M. J., Kim, J. T., Park, S. H., Park, H. J., & Shin, G. H. (2016). Development of food-grade curcumin nanoemulsion and its potential application to food beverage system: antioxidant property and in vitro digestion. *Journal of Food Science, 81*(3), N745-N753. doi:10.1111/1750-3841.13224

Karim, M. A., Rahman, M. M., Pham, N. D., & Fawzia, S. (2018). 3 - Food microstructure as affected by processing and its effect on quality and stability. In S. Devahastin (Ed.), *Food Microstructure and Its Relationship with Quality and Stability* (pp. 43-57): Woodhead Publishing.

Keenan, D. F., Resconi, V. C., Smyth, T. J., Botinestean, C., Lefranc, C., Kerry, J. P., & Hamill, R. M. (2015). The effect of partial-fat substitutions with encapsulated and unencapsulated fish oils on the technological and eating quality of beef burgers over storage. *Meat Science, 107*, 75-85. doi:https://doi.org/10.1016/j.meatsci.2015.04.013

Kha, T. C., Nguyen, M. H., Roach, P. D., & Stathopoulos, C. E. (2015). A storage study of encapsulated gac (Momordica cochinchinensis) oil powder and its fortification into foods. *Food and Bioproducts Processing, 96*, 113-125. doi:https://doi.org/10.1016/j.fbp.2015.07.009

Khan, R. S., Grigor, J., Winger, R., & Win, A. (2013). Functional food product development – Opportunities and challenges for food manufacturers. *Trends in Food Science & Technology, 30*(1), 27-37. doi:https://doi.org/10.1016/j.tifs.2012.11.004

Khaw, K.-Y., Parat, M.-O., Shaw, P. N., & Falconer, J. R. (2017). Solvent supercritical fluid technologies to extract bioactive compounds from natural sources: A review. *Molecules, 22*(7), 1186.

Kibar, E. A. A., Gönenç, I., & Us, F. (2010). Gelatinization of waxy, normal and high amylose corn starches. *The Journal of Food, 35*(4), 237-244.

Kong, F., & Singh, R. P. (2008). Disintegration of solid foods in human stomach. *Journal of Food Science, 73*(5), R67-R80. doi:10.1111/j.1750-3841.2008.00766.x

Kong, F., & Singh, R. P. (2009). Digestion of raw and roasted almonds in simulated gastric environment. *Food Biophysics, 4*(4), 365-377. doi:10.1007/s11483-009-9135-6

Kong, F., & Singh, R. P. (2010). A human gastric simulator (hgs) to study food digestion in human stomach. *Journal of Food Science, 75*(9), E627-E635. doi:10.1111/j.1750-3841.2010.01856.x

Kumar, D. D., Mann, B., Pothuraju, R., Sharma, R., Bajaj, R., & Minaxi. (2016). Formulation and characterization of nanoencapsulated curcumin using sodium caseinate and its incorporation in ice cream. *Food and Function, 7*(1), 417-424. doi:10.1039/c5fo00924c

Lamothe, S., Rémillard, N., Tremblay, J., & Britten, M. (2017). Influence of dairy matrices on nutrient release in a simulated gastrointestinal environment. *Food Research International, 92*, 138-146. doi:https://doi.org/10.1016/j.foodres.2016.12.026

Le Feunteun, S., & Mariette, F. (2008). Effects of acidification with and without rennet on a concentrated casein system: A kinetic NMR probe diffusion study. *Macromolecules, 41*(6), 2079-2086. doi:10.1021/ma702248z

Lentle, R. G., & Janssen, P. W. M. (2011). Introduction. In *The Physical Processes of Digestion* (pp. 1-7). New York, NY: Springer New York.

Let, M. B., Jacobsen, C., & Meyer, A. S. (2007). Lipid oxidation in milk, yoghurt, and salad dressing enriched with neat fish oil or pre-emulsified fish oil. *Journal of Agricultural and Food Chemistry, 55*(19), 7802-7809. doi:10.1021/jf070830x

Li, C., Yu, W., Wu, P., & Chen, X. D. (2020). Current in vitro digestion systems for understanding food digestion in human upper gastrointestinal tract. *Trends in Food Science & Technology, 96*, 114-126. doi:https://doi.org/10.1016/j.tifs.2019.12.015

Li, Q., & Zhao, Z. (2019). Acid and rennet-induced coagulation behavior of casein micelles with modified structure. *Food Chemistry, 291*, 231-238. doi:https://doi.org/10.1016/j.foodchem.2019.04.028

Li, S., Ye, A., & Singh, H. (2020). Effect of seasonal variations on the acid gelation of milk. *Journal of Dairy Science, 103*(6), 4965-4974. doi:https://doi.org/10.3168/jds.2019-17603

Lin, L., Zhang, L., Cai, X., Liu, Q., Zhang, C., & Wei, C. (2018). The relationship between enzyme hydrolysis and the components of rice starches with the same genetic background and amylopectin structure but different amylose contents. *Food Hydrocolloids, 84*, 406-413. doi:https://doi.org/10.1016/j.foodhyd.2018.06.029

Liu, D., Deng, Y., Sha, L., Abul Hashem, M., & Gai, S. (2017). Impact of oral processing on texture attributes and taste perception. *Journal of Food Science and Technology, 54*(8), 2585-2593. doi:10.1007/s13197-017-2661-1

Liu, D., Parker, H. L., Curcic, J., Kozerke, S., & Steingoetter, A. (2016). Emulsion stability modulates gastric secretion and its mixing with emulsified fat in healthy adults in a randomized magnetic resonance imaging study. *The Journal of Nutrition, 146*(10), 2158-2164.

Lu, X., Brennan, M. A., Guan, W., Zhang, J., Yuan, L., & Brennan, C. S. (2021). Enhancing the nutritional properties of bread by incorporating mushroom bioactive compounds: The manipulation of the pre-dictive glycaemic response and the phenolic properties. *Foods, 10*(4), 731.

Lu, Y., Mao, L., Hou, Z., Miao, S., & Gao, Y. (2019). Development of emulsion gels for the delivery of functional food ingredients: From structure to functionality. *Food Engineering Reviews, 11*(4), 245-258.

Lucey, J. A. (2008). Chapter 16 - Milk protein gels. In A. Thompson, M. Boland, & H. Singh (Eds.), *Milk Proteins* (pp. 449-481). San Diego: Academic Press.

Luo, N., Ye, A., Wolber, F. M., & Singh, H. (2019). Structure of whey protein emulsion gels containing capsaicinoids: Impact on in-mouth breakdown behaviour and sensory perception. *Food Hydrocolloids, 92*, 19-29. doi:https://doi.org/10.1016/j.foodhyd.2019.01.019

Luo, N., Ye, A., Wolber, F. M., & Singh, H. (2021). Effect of gel structure on the in vitro gastrointestinal digestion behaviour of whey protein emulsion gels and the bioaccessibility of capsaicinoids. *Molecules, 26*(5), 1379. Retrieved from https://www.mdpi.com/1420-3049/26/5/1379

MacFarlane, N. G. (2018). Digestion and absorption. *Anaesthesia & Intensive Care Medicine, 19*(3), 125-127.

Magallanes-Cruz, P. A., Flores-Silva, P. C., & Bello-Perez, L. A. (2017). Starch structure influences its digestibility: a review. *Journal of Food Science, 82*(9), 2016-2023.

Mao, L., Roos, Y. H., Biliaderis, C. G., & Miao, S. (2017). Food emulsions as delivery systems for flavor compounds: A review. *Critical Reviews in Food Science and Nutrition, 57*(15), 3173-3187.

Marcolino, V. A., Zanin, G. M., Durrant, L. R., Benassi, M. D. T., & Matioli, G. (2011). Interaction of curcumin and bixin with β-cyclodextrin: complexation methods, stability, and applications in food. *Journal of Agricultural and Food Chemistry, 59*(7), 3348-3357. doi:10.1021/jf104223k

Martin, G. J. O., Williams, R. P. W., & Dunstan, D. E. (2007). Comparison of casein micelles in raw and reconstituted skim milk. *Journal of Dairy Science, 90*(10), 4543-4551. doi:https://doi.org/10.3168/jds.2007-0166

Martinez-Ballesta, M., Gil-Izquierdo, A., Garcia-Viguera, C., & Dominguez-Perles, R. (2018). Nanoparticles and controlled delivery for bioactive compounds: outlining challenges for new "smart-foods" for health. *Foods, 7*(5). doi:10.3390/foods7050072

Martins, A., Barros, L., Carvalho, A. M., Santos-Buelga, C., Fernandes, I. P., Barreiro, F., & Ferreira, I. C. (2014). Phenolic extracts of Rubus ulmifolius Schott flowers: Characterization, microencapsulation and incorporation into yogurts as nutraceutical sources. *Food & Function, 5*(6), 1091-1100.

McClements, D. J. (2018). Recent developments in encapsulation and release of functional food ingredients: delivery by design. *Current Opinion in Food Science, 23*, 80-84.

McClements, D. J., Decker, E. A., Park, Y., & Weiss, J. (2008). Designing food structure to control stability, digestion, release and absorption of lipophilic food components. *Food Biophysics, 3*(2), 219-228. doi:10.1007/s11483-008-9070-y

McClements, D. J., Decker, E. A., & Weiss, J. (2007). Emulsion-based delivery systems for lipophilic bioactive components. *Journal of Food Science, 72*(8), R109-R124. doi:doi:10.1111/j.1750-3841.2007.00507.x

McClements, D. J., & Grossmann, L. (2021). A brief review of the science behind the design of healthy and sustainable plant-based foods. *NPJ science of food, 5*(1), 1-10.

McClements, D. J., & Jafari, S. M. (2018). Chapter 1 - General aspects of nanoemulsions and their formulation. In S. M. Jafari & D. J. McClements (Eds.), *Nanoemulsions* (pp. 3-20): Academic Press.

Menrad, K. (2003). Market and marketing of functional food in Europe. *Journal of Food Engineering, 56*(2-3), 181-188.

Minekus, M., Alminger, M., Alvito, P., Ballance, S., Bohn, T., Bourlieu, C., . . . Brodkorb, A. (2014). A standardised static in vitro digestion method suitable for food - an international consensus. *Food & Function, 5*(6), 1113-1124. doi:10.1039/c3fo60702j

Miranda, G., & Pelissier, J.-P. (1981). In vivo studies on the digestion of bovine caseins in the rat stomach. *Journal of Dairy Research, 48*(2), 319-326. doi:10.1017/S0022029900021749

Moghadam, F. V., Pourahmad, R., Mortazavi, A., Davoodi, D., & Azizinezhad, R. (2019). Use of fish oil nanoencapsulated with gum arabic carrier in low fat probiotic fermented milk. *Food science of animal resources, 39*(2), 309.

Molaveisi, M., Shahidi Noghabi, M., Parastouei, K., & Taheri, R. A. (2021). Fate of nano-phytosomes containing bioactive compounds of Echinacea extract in an acidic food beverage. *Food Structure, 27*, 100177. doi:https://doi.org/10.1016/j.foostr.2021.100177

Molet-Rodríguez, A., Torcello-Gómez, A., Salvia-Trujillo, L., Martín-Belloso, O., & Mackie, A. R. (2023). In vitro digestibility of O/W emulsions co-ingested with complex meals: Influence of the food matrix. *Food Hydrocolloids, 135*, 108121. doi:https://doi.org/10.1016/j.foodhyd.2022.108121

Mollet, B., & Rowland, I. (2002). Functional foods: at the frontier between food and pharma. *Current Opinion in Biotechnology, 13*(5), 483-485. doi:https://doi.org/10.1016/S0958-1669(02)00375-0

Moreno, D. A., & Ilic, N. (2018). Functional and bioactive properties of food: The challenges ahead. *Foods, 7*(9). doi:10.3390/foods7090139

Mudgil, D., & Barak, S. (2019). 3 - Dairy-Based Functional Beverages. In A. M. Grumezescu & A. M. Holban (Eds.), *Milk-Based Beverages* (pp. 67-93): Woodhead Publishing.

Mudie, D. M., Murray, K., Hoad, C. L., Pritchard, S. E., Garnett, M. C., Amidon, G. L., . . . Marciani, L. (2014). Quantification of gastrointestinal liquid volumes and distribution following a 240 ml dose of water in the fasted state. *Molecular Pharmaceutics, 11*(9), 3039-3047. doi:10.1021/mp500210c

Muhammad, D. R. A., Gonzalez, C. G., Sedaghat Doost, A., Van de Walle, D., Van der Meeren, P., & Dewettinck, K. (2019). Improvement of antioxidant activity and physical stability of chocolate beverage using colloidal cinnamon nanoparticles. *Food and Bioprocess Technology, 12*(6), 976-989. doi:10.1007/s11947-019-02271-5

Muhammad, D. R. A., Saputro, A. D., Rottiers, H., Van de Walle, D., & Dewettinck, K. (2018). Physicochemical properties and antioxidant activities of chocolates enriched with engineered cinnamon nanoparticles. *European Food Research and Technology, 244*(7), 1185-1202. doi:10.1007/s00217-018-3035-2

Mulet-Cabero, A.-I., Egger, L., Portmann, R., Ménard, O., Marze, S., Minekus, M., . . . Carrière, F. (2020). A standardised semi-dynamic in vitro digestion method suitable for food–an international consensus. *Food & Function, 11*(2), 1702-1720.

Mulet-Cabero, A.-I., Mackie, A. R., Brodkorb, A., & Wilde, P. J. (2020). Dairy structures and physiological responses: a matter of gastric digestion. *Critical Reviews in Food Science and Nutrition*, 1-16. doi:10.1080/10408398.2019.1707159

Mulet-Cabero, A.-I., Mackie, A. R., Wilde, P. J., Fenelon, M. A., & Brodkorb, A. (2019). Structural mechanism and kinetics of in vitro gastric digestion are affected by process-induced changes in bovine milk. *Food Hydrocolloids, 86*, 172-183. doi:https://doi.org/10.1016/j.foodhyd.2018.03.035

Mun, S., Kim, Y.-R., & McClements, D. J. (2015). Control of β-carotene bioaccessibility using starch-based filled hydrogels. *Food Chemistry, 173*, 454-461. doi:https://doi.org/10.1016/j.foodchem.2014.10.053

Mun, S., Kim, Y.-R., Shin, M., & McClements, D. J. (2015). Control of lipid digestion and nutraceutical bioaccessibility using starch-based filled hydrogels: Influence of starch and surfactant type. *Food Hydrocolloids, 44*, 380-389. doi:https://doi.org/10.1016/j.foodhyd.2014.10.013

Mun, S., & McClements, D. J. (2017). Influence of simulated in-mouth processing (size reduction and alpha-amylase addition) on lipid digestion and β-carotene bioaccessibility in starch-based filled hydrogels. *LWT-Food Science and Technology, 80*, 113-120. doi:https://doi.org/10.1016/j.lwt.2017.02.011

Mutsokoti, L., Panozzo, A., Pallares Pallares, A., Jaiswal, S., Van Loey, A., Grauwet, T., & Hendrickx, M. (2017). Carotenoid bioaccessibility and the relation to lipid digestion: A kinetic study. *Food Chemistry, 232*, 124-134. doi:https://doi.org/10.1016/j.foodchem.2017.04.001

N'Goma, J.-C. B., Amara, S., Dridi, K., Jannin, V., & Carrière, F. (2012). Understanding the lipid-digestion processes in the GI tract before designing lipid-based drug-delivery systems. *Therapeutic Delivery, 3*(1), 105-124. doi:10.4155/tde.11.138

Nacak, B., Öztürk-Kerimoğlu, B., Yıldız, D., Çağındı, Ö., & Serdaroğlu, M. (2021). Peanut and linseed oil emulsion gels as potential fat replacer in emulsified sausages. *Meat Science, 176*, 108464.

Nadia, J., Bronlund, J., Singh, R. P., Singh, H., & Bornhorst, G. M. (2021). Structural breakdown of starch-based foods during gastric digestion and its link to glycemic response: In vivo and in vitro considerations. *Comprehensive Reviews in Food Science and Food Safety, 20*(3), 2660-2698.

Nedovic, V., Kalusevic, A., Manojlovic, V., Levic, S., & Bugarski, B. (2011). An overview of encapsulation technologies for food applications. *Procedia Food Science, 1*, 1806-1815. doi:https://doi.org/10.1016/j.profoo.2011.09.265

Nielsen, N. S., & Jacobsen, C. (2009). Methods for reducing lipid oxidation in fish-oil-enriched energy bars. *International Journal of Food Science & Technology, 44*(8), 1536-1546. doi:doi:10.1111/j.1365-2621.2008.01786.x

Nieto, G., & Lorenzo, J. M. (2021). Use of olive oil as fat replacer in meat emulsions. *Current Opinion in Food Science, 40*, 179-186.

Niu, Z., Acevedo-Fani, A., McDowell, A., Barnett, A., Loveday, S. M., & Singh, H. (2020). Nanoemulsion structure and food matrix determine the gastrointestinal fate and in vivo bioavailability of coenzyme Q10. *Journal of Controlled Release, 327*, 444-455. doi:https://doi.org/10.1016/j.jconrel.2020.08.025

Oliveira, F. S., Ribeiro, A., Barros, L., Calhelha, R. C., Barreira, J. C., Junior, B. D., . . . Ferreira, I. C. (2017). Evaluation of Arenaria montana L. hydroethanolic extract as a chemopreventive food ingredient: A case study focusing a dairy product (yogurt). *Journal of Functional Foods, 38*, 214-220.

Ötles, S., & Cagindi, Ö. (2006). Cereal based functional foods and nutraceuticals. *Acta Scientiarum Polonorum Technologia Alimentaria, 5*(1), 107-112.

Oyenihi, A. B., & Smith, C. (2019). Are polyphenol antioxidants at the root of medicinal plant anti-cancer success? *Journal of Ethnopharmacology, 229*, 54-72. doi:https://doi.org/10.1016/j.jep.2018.09.037

Ozdal, T., Yolci-Omeroglu, P., & Tamer, E. C. (2020). 6 - Role of encapsulation in functional beverages. In A. M. Grumezescu & A. M. Holban (Eds.), *Biotechnological Progress and Beverage Consumption* (pp. 195-232): Academic Press.

Öztürk, B. (2017). Nanoemulsions for food fortification with lipophilic vitamins: Production challenges, stability, and bioavailability. *European Journal of Lipid Science and Technology, 119*(7). doi:10.1002/ejlt.201500539

Pan, Z., Ye, A., Li, S., Dave, A., Fraser, K., & Singh, H. (2021). Dynamic in vitro gastric digestion of sheep milk: influence of homogenization and heat treatment. *Foods, 10*(8), 1938.

Panthi, R. R., Kelly, A. L., Sheehan, J. J., Bulbul, K., Vollmer, A. H., & McMahon, D. J. (2019). Influence of protein concentration and coagulation temperature on rennet-induced gelation characteristics and curd microstructure. *Journal of Dairy Science, 102*(1), 177-189. doi:https://doi.org/10.3168/jds.2018-15039

Papillo, V. A., Arlorio, M., Locatelli, M., Fuso, L., Pellegrini, N., & Fogliano, V. (2019). In vitro evaluation of gastro-intestinal digestion and colonic biotransformation of curcuminoids considering different formulations and food matrices. *Journal of Functional Foods, 59*, 156-163. doi:https://doi.org/10.1016/j.jff.2019.05.031

Papillo, V. A., Locatelli, M., Travaglia, F., Bordiga, M., Garino, C., Coïsson, J. D., & Arlorio, M. (2019). Cocoa hulls polyphenols stabilized by microencapsulation as functional ingredient for bakery applications. *Food Research International, 115*, 511-518. doi:https://doi.org/10.1016/j.foodres.2018.10.004

Parada, J., & Aguilera, J. M. (2007). Food microstructure affects the bioavailability of several nutrients. *Journal of Food Science, 72*(2), R21-R32. doi:doi:10.1111/j.1750-3841.2007.00274.x

Park, S. J., Garcia, C. V., Shin, G. H., & Kim, J. T. (2018). Improvement of curcuminoid bioaccessibility from turmeric by a nanostructured lipid carrier system. *Food Chemistry, 251*, 51-57. doi:https://doi.org/10.1016/j.foodchem.2018.01.071

Park, S. J., Hong, S. J., Garcia, C. V., Lee, S. B., Shin, G. H., & Kim, J. T. (2019). Stability evaluation of turmeric extract nanoemulsion powder after application in milk as a food model. *Journal of Food Engineering, 259*, 12-20. doi:https://doi.org/10.1016/j.jfoodeng.2019.04.011

Pasrija, D., Ezhilarasi, P. N., Indrani, D., & Anandharamakrishnan, C. (2015). Microencapsulation of green tea polyphenols and its effect on incorporated bread quality. *LWT - Food Science and Technology, 64*(1), 289-296. doi:https://doi.org/10.1016/j.lwt.2015.05.054

Patel, H. A., Anema, S. G., Holroyd, S. E., Singh, H., & Creamer, L. K. (2007). Methods to determine denaturation and aggregation of proteins in low-, medium-and high-heat skim milk powders. *Le Lait, 87*(4-5), 251-268.

Patel, A., Patra, F., Shah, N., & Khedkar, C. (2018). Application of nanotechnology in the food industry: Present status and future prospects. In Impact of Nanoscience in the Food Industry (pp. 1-27).

Patricia, J. J., & Dhamoon, A. S. (2019). Physiology, Digestion.

Pereira, P. C. (2014). Milk nutritional composition and its role in human health. *Nutrition, 30*(6), 619-627.

Petrotos, K., Karkanta, F. , Gkoutsidis, P. , Giavasis, I. , Papatheodorou, K. , Ntontos, A. (2012). Production of novel bioactive yogurt enriched with olive fruit polyphenols. *International Journal of Biological, Biomolecular, Agricultural, Food and Biotechnological Engineering, 6*, 169-175. Retrieved from http://waset.org/publications/14830

Pimentel-González, D. J., Aguilar-García, M. E., Aguirre-Álvarez, G., Salcedo-Hernández, R., Guevara-Arauza, J. C., & Campos-Montiel, R. G. (2015). The process and maturation stability of chihuahua cheese with antioxidants in multiple emulsions. *Journal of Food Processing and Preservation, 39*(6), 1027-1035. doi:https://doi.org/10.1111/jfpp.12317

Pinilla, C. M. B., Thys, R. C. S., & Brandelli, A. (2019). Antifungal properties of phosphatidylcholine-oleic acid liposomes encapsulating garlic against environmental

fungal in wheat bread. *International Journal of Food Microbiology, 293*, 72-78. doi:https://doi.org/10.1016/j.ijfoodmicro.2019.01.006

Pletsch, E. A., & Hamaker, B. R. (2018). Brown rice compared to white rice slows gastric emptying in humans. *European Journal of Clininical Nutrition, 72*(3), 367-373.

Prasad, S., Gupta, S. C., Tyagi, A. K., & Aggarwal, B. B. (2014). Curcumin, a component of golden spice: From bedside to bench and back. *Biotechnology Advances*, 32(6), 1053-1064. doi:https://doi.org/10.1016/j.biotechadv.2014.04.004

Prasad, M., Jayaraman, S., Eladl, M. A., El-Sherbiny, M., Abdelrahman, M. A. E., Veeraraghavan, V. P., . . . Krishnamoorthy, K. (2022). A Comprehensive review on therapeutic perspectives of phytosterols in insulin resistance: A mechanistic approach. *Molecules*, *27*(5), 1595.

Prior, R. L., E. Wilkes, S., R. Rogers, T., Khanal, R. C., Wu, X., & Howard, L. R. (2010). Purified blueberry anthocyanins and blueberry juice alter development of obesity in mice fed an obesogenic high-fat diet. *Journal of Agricultural and Food Chemistry, 58*(7), 3970-3976. doi:10.1021/jf902852d

Puiggròs, F., Muguerza, B., Arola-Arnal, A., Aragonès, G., Suárez-Garcia, S., Bladé, C., . . . Suárez, M. (2017). Functional beverages. *Innovative Technologies in Beverage Processing*, 275-296.

Qazi, H. J., Majeed, H., Safdar, W., Antoniou, J., & Fang, Z. (2015). A novel approach for microencapsulation of nanoemulsions to overcome the oxidation of bioactives in aqueous phase. *Advance Journal of Food Science and Technology, 7*(6), 388-394.

Qazi, H. J., Ye, A., Acevedo-Fani, A., & Singh, H. (2021). In vitro digestion of curcumin-nanoemulsion-enriched dairy protein matrices: Impact of the type of gel structure on the bioaccessibility of curcumin. *Food Hydrocolloids, 117*, 106692.

Qazi, H. J., Ye, A., Acevedo-Fani, A., & Singh, H. (2022). Impact of recombined milk systems on gastrointestinal fate of curcumin nanoemulsion. *Frontiers in Nutrition, 9*.

Rafiee, Z., Barzegar, M., Sahari, M. A., & Maherani, B. (2018). Nanoliposomes containing pistachio green hull's phenolic compounds as natural bio-preservatives for mayonnaise. *European Journal of Lipid Science and Technology, 120*(9), 1800086. doi:https://doi.org/10.1002/ejlt.201800086

Raikos, V., & Ranawana, V. (2017). Designing emulsion droplets of foods and beverages to enhance delivery of lipophilic bioactive components – a review of recent advances. *International Journal of Food Science & Technology, 52*(1), 68-80. doi:doi:10.1111/ijfs.13272

Rao, J., Decker, E. A., Xiao, H., & McClements, D. J. (2013). Nutraceutical nanoemulsions: influence of carrier oil composition (digestible versus indigestible oil) on β-carotene bioavailability. *Journal of the Science of Food and Agriculture, 93*(13), 3175-3183. doi:10.1002/jsfa.6215

Rashidinejad, A., Birch, E. J., Sun-Waterhouse, D., & Everett, D. W. (2014). Delivery of green tea catechin and epigallocatechin gallate in liposomes incorporated into low-fat hard cheese. *Food Chemistry, 156*, 176-183. doi:https://doi.org/10.1016/j.foodchem.2014.01.115

Rashidinejad, A., Birch, E. J., Sun-Waterhouse, D., & Everett, D. W. (2015). Total phenolic content and antioxidant properties of hard low-fat cheese fortified with catechin as affected by invitro gastrointestinal digestion. *LWT - Food Science and Technology, 62*(1), 393-399. doi:10.1016/j.lwt.2014.12.058

Rauf, A., Imran, M., Orhan, I. E., & Bawazeer, S. (2018). Health perspectives of a bioactive compound curcumin: A review. *Trends in Food Science & Technology, 74*, 33-45. doi:https://doi.org/10.1016/j.tifs.2018.01.016

Rein, M. J., Renouf, M., Cruz-Hernandez, C., Actis-Goretta, L., Thakkar, S. K., & da Silva Pinto, M. (2013). Bioavailability of bioactive food compounds: a challenging journey to bioefficacy. *British Journal of Clinical Pharmacology*, *75*(3), 588-602. doi:doi:10.1111/j.1365-2125.2012.04425.x

Rein, M. J., Renouf, M., Cruz-Hernandez, C., Actis-Goretta, L., Thakkar, S. K., & Pinto, M. d. S. (2013). Bioavailability of bioactive food compounds: a challenging journey to bioefficacy. *British Journal of Clinical Pharmacology*, *75*(3), 588-602. doi:10.1111/j.1365-2125.2012.04425.x

Reyes-Jurado, F., Soto-Reyes, N., Dávila-Rodríguez, M., Lorenzo-Leal, A., Jiménez-Munguía, M., Mani-López, E., & López-Malo, A. (2021). Plant-based milk alternatives: Types, processes, benefits, and characteristics. *Food Reviews International*, 1-32.

Rezvankhah, A., Emam-Djomeh, Z., & Askari, G. (2020). Encapsulation and delivery of bioactive compounds using spray and freeze-drying techniques: A review. *Drying Technology*, *38*(1-2), 235-258.

Richardson, P. H., Jeffcoat, R., & Shi, Y.-C. (2000). High-Amylose Starches: From Biosynthesis to Their Use as Food Ingredients. *MRS Bulletin*, *25*(12), 20-24. doi:10.1557/mrs2000.249

Robert, P., Gorena, T., Romero, N., Sepulveda, E., Chavez, J., & Saenz, C. (2010). Encapsulation of polyphenols and anthocyanins from pomegranate (Punica granatum) by spray drying. *International Journal of Food Science & Technology*, *45*(7), 1386-1394. doi:https://doi.org/10.1111/j.1365-2621.2010.02270.x

Robert, P., Zamorano, M., González, E., Silva-Weiss, A., Cofrades, S., & Giménez, B. (2019). Double emulsions with olive leaves extract as fat replacers in meat systems with high oxidative stability. *Food Research International*, *120*, 904-912. doi:https://doi.org/10.1016/j.foodres.2018.12.014

Rodríguez, J., Martín, M. J., Ruiz, M. A., & Clares, B. (2016). Current encapsulation strategies for bioactive oils: From alimentary to pharmaceutical perspectives. *Food Research International, 83*, 41-59. doi:https://doi.org/10.1016/j.foodres.2016.01.032

Roman, M. J., Burri, B. J., & Singh, R. P. (2012). Release and bioaccessibility of β-carotene from fortified almond butter during in vitro digestion. *Journal of Agricultural and Food Chemistry, 60*(38), 9659-9666. doi:10.1021/jf302843w

Roy, D., Ye, A., Moughan, P. J., & Singh, H. (2021). Impact of gastric coagulation on the kinetics of release of fat globules from milk of different species. *Food & Function, 12*(4), 1783-1802. doi:10.1039/D0FO02870C

Ruhee, R. T., Roberts, L. A., Ma, S., & Suzuki, K. (2020). Organosulfur compounds: A review of their anti-inflammatory effects in human health. *Frontiers in Nutrition, 7*, 64.

Sabet, S., Rashidinejad, A., Qazi, H. J., & McGillivray, D. J. (2021). An efficient small intestine-targeted curcumin delivery system based on the positive-negative-negative colloidal interactions. *Food Hydrocolloids, 111*, 106375. doi:https://doi.org/10.1016/j.foodhyd.2020.106375

Salvia-Trujillo, L., Qian, C., Martín-Belloso, O., & McClements, D. J. (2013). Influence of particle size on lipid digestion and β-carotene bioaccessibility in emulsions and nanoemulsions. *Food Chemistry, 141*(2), 1472-1480. doi:https://doi.org/10.1016/j.foodchem.2013.03.050

Salvia-Trujillo, L., Verkempinck, S. H. E., Sun, L., Van Loey, A. M., Grauwet, T., & Hendrickx, M. E. (2017). Lipid digestion, micelle formation and carotenoid bioaccessibility kinetics: Influence of emulsion droplet size. *Food Chemistry, 229*, 653-662. doi:https://doi.org/10.1016/j.foodchem.2017.02.146

Samadarsi, R., Mishra, D., & Dutta, D. (2020). Mangiferin nanoparticles fortified dairy beverage as a low glycemic food product: its quality attributes and antioxidant

properties. *International Journal of Food Science & Technology, 55*(2), 589-600. doi:https://doi.org/10.1111/ijfs.14310

Sandoval-Castilla, O., Lobato-Calleros, C., Aguirre-Mandujano, E., & Vernon-Carter, E. J. (2004). Microstructure and texture of yogurt as influenced by fat replacers. *International Dairy Journal, 14*(2), 151-159. doi:https://doi.org/10.1016/S0958-6946(03)00166-3

Sarkar, A., Ye, A., & Singh, H. (2016). On the role of bile salts in the digestion of emulsified lipids. *Food Hydrocolloids, 60*, 77-84.

Sawale, P. D., Patil, G. R., Hussain, S. A., Singh, A. K., & Singh, R. R. B. (2017). Effect of incorporation of encapsulated and free Arjuna herb on storage stability of chocolate vanilla dairy drink. *Food Bioscience, 19*, 142-148. doi:https://doi.org/10.1016/j.fbio.2017.07.005

Scholz-Ahrens, K. E., Ahrens, F., & Barth, C. A. (2020). Nutritional and health attributes of milk and milk imitations. *European Journal of Nutrition, 59*(1), 19-34.

Schwanz Goebel, J. T., Kaur, L., Colussi, R., Elias, M. C., & Singh, J. (2019). Microstructure of indica and japonica rice influences their starch digestibility: A study using a human digestion simulator. *Food Hydrocolloids, 94*, 191-198. doi:https://doi.org/10.1016/j.foodhyd.2019.02.038

Serdaroğlu, M., Öztürk, B., & Urgu, M. (2016). Emulsion characteristics, chemical and textural properties of meat systems produced with double emulsions as beef fat replacers. *Meat Science, 117*, 187-195.

Šeregelj, V., Pezo, L., Šovljanski, O., Lević, S., Nedović, V., Markov, S., . . . Ćetković, G. (2021). New concept of fortified yogurt formulation with encapsulated carrot waste extract. *LWT - Food Science and Technology, 138*, 110732. doi:https://doi.org/10.1016/j.lwt.2020.110732

Serra, M., Trujillo, A. J., Guamis, B., & Ferragut, V. (2009). Evaluation of physical properties during storage of set and stirred yogurts made from ultra-high pressure homogenization-treated milk. *Food Hydrocolloids, 23*(1), 82-91. doi:https://doi.org/10.1016/j.foodhyd.2007.11.015

Sessa, M., Ferrari, G., & Donsì, F. (2015). Novel edible coating containing essential oil nanoemulsions to prolong the shelf life of vegetable products (Vol. 43).

Sethi, S., Tyagi, S. K., & Anurag, R. K. (2016). Plant-based milk alternatives an emerging segment of functional beverages: a review. *Journal of Food Science and Technology, 53*(9), 3408-3423. doi:10.1007/s13197-016-2328-3

Shahidi, F. (2009). Nutraceuticals and functional foods: Whole versus processed foods. *Trends in Food Science & Technology, 20*(9), 376-387. doi:https://doi.org/10.1016/j.tifs.2008.08.004

Shaikh, J., Ankola, D. D., Beniwal, V., Singh, D., & Kumar, M. N. V. R. (2009). Nanoparticle encapsulation improves oral bioavailability of curcumin by at least 9-fold when compared to curcumin administered with piperine as absorption enhancer. *European Journal of Pharmaceutical Sciences,* 37(3), 223-230. doi:https://doi.org/10.1016/j.ejps.2009.02.019

Sharma, A., Jana, A. H., & Chavan, R. S. (2012). Functionality of milk powders and milk-based powders for end use applications—A Review. *Comprehensive Reviews in Food Science and Food Safety, 11*(5), 518-528. doi:https://doi.org/10.1111/j.1541-4337.2012.00199.x

Shen, Z., Apriani, C., Weerakkody, R., Sanguansri, L., & Augustin, M. A. (2011). Food matrix effects on in vitro digestion of microencapsulated tuna oil powder. *Journal of Agricultural and Food Chemistry, 59*(15), 8442-8449. doi:10.1021/jf201494b

Shoba, G., Joy, D., Joseph, T., Majeed, M., Rajendran, R., & Srinivas, P. S. (1998). Influence of piperine on the pharmacokinetics of curcumin in animals and human volunteers. *Planta Medica*, 64(4), 353-356. doi:10.1055/s-2006-957450

Siegel, J., Urbain, J., Adler, L., Charkes, N., Maurer, A., Krevsky, B., . . . Malmud, L. (1988). Biphasic nature of gastric emptying. *Gut*, *29*(1), 85-89.

Silva, H. D., Poejo, J., Pinheiro, A. C., Donsì, F., Serra, A. T., Duarte, C. M. M., . . . Vicente, A. A. (2018). Evaluating the behaviour of curcumin nanoemulsions and multilayer nanoemulsions during dynamic in vitro digestion. *Journal of Functional Foods*, 48, 605-613. doi:https://doi.org/10.1016/j.jff.2018.08.002

Singh, H. (2007). Interactions of milk proteins during the manufacture of milk powders. *Lait*, *87*(4-5), 413-423. Retrieved from https://doi.org/10.1051/lait:2007014

Singh, H. (2016). Nanotechnology applications in functional foods; opportunities and challenges. *Preventive Nutrition and Food Science*, *21*(1), 1-8. doi:10.3746/pnf.2016.21.1.1

Singh, H., & Acevedo-Fani, A. (2022). New perspectives on the delivery of nutrients and bioactive compounds through gastric restructuring of foods lipid molecular assemblies: Structure, digestion, absorption and application as delivery carrier (SY (T8) 6). *Journal of Nutritional Science and Vitaminology*, *68*(Supplement), S149-S151.

Singh, H., & Gallier, S. (2014). Chapter 2 - Processing of food structures in the gastrointestinal tract and physiological responses. In M. Boland, M. Golding, & H. Singh (Eds.), *Food Structures, Digestion and Health* (pp. 51-81). San Diego: Academic Press.

Singh, J., Dartois, A., & Kaur, L. (2010). Starch digestibility in food matrix: a review. *Trends in Food Science & Technology*, *21*(4), 168-180. doi:https://doi.org/10.1016/j.tifs.2009.12.001

Singh, J., Kaur, L., & Singh, H. (2013). Chapter Four - Food microstructure and starch digestion. In J. Henry (Ed.), *Advances in Food and Nutrition Research* (Vol. 70, pp. 137-179): Academic Press.

Siyar, Z., Motamedzadegan, A., Mohammadzadeh Milani, J., & Rashidinejad, A. (2021). The effect of the liposomal encapsulated saffron extract on the physicochemical properties of a functional ricotta cheese. *Molecules, 27*(1), 120.

Solans, C., Izquierdo, P., Nolla, J., Azemar, N., & Garcia-Celma, M. J. (2005). Nano-emulsions. *Current Opinion in Colloid & Interface Science, 10*(3), 102-110. doi:https://doi.org/10.1016/j.cocis.2005.06.004

Somaratne, G., Ferrua, M. J., Ye, A., Nau, F., Floury, J., Dupont, D., & Singh, J. (2020). Food material properties as determining factors in nutrient release during human gastric digestion: a review. *Critical Reviews in Food Science and Nutrition, 60*(22), 3753-3769. doi:10.1080/10408398.2019.1707770

Steingoetter, A., Buetikofer, S., Curcic, J., Menne, D., Rehfeld, J. F., Fried, M., . . . Wooster, T. J. (2017). The dynamics of gastric emptying and self-reported feelings of satiation are better predictors than gastrointestinal hormones of the effects of lipid emulsion structure on fat digestion in healthy adults—a Bayesian inference approach. *The Journal of Nutrition, 147*(4), 706-714.

Steingoetter, A., Fox, M., Treier, R., Weishaupt, D., Marincek, B., Boesiger, P., . . . Schwizer, W. (2006). Effects of posture on the physiology of gastric emptying: A magnetic resonance imaging study. *Scandinavian Journal of Gastroenterology, 41*(10), 1155-1164. doi:10.1080/00365520600610451

Su, X., Wu, F., Zhang, Y., Yang, N., Chen, F., Jin, Z., & Xu, X. (2019). Effect of organic acids on bread quality improvement. *Food Chemistry, 278*, 267-275.

Szewczyk, K., Chojnacka, A., & Górnicka, M. (2021). Tocopherols and tocotrienols—Bioactive dietary compounds; what is certain, what is doubt? *International Journal of Molecular Sciences, 22*(12), 6222.

Tan, P. Y., Tan, T. B., Chang, H. W., Tey, B. T., Chan, E. S., Lai, O. M., . . . Tan, C. P. (2018). Effects of storage and yogurt matrix on the stability of tocotrienols encapsulated in chitosan-alginate microcapsules. *Food Chemistry, 241*, 79-85. doi:https://doi.org/10.1016/j.foodchem.2017.08.075

Tang, P. L., Cham, X. Y., Hou, X., & Deng, J. (2022). Potential use of waste cinnamon leaves in stirred yogurt fortification. *Food Bioscience, 48*, 101838. doi:https://doi.org/10.1016/j.fbio.2022.101838

Tao, J., Zhu, Q., Qin, F., Wang, M., Chen, J., & Zheng, Z.-P. (2017). Preparation of steppogenin and ascorbic acid, vitamin E, butylated hydroxytoluene oil-in-water microemulsions: Characterization, stability, and antibrowning effects for fresh apple juice. *Food Chemistry, 224*, 11-18. doi:https://doi.org/10.1016/j.foodchem.2016.12.045

Tolve, R., Bianchi, F., Lomuscio, E., Sportiello, L., & Simonato, B. (2023). Current advantages in the application of microencapsulation in functional bread development. *Foods, 12*(1), 96.

Topolska, K., Florkiewicz, A., & Filipiak-Florkiewicz, A. (2021). Functional food—Consumer motivations and expectations. *International Journal of Environmental Research and Public Health, 18*(10), 5327.

Tornesello, A. L., Borrelli, A., Buonaguro, L., Buonaguro, F. M., & Tornesello, M. L. (2020). Antimicrobial peptides as anticancer agents: functional properties and biological activities. *Molecules, 25*(12), 2850.

Torres, O., Tena, N. M., Murray, B., & Sarkar, A. (2017). Novel starch based emulsion gels and emulsion microgel particles: Design, structure and rheology. *Carbohydrate Polymers, 178*, 86-94. doi:https://doi.org/10.1016/j.carbpol.2017.09.027

Tunick, M. H., Ren, D. X., Van Hekken, D. L., Bonnaillie, L., Paul, M., Kwoczak, R., & Tomasula, P. M. (2016). Effect of heat and homogenization on in vitro digestion of milk. *Journal of Dairy Science*, *99*(6), 4124-4139.

Ubbink, J. (2012). Soft matter approaches to structured foods: from "cook-and-look" to rational food design? *Faraday Discussions*, *158*(0), 9-35. doi:10.1039/C2FD20125A

Ubbink, J., & Krüger, J. (2006). Physical approaches for the delivery of active ingredients in foods. *Trends in Food Science & Technology*, *17*(5), 244-254. doi:https://doi.org/10.1016/j.tifs.2006.01.007

van der Bilt, A. (2009). 1 - Oral physiology, mastication and food perception. In D. J. McClements & E. A. Decker (Eds.), *Designing Functional Foods* (pp. 3-37): Woodhead Publishing.

Vitaglione, P., Barone Lumaga, R., Ferracane, R., Radetsky, I., Mennella, I., Schettino, R., . . . Fogliano, V. (2012). Curcumin bioavailability from enriched bread: the effect of microencapsulated ingredients. *Journal of Agricultural and Food Chemistry*, *60*(13), 3357-3366. doi:10.1021/jf204517k

Vítek, L., & Haluzík, M. (2016). The role of bile acids in metabolic regulation. *Journal of Endocrinology*, *228*(3), R85-R96.

Wada, Y., & Lönnerdal, B. (2014). Effects of different industrial heating processes of milk on site-specific protein modifications and their relationship to in vitro and in vivo digestibility. *Journal of Agricultural and Food Chemistry*, *62*(18), 4175-4185.

Wang, Q., Luan, Y., Tang, Z., Li, Z., Gu, C., Liu, R., . . . Wu, M. (2023). Consolidating the gelling performance of myofibrillar protein using a novel OSA-modified-starch-

stabilized Pickering emulsion filler: Effect of starches with distinct crystalline types. *Food Research International*, *164*, 112443. doi:https://doi.org/10.1016/j.foodres.2022.112443

Wang, S., & Copeland, L. (2013). Molecular disassembly of starch granules during gelatinization and its effect on starch digestibility: a review. *Food & Function*, *4*(11), 1564-1580.

Wang, X., Lin, Q., Ye, A., Han, J., & Singh, H. (2019). Flocculation of oil-in-water emulsions stabilised by milk protein ingredients under gastric conditions: Impact on in vitro intestinal lipid digestion. *Food Hydrocolloids*, *88*, 272-282. doi:https://doi.org/10.1016/j.foodhyd.2018.10.001

Wang, X., Ye, A., Dave, A., & Singh, H. (2021). In vitro digestion of soymilk using a human gastric simulator: Impact of structural changes on kinetics of release of proteins and lipids. *Food Hydrocolloids*, *111*, 106235. doi:https://doi.org/10.1016/j.foodhyd.2020.106235

Wang, X., Ye, A., Dave, A., & Singh, H. (2022). Structural changes in oat milk and an oat milk–bovine skim milk blend during dynamic in vitro gastric digestion. *Food Hydrocolloids*, *124*, 107311.

Wang, X., Ye, A., Lin, Q., Han, J., & Singh, H. (2018). Gastric digestion of milk protein ingredients: Study using an in vitro dynamic model. *Journal of Dairy Science*, *101*(8), 6842-6852. doi:https://doi.org/10.3168/jds.2017-14284

Wang, X., Ye, A., & Singh, H. (2020). Structural and physicochemical changes in almond milk during in vitro gastric digestion: impact on the delivery of protein and lipids. *Food & Function*, *11*(5), 4314-4326.

Weber, F. H., Clerici, M. T. P. S., Collares-Queiroz, F. P., & Chang, Y. K. (2009). Interaction of guar and xanthan gums with starch in the gels obtained from normal, waxy and high-

amylose corn starches. *Starch - Stärke, 61*(1), 28-34. doi:https://doi.org/10.1002/star.200700655

Wooster, T. J., Day, L., Xu, M., Golding, M., Oiseth, S., Keogh, J., & Clifton, P. (2014). Impact of different biopolymer networks on the digestion of gastric structured emulsions. *Food Hydrocolloids, 36*, 102-114. doi:https://doi.org/10.1016/j.foodhyd.2013.09.009

Wooster, T. J., Moore, S. C., Chen, W., Andrews, H., Addepalli, R., Seymour, R. B., & Osborne, S. A. (2017). Biological fate of food nanoemulsions and the nutrients they carry – internalisation, transport and cytotoxicity of edible nanoemulsions in Caco-2 intestinal cells. *RSC Advances, 7*(64), 40053-40066. doi:10.1039/C7RA07804H

Wyspiańska, D., Kucharska, A. Z., Sokół-Łętowska, A., & Kolniak-Ostek, J. (2019). Effect of microencapsulation on concentration of isoflavones during simulated in vitro digestion of isotonic drink. *Food Science & Nutrition, 7*(2), 805-816. doi:https://doi.org/10.1002/fsn3.929

Yang, L., Yang, C., Li, C., Zhao, Q., Liu, L., Fang, X., & Chen, X.-Y. (2016). Recent advances in biosynthesis of bioactive compounds in traditional Chinese medicinal plants. *Science Bulletin, 61*(1), 3-17.

Ye, A. (2021). Gastric colloidal behaviour of milk protein as a tool for manipulating nutrient digestion in dairy products and protein emulsions. *Food Hydrocolloids, 115*, 106599. doi:https://doi.org/10.1016/j.foodhyd.2021.106599

Ye, A., Cui, J., Dalgleish, D., & Singh, H. (2016). Formation of a structured clot during the gastric digestion of milk: Impact on the rate of protein hydrolysis. *Food Hydrocolloids, 52*, 478-486. doi:https://doi.org/10.1016/j.foodhyd.2015.07.023

Ye, A., Cui, J., Dalgleish, D., & Singh, H. (2017). Effect of homogenization and heat treatment on the behavior of protein and fat globules during gastric digestion of milk. *Journal of Dairy Science, 100*(1), 36-47. doi:https://doi.org/10.3168/jds.2016-11764

Ye, A., Cui, J., Taneja, A., Zhu, X., & Singh, H. (2009). Evaluation of processed cheese fortified with fish oil emulsion. *Food Research International, 42*(8), 1093-1098. doi:https://doi.org/10.1016/j.foodres.2009.05.006

Ye, A., Liu, W., Cui, J., Kong, X., Roy, D., Kong, Y., . . . Singh, H. (2019). Coagulation behaviour of milk under gastric digestion: Effect of pasteurization and ultra-high temperature treatment. *Food Chemistry, 286*, 216-225. doi:https://doi.org/10.1016/j.foodchem.2019.02.010

Ye, Q., Ge, F., Wang, Y., Woo, M. W., Wu, P., Chen, X. D., & Selomulya, C. (2021). On improving bioaccessibility and targeted release of curcumin-whey protein complex microparticles in food. *Food Chemistry, 346*, 128900. doi:https://doi.org/10.1016/j.foodchem.2020.128900

Zaidel, D. N. A., Sahat, N. S., Jusoh, Y. M. M., & Muhamad, I. I. (2014). Encapsulation of anthocyanin from roselle and red cabbage for stabilization of water-in-oil emulsion. *Agriculture and Agricultural Science Procedia, 2*, 82-89. doi:https://doi.org/10.1016/j.aaspro.2014.11.012

Zhang, R., & McClements, D. J. (2018). Chapter 18 - Characterization of gastrointestinal fate of nanoemulsions. In S. M. Jafari & D. J. McClements (Eds.), *Nanoemulsions* (pp. 577-612): Academic Press.

Zhao, X., Li, D., Wang, L.-j., & Wang, Y. (2022). Rheological properties and microstructure of a novel starch-based emulsion gel produced by one-step emulsion gelation: Effect of oil content. *Carbohydrate Polymers, 281*, 119061. doi:https://doi.org/10.1016/j.carbpol.2021.119061

Zheng, B., Peng, S., Zhang, X., & McClements, D. J. (2018). Impact of delivery system type on curcumin bioaccessibility: comparison of curcumin-loaded nanoemulsions with

commercial curcumin supplements. *Journal of Agricultural and Food Chemistry, 66*(41), 10816-10826. doi:10.1021/acs.jafc.8b03174

Zheng, B., Zhang, X., Peng, S., & McClements, D. J. (2019). Impact of curcumin delivery system format on bioaccessibility: nanocrystals, nanoemulsion droplets, and natural oil bodies. *Food & Function, 10*(7), 4339-4349.

Zheng, B., Zhou, H., & McClements, D. J. (2021). Nutraceutical-fortified plant-based milk analogs: Bioaccessibility of curcumin-loaded almond, cashew, coconut, and oat milks. *LWT - Food Science and Technology, 147*, 111517. doi:https://doi.org/10.1016/j.lwt.2021.111517

Zheng, M., Ye, A., Singh, H., & Zhang, Y. (2021). The in vitro digestion of differently structured starch gels with different amylose contents. *Food Hydrocolloids, 116*, 106647.

Zhong, J., Yang, R., Cao, X., Liu, X., & Qin, X. (2018). Improved physicochemical properties of yogurt fortified with fish oil/γ-oryzanol by nanoemulsion technology. *Molecules, 23*(1), 56. Retrieved from http://www.mdpi.com/1420-3049/23/1/56

Zhu, F. (2017). Encapsulation and delivery of food ingredients using starch based systems. *Food Chemistry, 229*, 542-552. doi:https://doi.org/10.1016/j.foodchem.2017.02.101

Zou, L., Zheng, B., Zhang, R., Zhang, Z., Liu, W., Liu, C., Liu, W., Zhang, G., Xiao, H., & McClements, D. J. (2016). Influence of lipid phase composition of excipient emulsions on curcumin solubility, stability, and bioaccessibility. *Food Biophysics,* 11(3), 213-225. doi:10.1007/s11483-016-9432-9